DROP AND STATIC TESTS ON A TENTH-SCALE MODEL OF AN AIR CUSHION LANDING SYSTEM (ACLS)

AIR FORCE INSTITUTE OF TECHNOLOGY

SEPTEMBER 1973

DISCLAIMER NOTICE

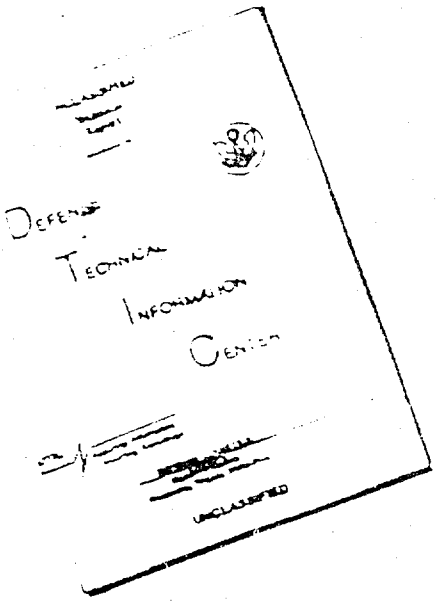

THIS DOCUMENT IS BEST QUALITY AVAILABLE. THE COPY FURNISHED TO DTIC CONTAINED A SIGNIFICANT NUMBER OF PAGES WHICH DO NOT REPRODUCE LEGIBLY.

NOTICE

When Government drawings, specifications, or other data are used for any purpose other than in connection with a definitely related Government procurement operation, the United States Government thereby incurs no responsibility nor any obligation whatsoever; and the fact that the government may have formulated, furnished, or in any way supplied the said drawings, specifications, or other data, is not to be regarded by implication or otherwise as in any manner licensing the holder or any other person or corporation, or conveying any rights or permission to manufacture, use, or sell any patented invention that may in any way be related thereto.

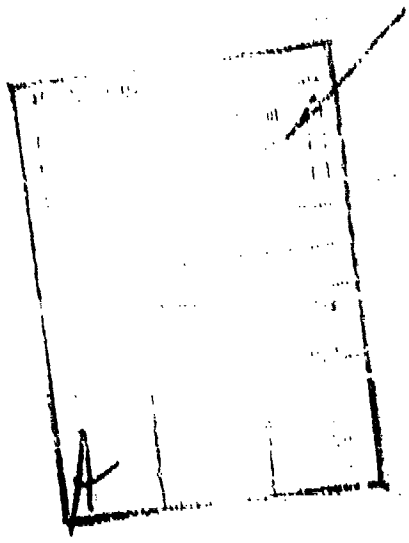

Copies of this report should not be returned unless return is required by security considerations, contractual obligations, or notice on a specific document.

AIR FORCE/56780/30 November 1973 — 100

UNCLASSIFIED
Security Classification

AD 770 026

DOCUMENT CONTROL DATA - R & D

(Security classification of title, body of abstract and indexing annotation must be entered when the overall report is classified)

1. ORIGINATING ACTIVITY (Corporate author)	2a. REPORT SECURITY CLASSIFICATION
Air Force Institute of Technology (AFIT-ER) Wright-Patterson Air Force Base, Ohio 45433	Unclassified
	2b. GROUP

3. REPORT TITLE

DROP AND STATIC TESTS ON A TENTH-SCALE MODEL OF AN AIR CUSHION LANDING SYSTEM (ACLS)

4. DESCRIPTIVE NOTES (Type of report and inclusive dates)

Thesis

5. AUTHOR(S) (First name, middle initial, last name)

Anthony Rodrigues
Captain, USAF

6. REPORT DATE	7a. TOTAL NO. OF PAGES	7b. NO. OF REFS
September 1973	148	3

8a. CONTRACT OR GRANT NO	9a. ORIGINATOR'S REPORT NUMBER(S)
b. PROJECT NO 1369	GA/ME/73-3
c. Task No. 02	9b. OTHER REPORT NO(S) (Any other numbers that may be assigned this report)
d.	AFFDL-TR-73-46

10. DISTRIBUTION STATEMENT

Approved for public release; distribution unlimited.

11. SUPPLEMENTARY NOTES	12. SPONSORING MILITARY ACTIVITY
	Air Force Flight Dynamics Laboratory Wright-Patterson AFB, Ohio 45433

13. ABSTRACT

An experimental investigation of the performance of an Air Cushion Landing System (ACLS) on a one-tenth scale model of a CC-115 Canadian aircraft is discussed. Several different types of tests wereconducted on an extended version of the ACLS trunk at simulated full-scale trunk pressures of 315 psfg, out of ground effect, and 342 psfg, in ground effect. Cushion pressure was 160 psfg, in ground effect during hover. The experiments involved: vertical drop tests to measure the effects of sink rate and initial attitude between full-scale sink rates of 3.0 and 12.5 fps, and attitudes of pitch and roll from 0.0 to 12.0 and 0.0 to 7.5 degrees, respectively; static equilibrium tests to measure vertical stiffness, roll stiffness, pitch stiffness, and floor pressure exerted by the ACLS with loads up to 4.1 times the aircraft landing weight; and braking tests to obtain the effects of changing brake pillow thickness between simulated full-scale heights of 0.0 inches and 26.0 inches.

The results of the vertical drop tests revealed that the air cushion will absorb most of the landing impact load except at initial attitudes of 12.0 degrees pitch, where the aircraft fuselage could touch the ground. Vertical stiffness test results showed the extended version of the ACLS trunk to be 39% stiffer than a previous shorter version between vertical load ranges of 0.5 and 1.9 times the aircraft landing weight. Floor pressure tests verified that the ACLS aircraft could land on low strength runways and never exert pressures higher than 3.8 psi above the atmospheric, full scale. Braking tests concluded that the maximum deceleration of the aircraft was about 0.34 g, and that increasing pillow thickness above 10.8 inches, full scale, would not increase that deceleration rate.

DD FORM 1 NOV 68 1473

UNCLASSIFIED
Security Classification

14. KEY WORDS	LINK A		LINK B		LINK C	
	ROLE	WT	ROLE	WT	ROLE	WT
Air Cushion Landing System Landing Gear CC-115						

*U.S.Government Printing Office: 1973 — 758-428/262

DROP AND STATIC TESTS ON A TENTH-SCALE MODEL OF AN AIR CUSHION LANDING SYSTEM (ACLS)

ANTHONY RODRIGUES, CAPT, USAF

1-2

FOREWORD

This work was conducted in support of an Air Force Flight Dynamics Laboratory in-house exploratory development effort on air cushion landing systems (Project 1369). The author conducted this work in partial fulfillment of the requirements for the degree of Master of Science from the Air Force Institute of Technology.

The author wishes to express his thanks to Dr. Andrew J. Shine, his Thesis advisor, for his valuable help and guidance throughout the independent study period.

The author is particularly indebted to Major John C. Vaughan, III, Mr. Shade Campbell, and Mr. David J. Pool of the Mechanical Branch, Vehicle Equipment Division, Air Force Flight Dynamics Laboratory, Wright-Patterson Air Force Base, Ohio, for their valuable and frequent assistance and suggestions during the course of this experimental investigation. Without their aid and advice, this study could not have been conducted.

This report was submitted by the author in March 1973.

This technical report has been reviewed and is approved.

K. N. Digges

KENNERLY H. DIGGES
Chief, Mechanical Branch
Vehicle Equipment Division

ABSTRACT

An experimental investigation of the performance of an Air Cushion Landing System (ACLS) on a one-tenth scale model of a CC-115 Canadian aircraft is discussed. Several different types of tests were conducted on an extended version of the ACLS trunk at simulated full-scale trunk pressures of 315 psfg, out of ground effect, and 342 psfg, in ground effect. Cushion pressure was 160 psfg, in ground effect, during hover. The experiments involved: vertical drop tests to measure the effects of sink rate and initial attitude between full-scale sink rates of 3.0 and 12.5 fps, and attitudes of pitch and roll from 0.0 to 12.0 and 0.0 to 7.5 degrees, respectively; static equilibrium tests to measure vertical stiffness, roll stiffness, pitch stiffness, and floor pressure exerted by the ACLS with loads up to 4.1 times the aircraft landing weight; and braking tests to obtain the effects of changing brake pillow thickness between simulated full-scale heights of 0.0 inches and 26.0 inches.

The results of the vertical drop tests revealed that the air cushion will absorb most of the landing impact load except at initial attitudes of 12.0 degrees pitch, where the aircraft fuselage could touch the ground. Vertical stiffness test results showed the extended version of the ACLS trunk to be 39% stiffer than a previous shorter version between vertical load ranges of 0.5 and 1.9 times the aircraft landing weight. Floor pressure tests verified that the ACLS aircraft could land on low strength runways and never exert pressures higher than

3.8 psi above the atmospheric, full scale. Braking tests concluded t maximum deceleration of the aircraft was about 0.34 g, and that increasing pillow thickness above 10.8 inches, full scale, would not increase that deceleration rate.

Contents

List of Figures

List of Figures

List of Figures

List of Figures

List of Tables

List of Tables

List of Symbols

Symbol	Description	Unit
A_C	Area of cushion	ft^2
A_D	Braking deceleration	g_e's
A_T	Area of trunk contact	ft^2
c.g.	Center of gravity	-
c.p.	ACLS center of pressure	-
D	Deflection of ACLS	inches
d	Drop height	inches
F	Brake drag	pounds
F_B	Load on brake blocks	pounds
$G_{c.g.}$	Load at model center of gravity	g-load
G_T	Ground tangent line	-
g_e	Gravity acceleration constant (32.2 ft/sec^2)	-
H_L	Height of center of gravity above floor	inches
I	Moment of inertia	slug-ft^2
IGE	In ground effect	-
L	Trunk length	inches
L_P	Pitch torque load	pounds
L_R	Roll torque load	pounds
ℓ	Length from pivot point to model center of gravity	inches
M	Mass	slugs
OGE	Out of ground effect	-
P_C	Cushion pressure	psfg

List of Symbols

Symbol	Description	Unit
P_T	Trunk pressure	psfg
T	Period of oscillation	minutes
t	Time	seconds
v_t	Sink rate	fps
W_A	Total weight of model on ACLS	pounds
μ	Coefficient of static friction	-
θ	Pitch angle	degrees
τ_{P_+}	Positive pitch torque	ft-lbs
τ_{P_-}	Negative pitch torque	ft-lbs
τ_R	Roll torque	in-lbs
ϕ	Roll angle	degrees

DROP AND STATIC TESTS ON A TENTH-SCALE MODEL OF AN AIR CUSHION LANDING SYSTEM (ACLS)

I. Introduction

Background

The Air Cushion Landing System (ACLS) Project is a development program being conducted by joint cooperation between the Air Force Flight Dynamics Laboratory at Wright-Patterson AFB, Ohio, and the Canadian government. The system eliminates the need for a conventional landing gear by replacing it with a cushion of air directly beneath the fuselage of the aircraft. The cushion supports the weight of the aircraft during takeoff, landing, and taxiing. Since this cushion supports the weight of the aircraft over a large area, the pressure on the landing surface is low (1 - 4 psi above atmospheric pressure). Thus ACLS allows large aircraft to land on snow, tundra, and other unprepared types of runways. In addition, the ACLS provides a weight savings compared to the conventional landing gear as that on the C-5.

The cushion of air is formed through the use of an elongated doughnut-shaped trunk, which is physically attached to the bottom of the aircraft fuselage (see Fig. 1). Air is supplied to the trunk from a source on the aircraft, and it flows from the trunk through hundreds of tiny holes on the bottom of the trunk. The air from these holes forms a continuous jet curtain around the periphery of the trunk. The curtain thus acts as a seal against air escaping from the cushion region and secures a pressure of 1 to 4 psi above atmospheric under the fuselage, and this pressure, or air cushion, supports the entire weight of the

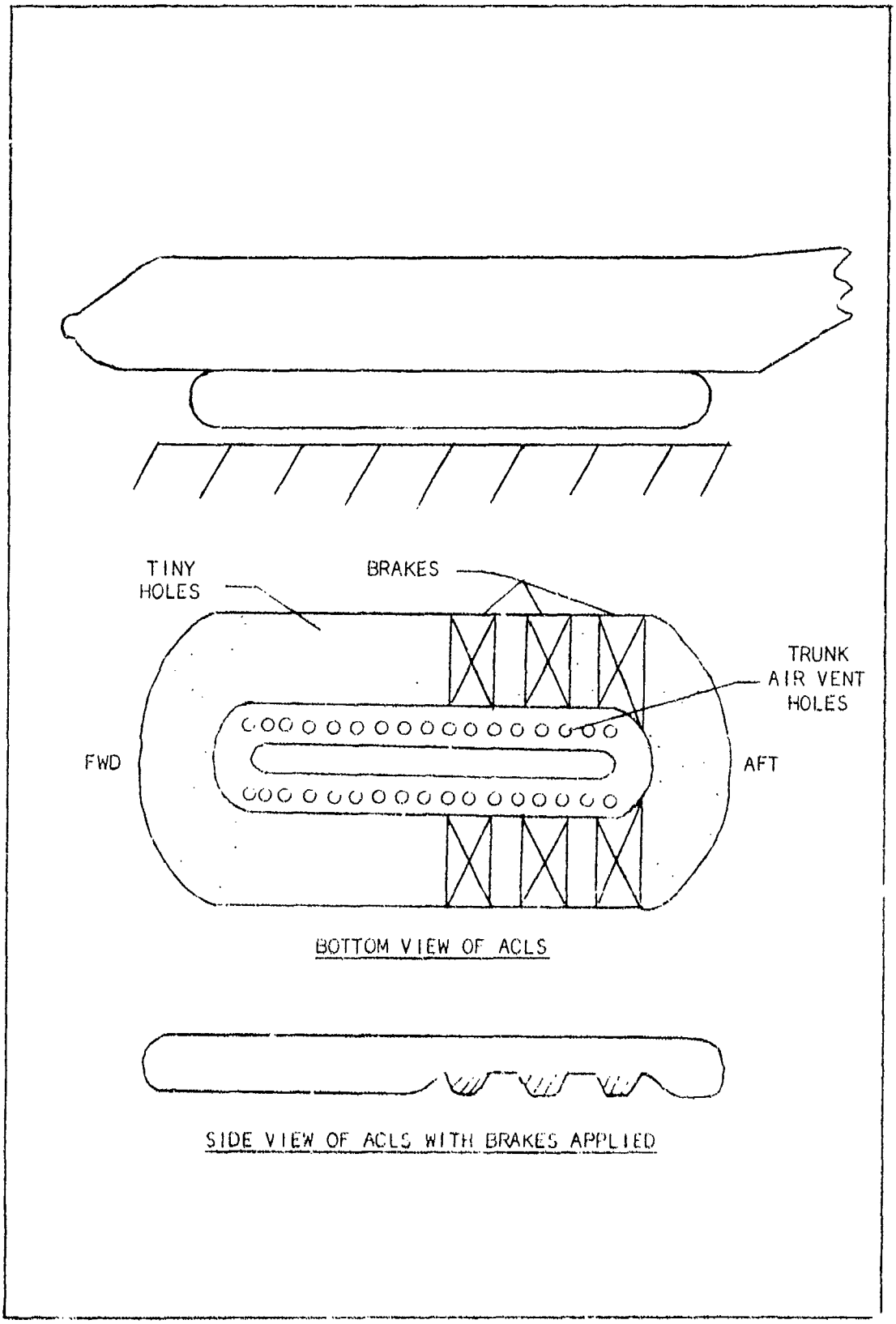

Fig. 1. ACLS Components

aircraft as it approaches the ground. The trunk is constructed of rubber and nylon and stretches approximately 300% from an uninflated state in order to be in the proper landing mode. During flight, the trunk is deflated and hugs the fuselage of the aircraft (Ref 2:7).

Braking is performed by pressing a braking material against the ground. The braking material is secured to each of six pillows which are attached to the bottom of the trunk as shown in Fig. 1. When braking is desired the pillows are inflated, and this presses the braking material against the landing surface and raises that portion of the trunk to which the brakes are attached above the surface. As the trunk is raised, the jet curtain is broken, allowing cushion pressure to decrease and placing part of the aircraft weight on the brakes instead of the air cushion. Steering is accomplished through the use of differential braking as is done on a caterpillar tractor. Right brakes are applied to turn right and the left to turn left (Ref 2:7).

Present program development is being geared to a full-scale flight test of the ACLS on a deHavilland CC-115 Canadian aircraft (C-8 Buffalo is the U.S. version of the aircraft). As such, all recent testing of the system has been done using scaled models of this aircraft with ACLS attached. Some of the tests have been accomplished by the Air Force Flight Dynamics Laboratory (AFFDL) at Wright-Patterson AFB, Ohio, on a quarter-scale model of the CC-115 and other tests by Bell Aerospace Company of Buffalo, New York, on a tenth-scale model of the CC-115. Model testing of the system is required to help substantiate design. Theoretical prediction of ACLS functions is difficult; since operation of the system involves many interacting events such as trunk deflections,

transient increases in cushion and trunk pressure, variations in back pressure, and forward and reverse flow through the air supply equipment of the system (Ref 3:1).

The quarter-scale tests conducted by AFFDL involved vertical drop tests which determined the effects of vertical velocity and attitude during a landing with the ACLS and vertical static load deflection tests of the system. The model was dropped simulating sink rates of 9, 11, and 12.5 fps and at various attitudes of pitch up to 10 degrees and roll of 0.0 and +7.5 degrees. Static loading of the model was accomplished up to twice the weight of the model to obtain static stiffness (Ref 3:ii).

Some of the tenth-scale tests accomplished by the Bell Aerospace Company also involved drop tests and static stiffness tests of the model. These drop tests were conducted at sink rates from 5 fps to 12.7 fps with various attitudes of pitch up to 8.5 degrees and roll up to 6.2 degrees. The model was statically loaded up to 1.5 times its weight (Ref 1:362).

The AFFDL tests were accomplished at a different full-scale center of gravity location than the Bell tests, but both series of tests were done with a shorter version of the trunk than is being presently proposed. The full-scale difference in length between the two trunks is 17.5 inches. The Bell Aerospace Company did perform forward velocity tests on the longer trunk, but these tests will not concern this report. In addition, AFFDL drop tests were accomplished at a different design trunk pressure than the Bell tests.

This study was conducted to gather more data on the ACLS and particularly on the longer version of the trunk. The tests of this report involve only the long trunk, and the drop and vertical static

stiffness tests of this report will be compared to similar tests done by Bell and AFFDL to show differences between long and short trunk responses.

Definition of Terms

The following are certain terms and phrases that will be used throughout the remainder of this report:

1. Cushion Pressure P_C. Pressure of the air within the cavity created by the fuselage, ground, and the doughnut-shaped trunk. In a hover near the ground or taxiing condition, the cushion pressure is the pressure supporting the weight of the aircraft. The design cushion pressure is determined from the fact that a certain pressure is required to support the weight of the aircraft in a hover condition. The design cushion pressure of the model was found to be 16 psfg.

2. Trunk Pressure P_T. Pressure of the air contained within the doughnut-shaped bag or trunk. This pressure keeps the bag inflated to desired design conditions and provides the desired velocity of the tiny jets issuing from the numerous holes. Air for trunk pressure is supplied from onboard fans. This air leaves the trunk through the tiny holes on the trunk bottom and also through trunk vent holes in the cushion cavity. These vents supply air to the cushion. Thus, to maintain a specific cushion pressure, a certain trunk pressure is required. The trunk pressure is adjusted by covering or uncovering the vent holes.

3. Out of Ground Effect OGE. This is a design point for the system. In model testing under this condition, the model is raised above the ground until cushion pressure is 0.0 psfg. At that point the design trunk pressure is obtained by covering or uncovering trunk air vent holes located in the cushion cavity.

4. In Ground Effect IGE. This is another design point for the system. For this case, in model testing, the model is left in its hover condition on the ground with full weight of the model being supported by cushion pressure. While in this condition, the design trunk pressure is again obtained by adjusting trunk air vent holes in the cushion cavity.

5. Center of Pressure C.P. This point is the geometric center of the ACLS consisting of the trunk or bag and cushion (see Fig. 2). It is the point where the resultant force generated by the ACLS is located. On the aircraft the c.p. is forward of the center of gravity.

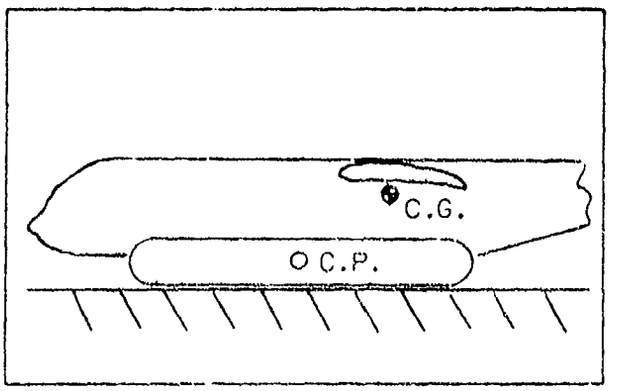

Fig. 2. Location of C.P.

6. Scaling Parameters. These parameters are factors used to obtain full-scale values from scale model results. The scaling parameters have been previously determined using a dimensional analysis based on a constant Froude number of air flow beneath the ACLS and a constant linear acceleration of the aircraft (Ref 3:5). In this report all values given will be the actual values obtained from a 1/10-scale model of the CC-115 aircraft, unless otherwise specified as full-scale values. Table I shows the terms applicable to this report and the necessary multiplying factor needed to obtain full-scale values from 1/10-scale terms.

7. g-Load. A 1 g-load in the vertical direction corresponds to a force equal to the weight of the aircraft. The g-load does not directly refer to the acceleration of the model. To obtain acceleration in terms of $g_e = 32.2$ ft/sec^2, 1 g should be subtracted from the value of the g-load.

TABLE I

1/10 Scaling Parameters

Term	Model Value	Scale Factor	Full-Scale Value
Acceleration, linear	a	1	a
Area	A	10^2	10^2A
Density	ρ	1	ρ
Force	F	10^3	10^3F
Length	L	10	10L
Mass	M	10^3	10^3M
Moment of Inertia	I	10^5	10^5I
Pitch	θ	1	θ
Pressure	P	10	10P
Pressure Ratio	P_1/P_2	1	P_1/P_2
Roll	ϕ	1	ϕ
Sink Rate or Velocity	v_t	$10^{1/2}$	$10^{1/2}v_t$
Time	t	$10^{1/2}$	$10^{1/2}$t
Volume	V	10^3	10^3V
Weight	W	10^3	10^3W

(From Ref 3:6)

Thus an object at rest on the floor is at a +1 g-load condition and 0 g_e acceleration in the vertical direction. A +1 g-load points up and away from the floor, and is the floor's reaction to model weight.

8. Pitch and Roll Directions. When referring to pitch and roll angles, the sense of angle rotation will be represented by the sign of the angle as shown in Fig. 3.

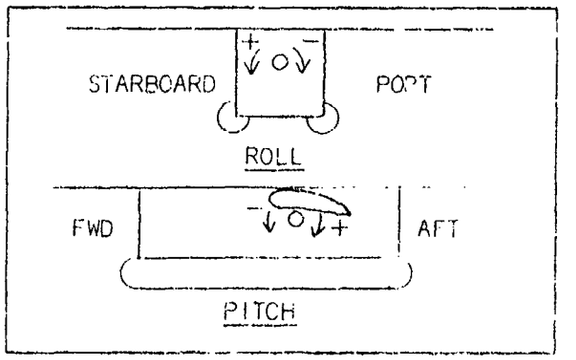

Fig. 3. Sense of Roll and Pitch Angles

9. Load on the ACLS. This load consists of all the force acting on the ACLS including the weight of the model. Thus a load on the ACLS of 140 pounds consists of 39.1 pounds of model weight and 100.9 pounds of additional load on the model.

10. Static Stiffness. This is a measure of the rigidity of the ACLS trunk and cushion under vertical and moment loading conditions. Vertical, or level, static stiffness measures the rigidity under downward loads on the ACLS, while pitch and roll stiffness measures rigidity under moments about the center of gravity in the roll and pitch planes

11. Area of Trunk Contact. When loads much above 1 g-load are felt by the ACLS, the trunk shape near the ground tangent deviates from its rounded shape and begins to flatten. The trunk does not make surface-to-surface contact with the floor, but the trunk is flattened by the pressure between it and the floor. Thus, area of trunk contact is the amount of area of the trunk that is flattened under load.

12. Cushion Area. The cushion pressure is exerted on a cushion area which is the area inside the normal trunk ground tangent line (see Fig. 4). The area under B is constant while that under A and C

depends on the amount of bag deflection and the value of cushion pressure during loading. The change in A and C has been found to be minimal since the trunk tends to flatten outside the hover ground tangent line. Therefore, the tests in this report assume a constant area for A, B, C, during all vertical loads above model weight.

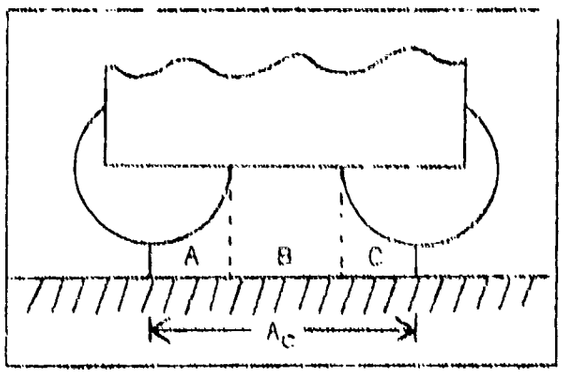

Fig. 4. Cushion Area

Purpose

The ACLS is a rapidly emerging technology, but more data are needed on the actual operation of the system in order to verify design criteria and confirm results of previous testing. Furthermore, the extension of the length of the trunk has created a need for more operational data of the extended trunk system. As has been stated, an analytical or computer approach to obtain this desired data is difficult due to the many interacting phenomena. Thus scale model experimental testing becomes the most effective method of gathering good data on the many interacting variables of cushion pressure, trunk pressure, bag deflection, and trunk area contact of the ACLS. In that light the purpose of this study was to experimentally examine the following:

1. Effects of vertical velocity and attitude of the aircraft on the ACLS performance during landing, in terms of cushion pressure, trunk pressure, and g-load at c.g.
2. Static stiffness of the ACLS in level, pitched, and rolled attitudes.

3. Static relationships of ag cushion pressure, trunk pressure, load on aircraft, bag deflection, and area of trunk contact.
4. Effects of aircraft load on the static pressure footprint of the ACLS.
5. Effects of brake pillow height (thickness of brake pillows from the bottom of the trunk to the contact with the landing surface) on cushion pressure, trunk pressure, and braking deceleration.

In addition, the experimental data gathered from 1, above, is compared to previous tests conducted on one-quarter and one-tenth scale models; and the results from 2 (level attitude only) and 4, above, are compared to previous one-quarter scale model tests. The quarter-scale data quoted in this report have been converted from quarter-scale values to tenth-scale terms.

All previous testing similar to that of this study was conducted using a trunk shorter in length than that being presently proposed. The tests of this study differ from previous testing in that the longer version of the trunk was used on all experiments.

Scope

A one-tenth scale model of the CC-115 Buffalo aircraft was used to conduct these tests. The model was dynamically and geometrically similar to the full-scale version according to the full-scale design parameters as found in Table II.

The effects of vertical velocity and attitude upon landing were determined through the use of drop tests. Vertical velocity was varied between 0.0 and 12.5 fps (full-scale value), while roll and pitch ranges

TABLE II

CC-118 Full-Scale Design Parameters

Landing weight	39,100 lbs
Length (nose to tail)	79 ft
Maximum sink speed	12.6 fps
Maximum g-load	3.6 g
Maximum landing pitch angle	12 degrees
Maximum landing roll angle	± 7.6 degrees
Moments of Inertia	
Pitch	280,780 slug-ft^2
Roll	223,846 slug-ft^2
Yaw	466,000 slug-ft^2
Wing span	79 ft
Trunk pressure, OGE	315 psfg
Trunk pressure, IGE	342 psfg
Cushion area	244 ft^2

were 0.0 to -7.5 degrees and 0.0 to 12.0 degrees, respectively. Roll and pitch were observed alone and in combination with each other. These drop tests were conducted at two different initial design points (full-scale values) of the ACLS:

$$\text{IGE, } P_T = 342 \text{ psfg}$$

$$\text{OGE, } P_T = 315 \text{ psfg}$$

Static tests in vertical stiffness, ACLS relationships, and pressure footprints were examined from zero load on the ACLS up to four times maximum landing weight of the aircraft. This range exceeds the maximum g-load of the aircraft by 1/2 g. The loads on the ACLS were applied as follows for vertical stiffness and ACLS relationships:

1. Load over c.p.--OGE and IGE design modes. The load over the c.p. was in addition to the model weight acting at the c.g.
2. Load over c.g.--OGE design mode.

Pressure footprint was examined at OGE mode with load over the c.g.

Roll stiffness was observed from 0.0 inch-pounds of torque to 46 inch-pounds of torque, while pitch stiffness was examined from -30.8 foot-pounds of torque to 20.2 foot-pounds of torque.

Braking tests were conducted with brake heights from 0.0 inches to 2.60 inches.

The data and results gathered from this study are presented in the form of graphs and tables in this report.

II. Apparatus

Introduction

This section will describe only that apparatus common to all of the tests. This equipment consisted of the one-tenth scale model, cushion and trunk pressure manometers, stroboscope, a barometer, and the platform used to conduct the testing. Other equipment used will be described with the section to which that equipment is peculiar.

One-Tenth Scale Model

The model used for these tests was a one-tenth scale model of the CC-115 Buffalo aircraft with the ACLS installed. Designed and built by Bell Aerospace Company, the model is dynamically and geometrically similar to its full-scale version. Figure 5 shows a sketch of the scale model with its dimensions. As the drawing indicates, the model is 94.8 inches long with a wingspan of 115.2 inches. It is made of lightweight materials consisting of balsa wood bulkheads and stringers with a molded fiber glass skin 0.025 inches thick (Ref 1:346). The original horizontal stabilizer provided with the model was not used. It was necessary to use a lighter weight tail to keep the model center of gravity in the desired location.

The trunk attached to the model was fabricated from an unstretchable material consisting of 2-3/4 ounces per square yard polyurethane coated nylon. The trunk is constructed to a shape associated with nominal ACLS

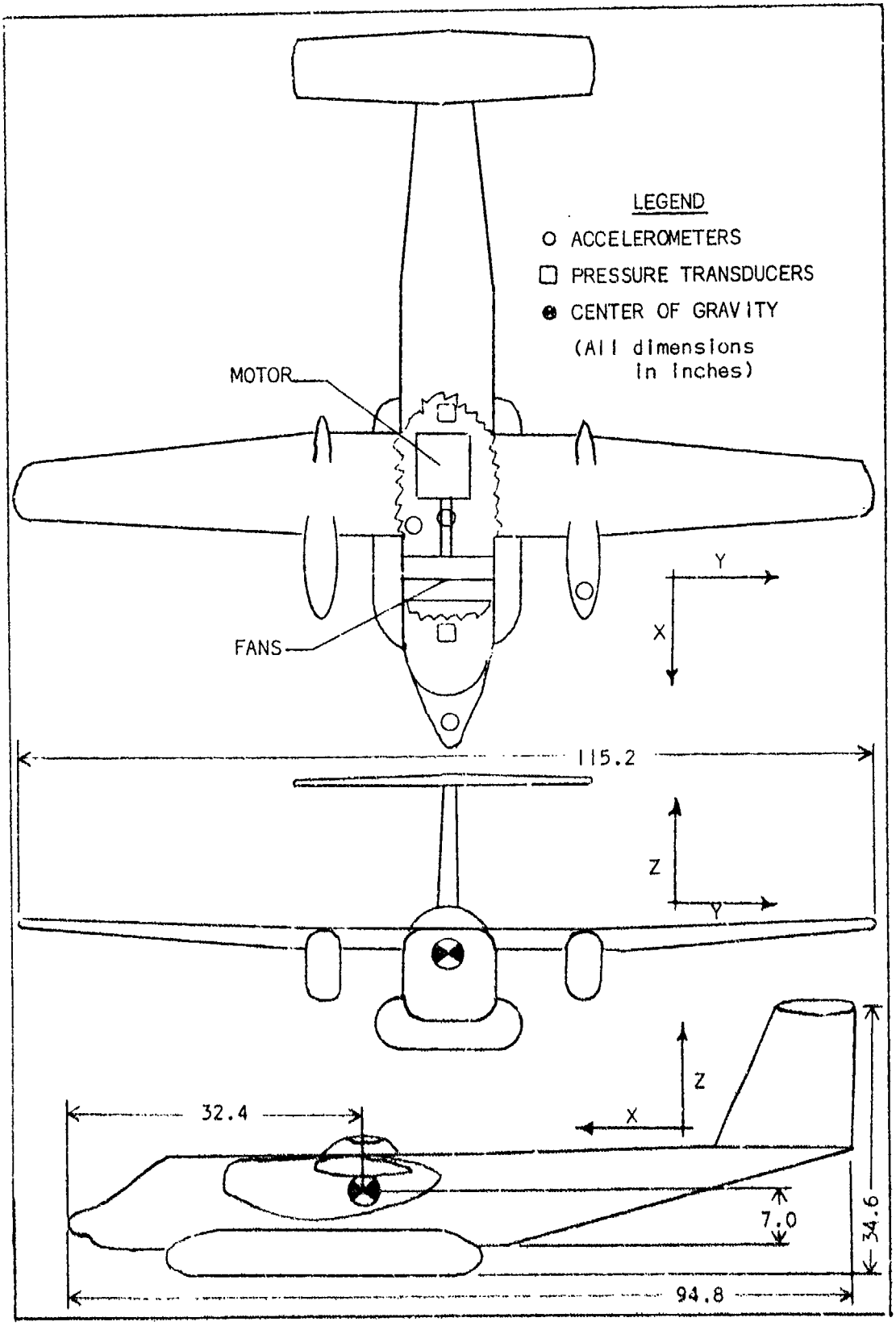

Fig. 5. Tenth-Scale Model of CC-115

operating pressures during ground taxiing, and it is mechanically attached with a metal strip fastener to the fuselage of the model (Ref 1:350). Nylon tape was placed over the metal fastener to insure no leakage. It should be noted that the full-scale version of the trunk consists of a stretchable material instead of unstretchable as was used in these tests. A stretchable material trunk could not be used since material is not presently available with the necessary load-elongation characteristics (Ref 3:17).

Air is supplied to the trunk by two lightweight centrifugal fans situated in the forward section of the model fuselage (see Fig. 5). These fans are powered by a 1.4 horsepower A.C. electric motor (200 volts, 3-phase, 400 cycles) which is placed aft of the fans (Ref 1:350). The motor was electrically powered as indicated by Fig. 6. Control of motor rpm was accomplished at the rectifier by varying output voltage of the rectifier to the inverter. Because the power necessary to operate the motor was not directly available, the apparatus and connections shown schematically by Fig. 6 were necessary. Fan performance was previously calibrated and adjusted by the Bell Aerospace Company to simulate 640 to 800 horsepower per fan, which is the horsepower range to be used in the full-scale air power supply. In these tests only the 640 horsepower case, which is simulated by a fan rpm of 8600 was used. An electric cable was run from the aircraft inverter to the motor installed in the fuselage to provide power to the motor. The cable was so suspended as to not add weight to the model or affect its motion during testing. Although only used for drop tests, two pressure transducers and four accelerometers were installed within the fuselage of the model as is indicated by Fig. 5. It was

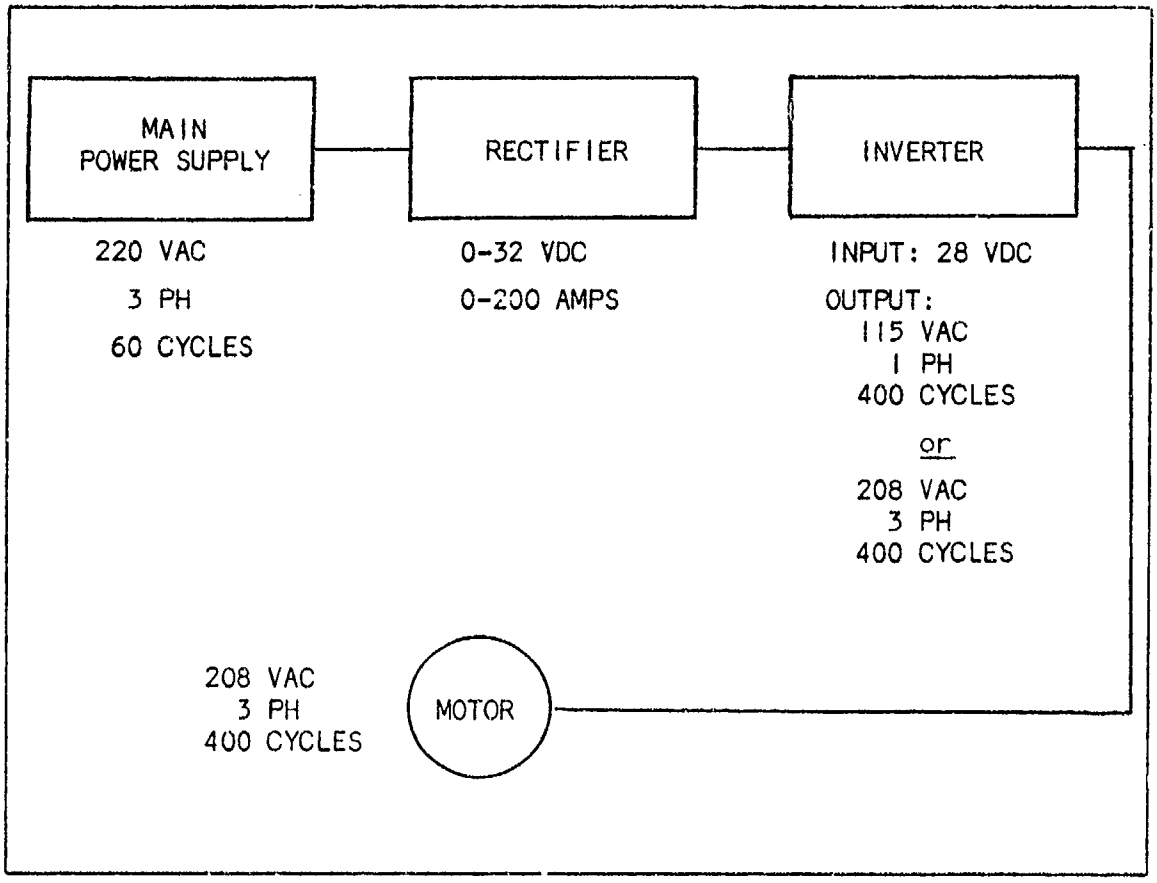

Fig. 6. Motor Power Supply

necessary to keep this equipment in the model for all tests in order to maintain the desired weight and center of gravity location of the model.

The model was fixed at a weight of 39.1 pounds with the center of gravity located as shown in Fig. 5: 32.4 inches aft of nose in the x direction, 7.0 inches above the bottom of the fuselage hard structure in the z direction, and 0.0 inches in the y direction. Moments of inertia of this model were found to be 2.71 slug ft^2 in pitch, 4.55 slug ft^2 in yaw, and 2.05 slug ft^2 in roll. Details concerning methods of checking model similarity, trunk construction, pressure transducers, and accelerometers are contained in Appendix A.

Cushion and Trunk Pressure Manometers, Stroboscope, Barometer

Before conducting each test the desired design conditions of trunk pressure, cushion pressure, and fan rpm had to be established. After each test, atmospheric temperature and pressure were checked. Cushion pressure and trunk pressure were obtained using water manometers that were leveled and zeroed before each test. Fan rpm was verified using a stroboscope. Atmospheric conditions were recorded from a mercury filled barometer for pressure and a centigrade thermometer for temperature. More detail on this equipment is found in Appendix B.

Testing Platform

All tests were conducted in Room 102, Building 255, Wright-Patterson Air Force Base, Ohio. Within this room was a wooden platform 122.0 inc long, 98.0 inches wide, and 30.5 inches high, on which the model was situated for all testing.

III. Drop Tests

Purpose

Drop tests were conducted to measure the effects of vertical velocity and attitude of the aircraft on the performance of the Air Cushion Landing System during a landing. These effects were observed in the reactions of cushion pressure, trunk pressure, and g-loads at the center of gravity of the model. Tests were run at two full-scale design conditions: trunk pressure at 342 psfg, IGE, and trunk pressure at 315 psfg, OGE. When an aircraft with the ACLS approaches the runway for a landing, it is considered in an OGE condition, and trunk pressure should be held at 315 psfg. When the CC-115 aircraft is IGE, trunk pressure trim valves are automatically opened. Vent holes (Fig. 1) are exposed and the valves adjust to keep the trunk pressure at 342 psfg. The model does not have the capability to change pressures as it approaches the platform. If trunk pressure was set at 34 psfg, IGE, and the model was raised above the platform, the trunk pressure dropped to 26 psfg. When trunk pressure was set at 32 psfg, OGE, and lowered to the platform, trunk pressure rose to 39 psfg. It was thus decided to run tests at both design points to cover the full range of possible pressures during an actual landing. The AFFDL quarter-scale model tests were run IGE while Bell tenth-scale model tests were run OGE. Therefore, the model was released at a lower than normal pressure during the AFFDL tests, while the model bounced at a higher than normal pressure during the Bell tests. Conducting tests at both conditions also enabled a more complete comparison to be made to the short trunk tests.

Equipment and Procedures (IGE and OGE)

The same equipment was used to conduct OGE and IGE tests. Two Statham differential pressure transducers were mounted in the model fuselage to measure trunk pressure and cushion pressure with a range of ±0.5 psi. Four Consolidated Electrodynamics Corporation accelerometers with ranges of ±5 g's were used to measure g-loads or accelerations at the nose, port nacelle, center of gravity, and along the longitudinal axis of the model. Although this report discusses only the data from the c.g. accelerometer, the data from the other accelerometers were recorded and can be used for angular acceleration determination in pitch and roll.

The signals received by the transducers and accelerometers were fed into a Bell and Howell Datatape, VR-3700B, recorder and signal conditioning unit from which the data were simultaneously sent to a magnetic tape and a Honeywell Visicorder. The raw data were received at the Honeywell Visicorder in the form of traces on photosensitive paper. From these traces the final data were reduced.

A detailed description and location of pressure transducers and receiving equipment is given in Appendix B. In addition to the above measuring equipment, two high-speed motion picture cameras (500 frames per second) were used to observe model reactions during a drop.

In order to simulate vertical velocity the model was treated much like an object released from a certain height and allowed to fall to the ground under the effects of gravity. Assuming no drag on the object, the distance through which it falls can be calculated from

$$d = v_t^2/2g_e \qquad (1)$$

Thus for a specific terminal velocity, the object must be raised to a specific height and released. It was also assumed and verified that drag on the model was negligible during a drop. Maximum drop height was 2.9 inches which simulated a full-scale velocity of 12.5 fps, or 4.0 fps in tenth-scale terms.

The model was supported above the platform as shown in the photograph in Fig. 7. Cables and pressure tubing to the model were suspended so as not to interfere with model reactions or weight during and after the drop. Drop height was measured from the lowest point on the inflated trunk to the platform by means of a wooden spacer bar as shown in the photograph in Fig. 8. As such, the model attained the desired sink rate as soon as the trunk touched the ground. Briefly, a test run consisted of adjusting trunk pressure to desired design condition, adjusting model attitude to desired pitch and roll, placing model at desired drop height, turning on recording equipment and movie cameras, and releasing model from its support.

Specific details on the test drop procedures and data reduction are explained in Appendix B.

General Results of All Drop Tests

A drop test involved some key events which can be defined as follows:

Release--the instant the model is released from its support, g-load = 0.0 g, time = 0.0 seconds.

Touch--the time when the trunk touches the platform as indicated by the first increase in trunk pressure from initial conditions.

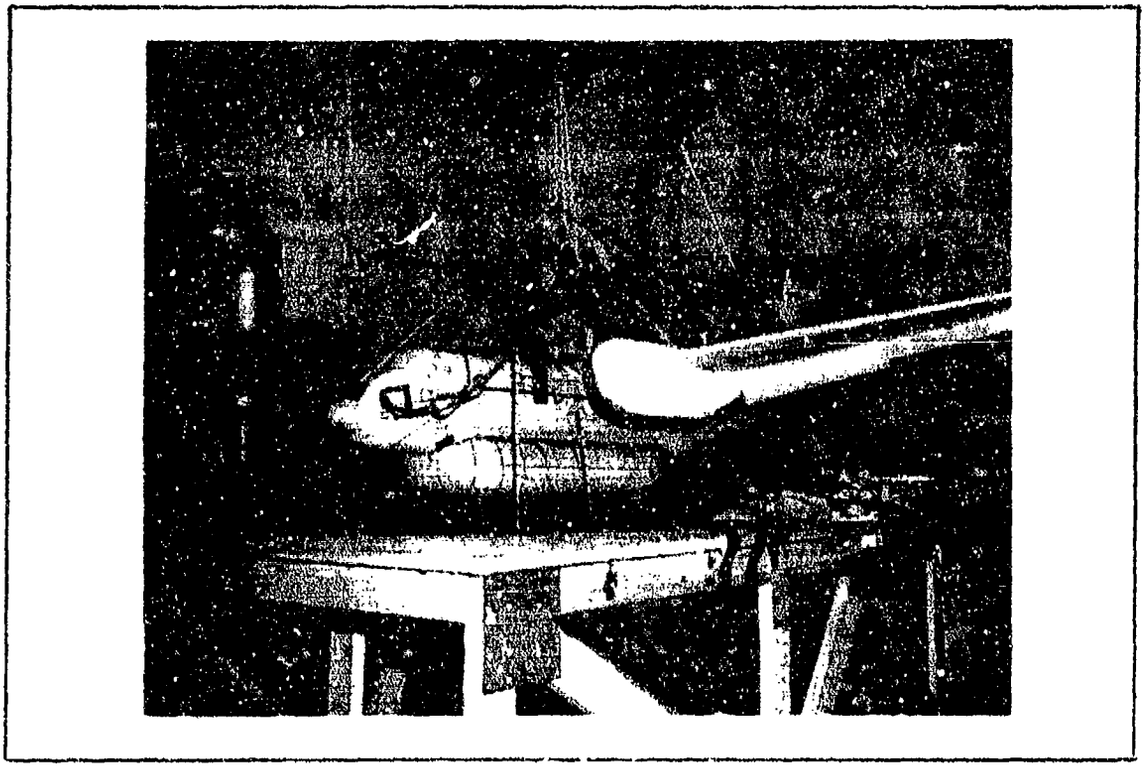

Fig. 7. Model Support for Drop Test

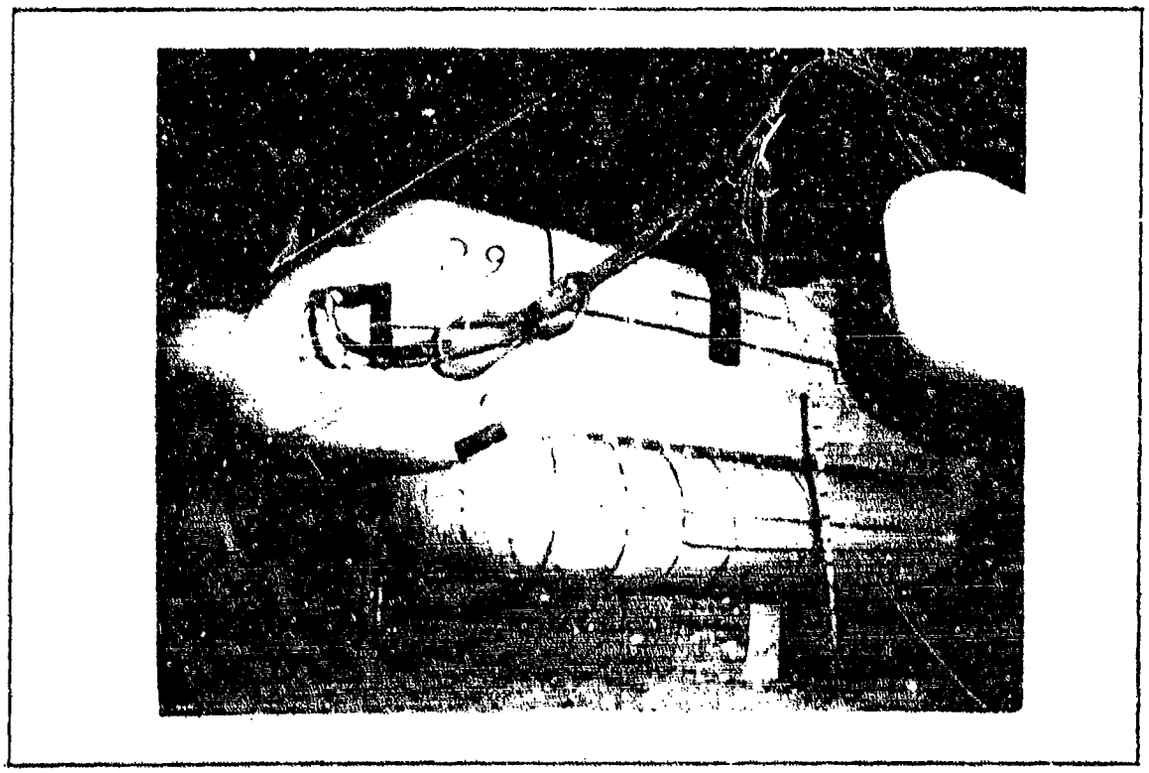

Fig. 8. Drop Height Measurement

Peak Pressures--the time of highest pressure in trunk and cushion due to the drop.

Peak Load--the time of highest accelerations or g-loads encountered during the drop.

Top of First Bounce--the midpoint of the time span when g-loads and cushion pressure approach or reach a zero value. After the model reaches peak pressure and g-load conditions, cushion and trunk pressure react to push the model away from the platform. The top of the first bounce is the peak of that upward travel.

Figure 9 is a plot of a typical drop test at a full-scale sink rate of 12.5 fps with -7.5 degrees initial roll angle. The key events are pointed out directly on the curve. Cushion pressure at release is always zero while trunk pressure starts out at a value depending on the initial design mode of OGE or IGE. The graph of Fig. 9 is for the IGE mode and trunk pressure begins at 25 psfg. OGE mode trunk pressure begins at 32 psfg. Touch times vary from 0.030 seconds to 0.130 seconds depending on the desired sink rate. Since Fig. 9 is that of a 12.5 fps drop, touch occurred at approximately 0.13 seconds. At touch, trunk pressure is still at its initial value; but cushion pressure has begun to increase since the model is approaching the floor of the platform and beginning to enclose the cushion air beneath the fuselage. Loads are still at a zero level since no appreciable forces are yet felt by the model. Peak trunk pressures generally occurred 0.160 to 0.210 seconds after release, reaching levels from 43 to 62 psfg depending on attitude, sink rate, and OGE or IGE design mode. If the model hard structure did

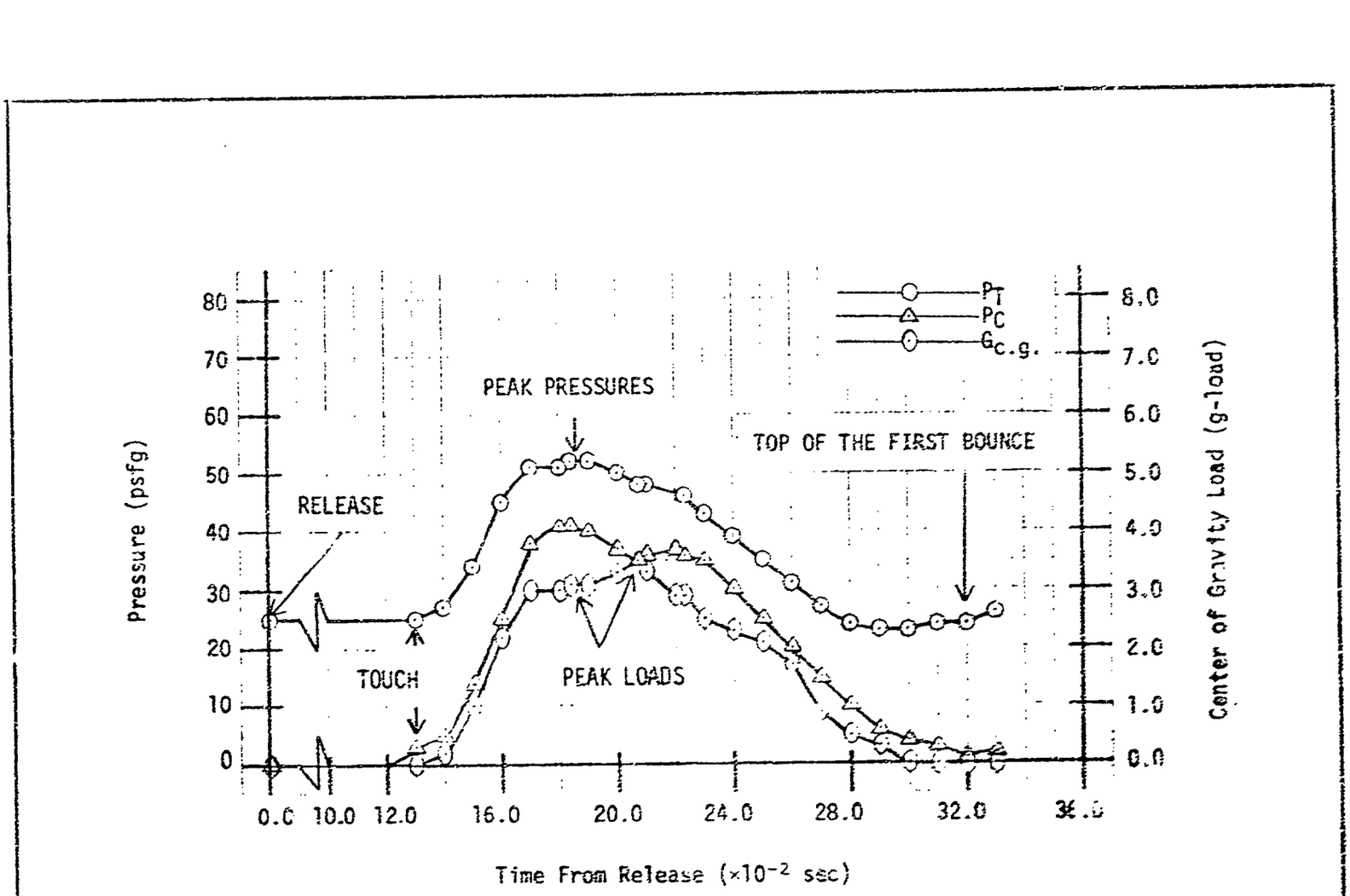

Fig. 9. Typical Drop Test, 12.5 fps, θ = 0.0, ϕ = -7.5, IEE

not make contact with the platform, peak cushion and trunk pressures occurred at approximately the same time (±0.005 seconds). Hard structure contact forced peak cushion pressure to occur as much as 0.07 seconds after peak trunk pressure. Peak cushion pressures reached values from 32 to 49 psfg depending on attitude, sink rate, and OGE or IGE design mode.

Peak loads occurred at approximately the same instant or slightly after peak pressures (±0.002 seconds), since they are a result of pressure reactions. Peak loads varied from 2.2 to 4.3 g-loads for tests without an initial 12 degrees of pitch, depending on the other initial conditions. A pitch angle of 12 degrees caused hard structure contact and resulted in g-loads from 2.7 to 5.1 g depending on sink rate. In the 12-degree pitch cases g-loads peaked immediately after peak trunk pressure occurred.

The top of the first bounce generally occurred from 0.300 to 0.350 seconds after release depending on initial conditions. At this point, the trunk pressure sought a pressure level near its initial value at release, and it usually came within ±2 psf of that initial value. Cushion pressure approached a level from 0 to 2 psfg. Both cushion and trunk pressures sought their initial values since the model is out of ground effect at the top of the first bounce, as it was at release. The most important reactions and greatest changes in pressure and g-load occur during this period up to the first bounce.

An important observation concerning all but the initial 12-degree pitch drop tests can be made by a simple calculation of cushion pressure times cushion area at peak g-loading. The g-loading of the aircraft is

a measure of its effective weight at the center of gravity at any instant. If the cushion absorbs all the load due to impact, then the value of g-loading times the weight of the aircraft would equal cushion pressure times the area of the cushion. The results of these tests revealed that the g-loading, or effective weight of the model on the ACLS, equals a resultant force 10 to 20 pounds of force above $P_C \times A_C$. This result indicates that the cushion is absorbing almost all the impact load, resulting in a minimal amount of trunk flattening. It is the desire of the ACLS system that the cushion absorb as much of the load as possible. This result was not true for the 12-degree pitch tests with and without roll, since the model hard structure made contact with the floor of the platform at the time of peak g-load. In this case cushion pressure was much below trunk pressure at the time of contact, forcing the trunk and hard structure to absorb the impact load. Thus, test results indicate 12-degree pitch attitudes are prohibitive to a landing on the CC-115 with ACLS.

High-speed movies of the drop tests revealed some interesting model reactions due to initial attitude settings at all sink rates. Even though the model was dropped at an initial attitude of no roll or pitch, the model would pitch slightly aft, or positive, as it came close to the floor of the platform. The pitching is due to the fact that the center of gravity of the model is 2.2 inches aft of the center of pressure of the ACLS. As such, the model would land on the rear portion of the trunk first and then pitch slightly forward. When the model was placed in an initial -7.5 degree roll attitude and no pitch, it would remain in that rolled attitude until all bounces dampened out. At that

point the model would roll out of its initial -7.5 degree roll to a level attitude. This roll effect was also observed in the AFFDL quarter-scale tests (Ref 3:36). There was less bouncing after the first bounce in the rolled condition than with no roll.

With an initial 6 degrees of pitch and no roll, the movies showed the model would remain at the 6-degree pitch attitude until touch. At touch the model would pitch forward as much as 6 degrees depending on sink rate. When -7.5 degrees of roll was added to the initial conditions, the model would remain at the initial roll and pitch attitude until touch. After touch, the model pitched forward as with pure pitch but remained at the -7.5 degree roll attitude until most of the bouncing of the model dampened out; and then the model rolled to a level attitude.

An initial 12 degrees of pitch with and without roll caused the rear of the model's hard structure to make contact with the platform at all sink rates whether OGE or IGE design mode.

Results of IGE (In Ground Effect) Drop Tests

The IGE drop tests were conducted with an initial trunk pressure of approximately 34 psfg and an IGE hover cushion pressure of approximately 16 psfg. Drop tests in the IGE condition were conducted at the following full-scale sink speeds and attitudes:

Full Scale Speed (fps)	Model Speed (fps)	Pitch/Roll (Degrees)
12.5	4.0	0/0, 0/-7.5, 6/0, 6/-7.5, 12/0, 12/-7.5
11.0	3.5	0/0, 0/-7.5, 6/0, 6/-7.5, 12/0, 12/-7.5
8.0	2.5	0/0, 0/-7.5, 6/0, 6/-7.5, 12/0, 12/-7.5
5.0	1.6	0/0, 12/0
3.0	1.0	0/0, 12/0

These values were chosen to cover the full range of possible landing speeds and attitudes of the CC-115 aircraft during a landing.

Effects of Sink Rate on Peak Pressures and Loads at the Center of Gravity. Graphs on Figures 10 to 15 show the effects of full-scale sink rate on peak trunk and cushion pressures and peak loads at the center of gravity for each initial attitude. The graphs demonstrate a trend that a decrease in sink rate or vertical velocity will cause a decrease in the peak, or highest values, of pressures and loads which occur during the first bounce of the aircraft upon landing. The decrease is as one would intuitively expect, since forces on the structure would be lower at lower sink rates. The rate of decrease is affected by the initial attitude of the model during the drop. In the case of the 0.0 degree roll and 12.0 degree pitch drop, peak trunk and cushion pressures were not noticeably affected by decreases in vertical velocity below 11.0 fps (see Fig. 14). In all other attitudes the decrease was significant. Depending on the initial attitude and sink rate from 3.0 to 12.5 fps, trunk pressure varied from 43 to 62 psfg; cushion pressure varied from 32 to 49 psfg; and g-loads varied from 2.2 to 4.2 g-loading, excluding hard structure contact where g-loading reached 5.1 g at 12.5 fps.

The quarter-scale tests conducted by AFFDL were run at the same conditions but with the model center of gravity directly over the ACLS center of pressure. The results of those tests showed that decreasing sink rate did not cause peak loads to decrease when the model was released with no roll or pitch. All other attitudes of the AFFDL tests showed that decrease in peak conditions was due to decrease in sink rate (Ref 3:32). The probable reason for the different results obtained with the two models lies in the location of the model center of gravity.

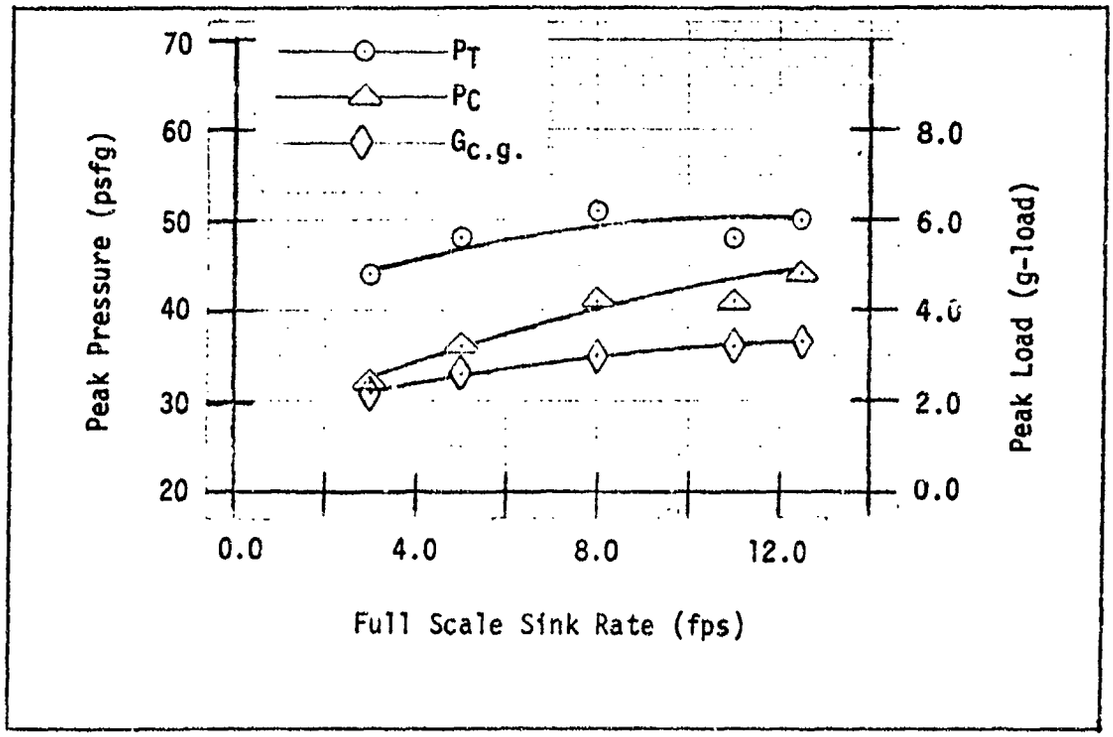

Fig. 10. Effects of Sink Rate on Peak Conditions, θ = 0.0, ϕ = 0.0

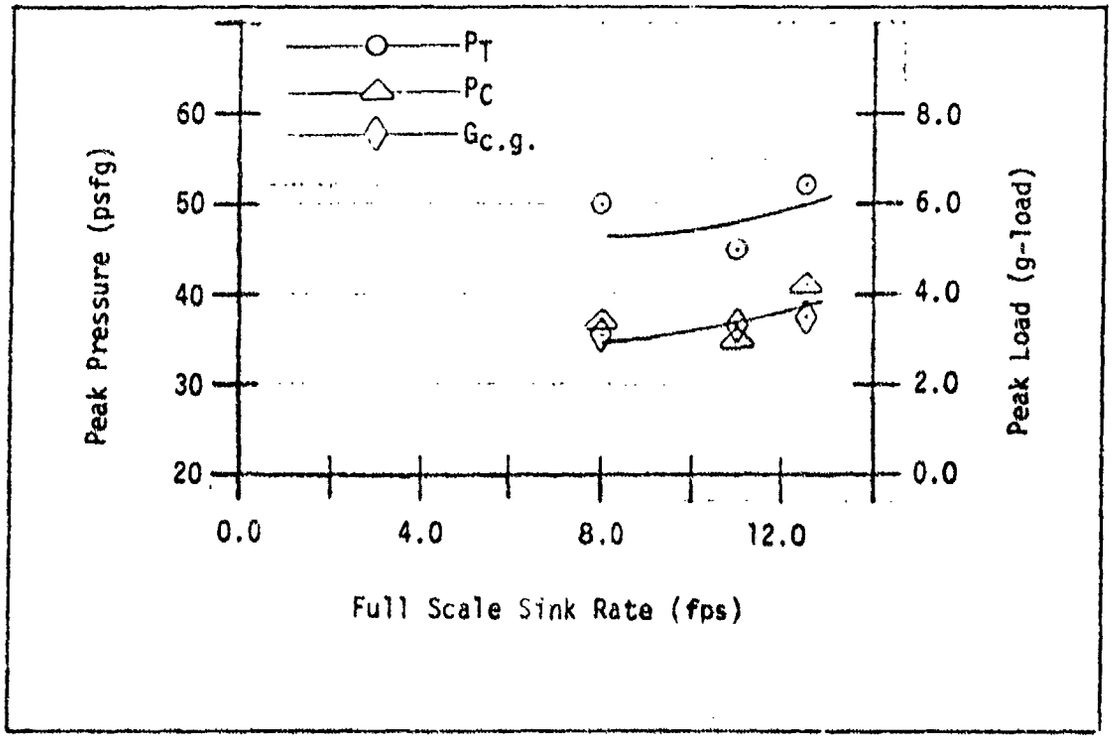

Fig. 11. Effects of Sink Rate on Peak Conditions, θ = 0.0, ϕ = -7.5

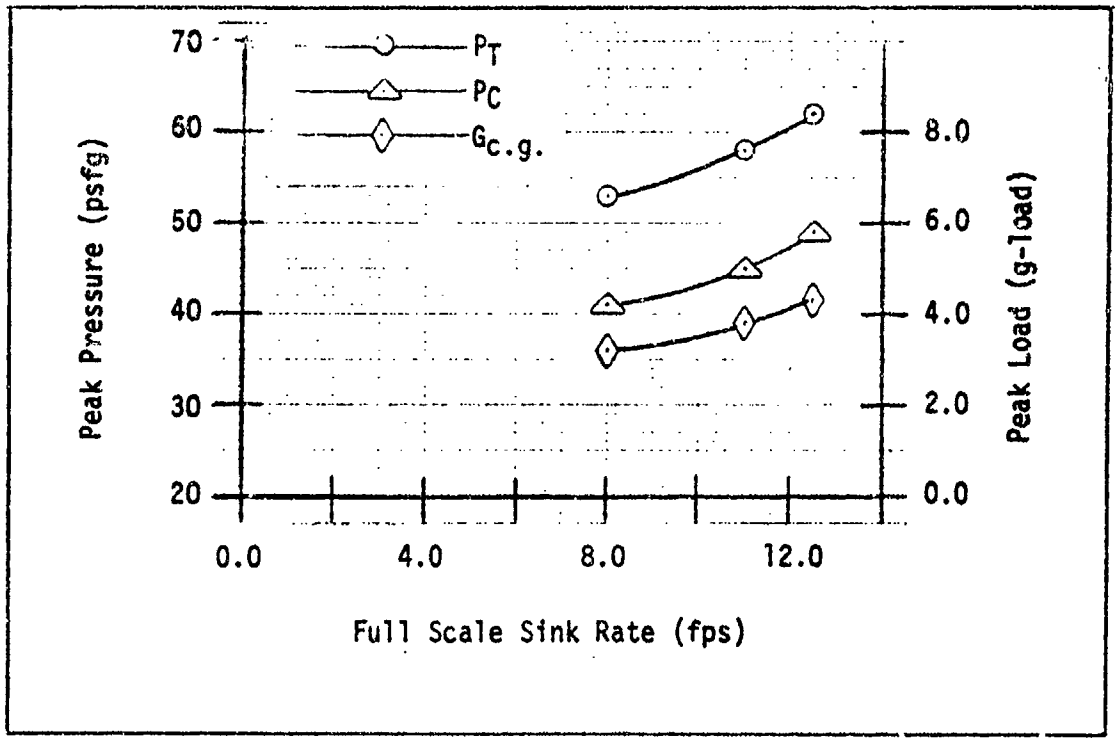

Fig. 12. Effects of Sink Rate on Peak Conditions, θ = 6.0, ϕ = 0.0

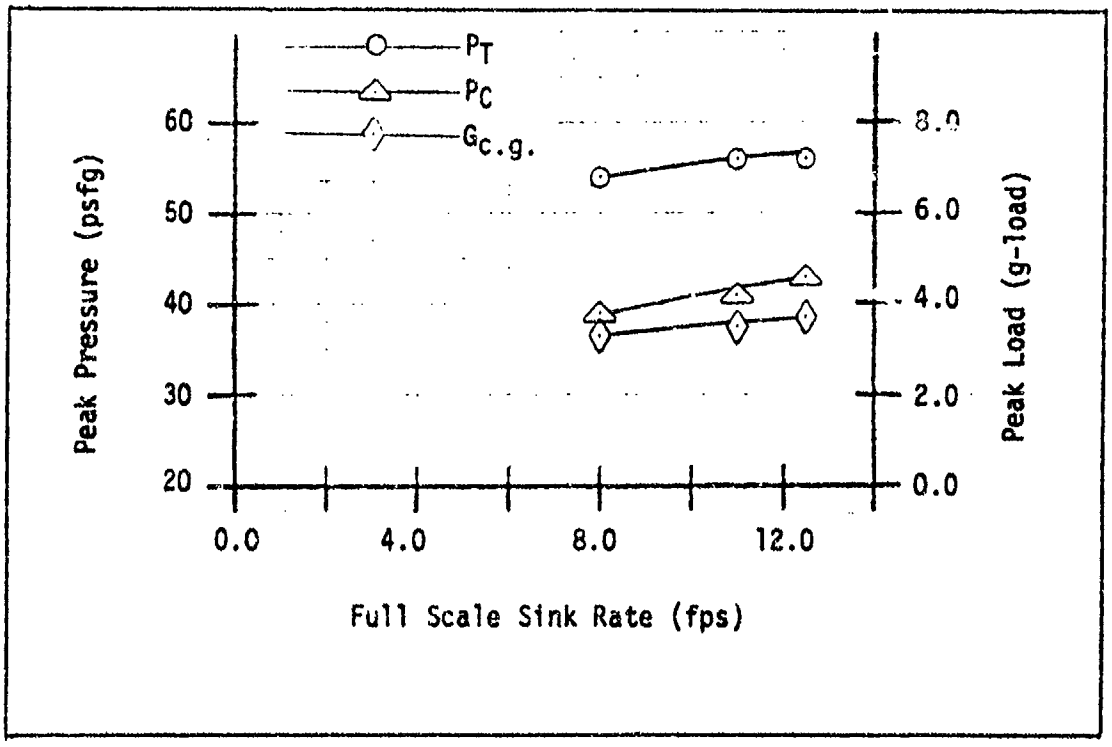

Fig. 13. Effects of Sink Rate on Peak Conditions, θ = 6.0, ϕ = -7.5

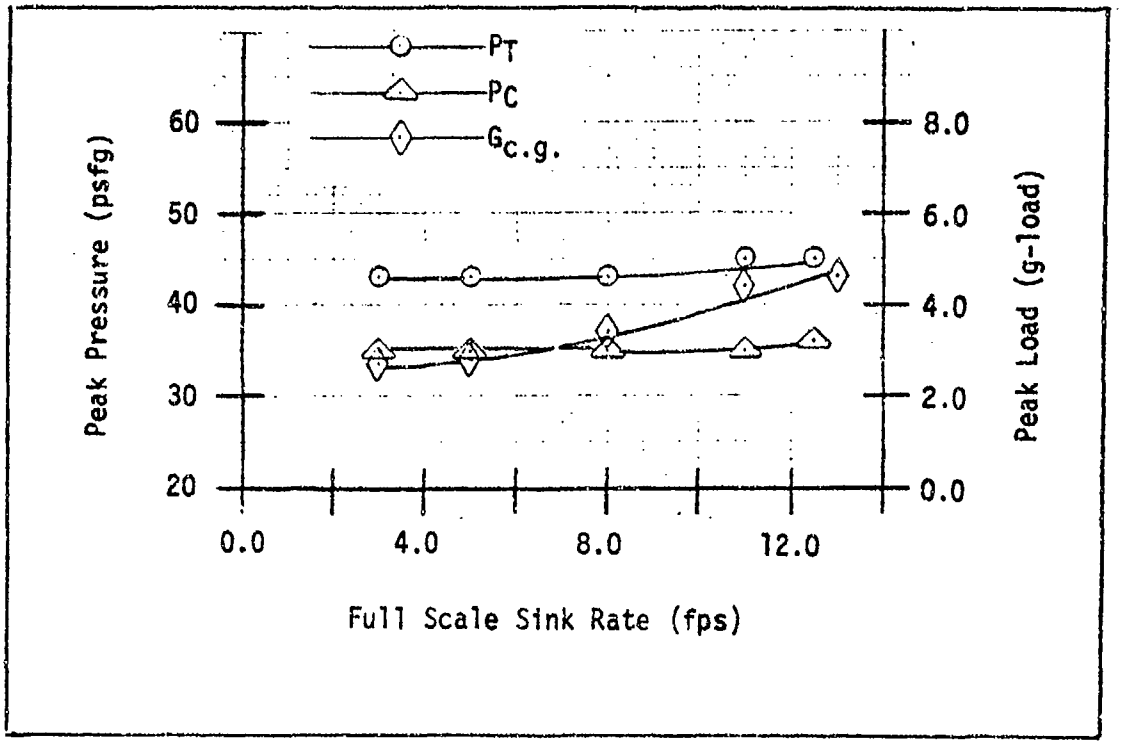

Fig. 14. Effects of Sink Rate on Peak Conditions, $\theta = 12.0$, $\phi = 0.0$

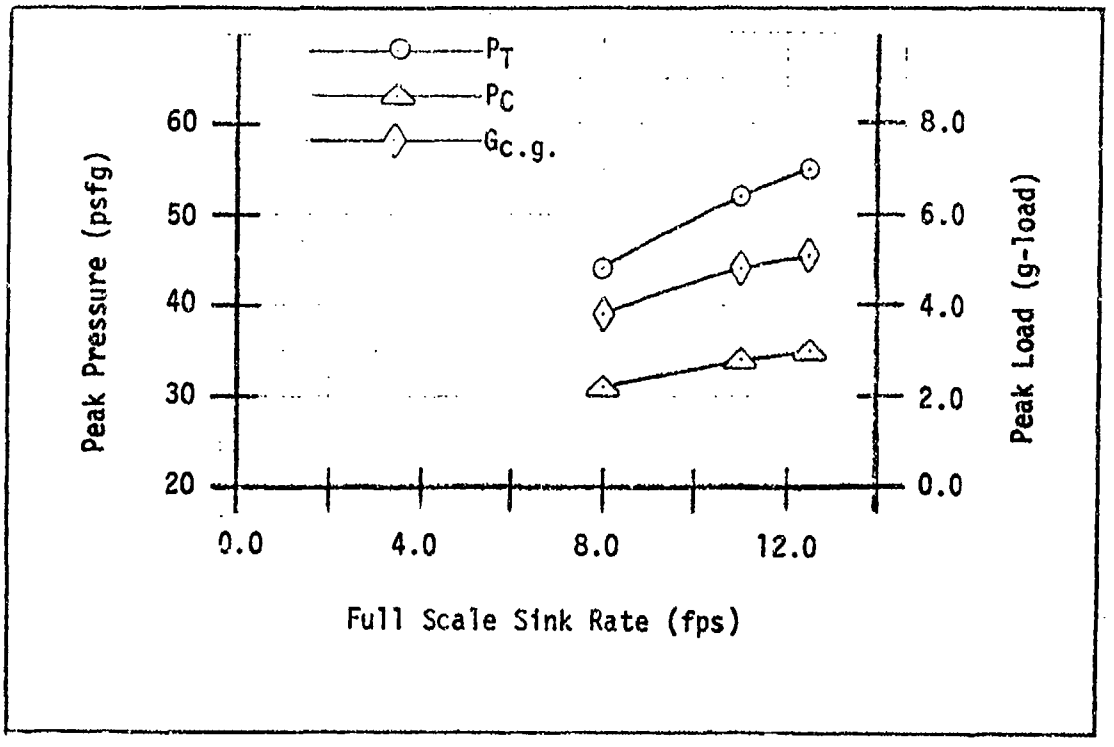

Fig. 15. Effects of Sink Rate on Peak Conditions, $\theta = 12.0$, $\phi = -7.5$

With the center of gravity over the center of pressure, as in the quarter-scale model, the weight and pressure loads occur directly on the center of the ACLS trunk and cushion during a level drop; and, therefore, this positioning results in an evenly distributed load over the ACLS for all sink rates.

Sink rate did not affect the test results in any other manner than indicated above. Therefore, only the 12.5 fps vertical velocity drops will be discussed. These drops covered the full range of desired attitudes and show the worst possible conditions for a landing. Pressure and g-load values at key events for the IGE tests at 11.0, 8.0, 5.0, and 3.0 fps are found in Appendix C.

Effects of Attitude on Trunk and Cushion Pressures. Figure 16 shows the effects of initial attitude on the response of trunk pressure. The increase in pitch angle from 0.0 degrees to 6.0 degrees increased the peak pressure 11 psf and delayed it about 0.04 seconds. Increasing the pitch to 12 degrees caused the model hard structure to hit the platform. This hit may account for the decrease in pressure and a more level pressure distribution over time than at 0.0 degrees and 6.0 degrees pitch. The model hard structure has probably absorbed a portion of the load that the trunk and cushion would have normally supported, and this fact caused decreased trunk pressure.

Roll does not appear to alter the basic shape of the trunk pressure-time curve except to increase the time for the peak condition to occur by about 0.03 seconds. Pressures peak at approximately the same level for both the 0.0 and -7.5 degree roll cases.

When roll is placed in combination with pitch, the responses of trunk pressure match very closely to those in which the model was pitched

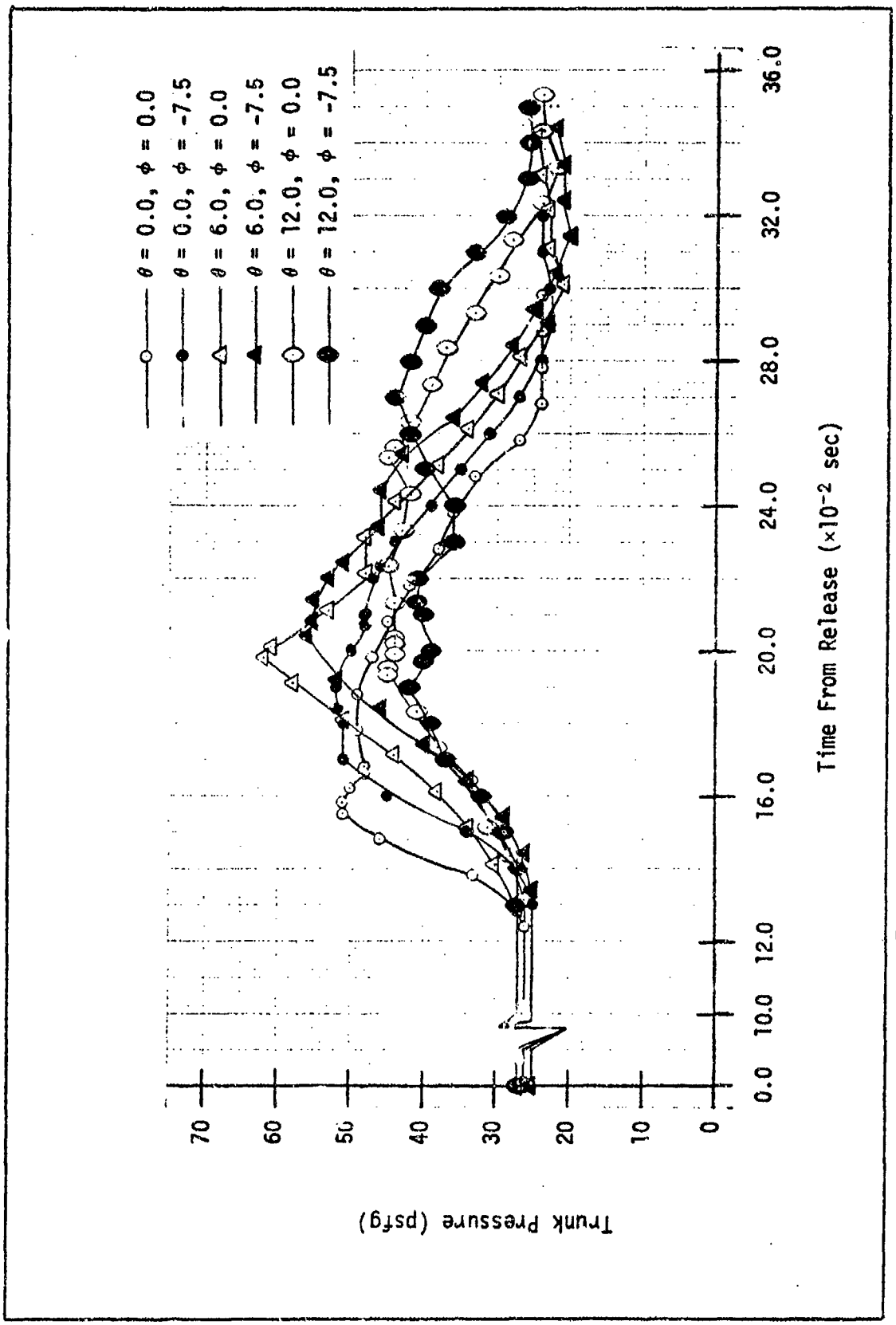

Fig. 16. Effects of Attitude on Trunk Pressure

but not rolled. The model hard structure also hit when the model landed at -7.5 degrees roll, 12.0 degrees pitch. The addition of roll to pitch seems to slightly decrease the trunk pressure by about 7 psf.

Figure 17 shows the effects of initial attitude on cushion pressure. Cushion pressure seems to react in the same manner as did trunk pressure between 0.0 and 6.0 degrees pitch. Cushion pressure at 6.0 degrees pitch was 5 psf higher at peak conditions than at 0.0 degrees pitch, and the peak at 6.0 degrees was of shorter duration. Cushion pressure at 12.0 degrees pitch showed two leveling periods on the approach to peak conditions. The leveling is due to hard structure contact with the platform. Due to the hard structure contact with the platform, peak cushion pressures at the 12.0 degree drops occurred as much as 0.09 seconds later than other attitudes tested. The area under the curves of Fig. 17 is a measure of the reaction force exerted on the fuselage during the drop. The area under the 12.0 degree pitch curves is considerably less than under the other two curves; and this indicates that the cushion did not absorb as much of the load as it would have if the model hard structure had not made contact with the platform. This, of course, is an undesirable condition. Load should be absorbed by the cushion.

As with the trunk pressure, roll does not alter the basic shape of cushion pressure-time curve. Peak pressures are 3 psf less than with no roll, and peak event time is delayed by about 0.02 seconds.

Combining roll and pitch makes the cushion pressure curves follow the same trend as for pure pitch with delayed event times and decreased pressures probably due to the roll angle.

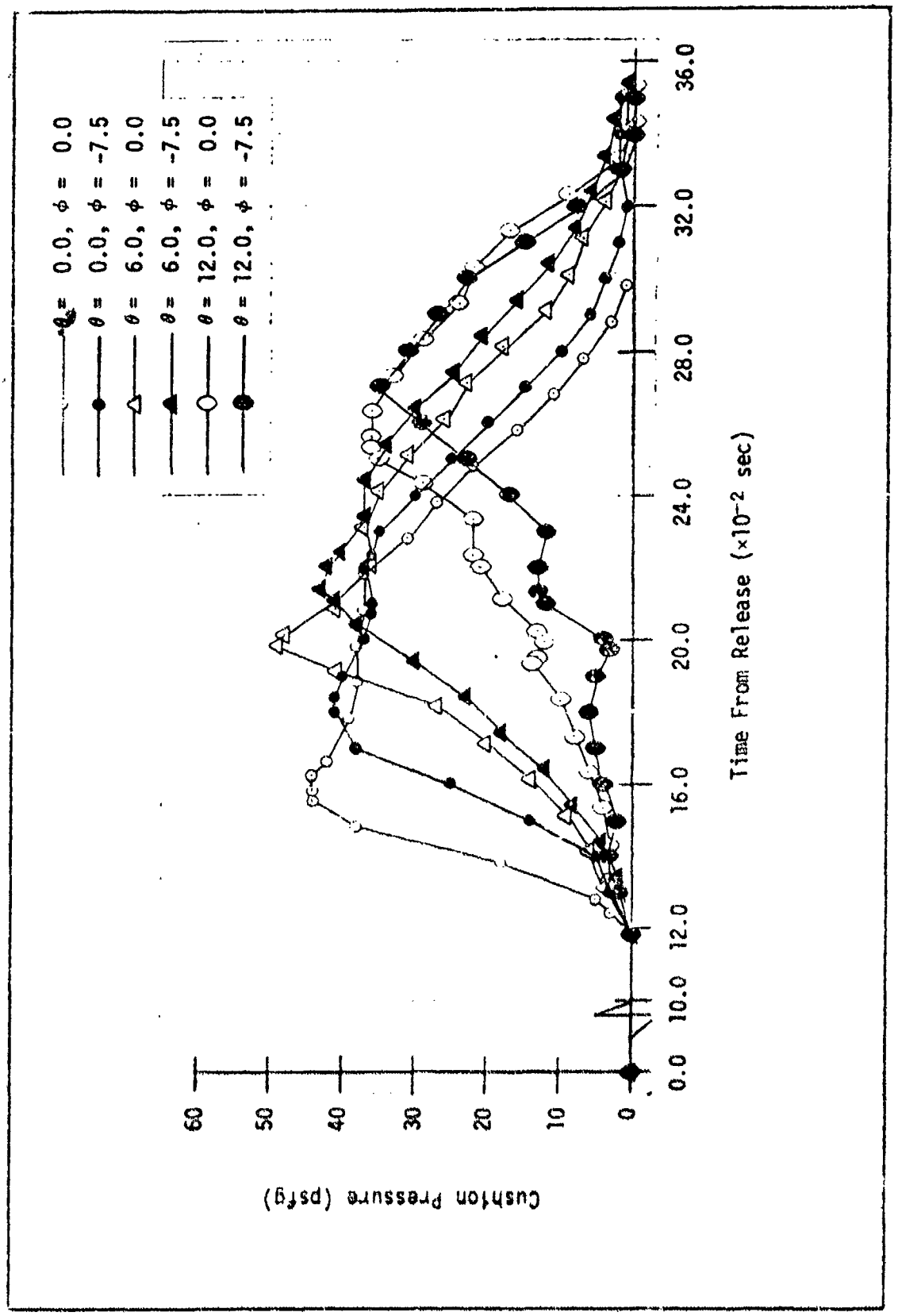

Fig. 17. Effects of Attitude on Cushion Pressure

Combined Dynamic Responses of Trunk Pressure, Cushion Pressure, and Center-of-Gravity Loads. Figures 18 to 23 show the dynamic responses of trunk pressure, cushion pressure, and center of gravity g-loads of the model for each attitude tested at the 12.5 fps full-scale sink rate. Drop tests conducted at lower sink rates provided the same basic shape of curve at each attitude as those discussed here, except that the curves rose to lower values of pressure and g-loads due to decreased sink rates. The graphs presented in this section depict responses during the time for the model to reach the top of the first bounce. Beyond that point, no significant variations in the responses were observed; and it is assumed that pilot control could change the responses of the system. Thus those events are not reported here.

Figures 18 and 19 show responses for a level drop and a -7.5 degree roll drop, respectively. Figure 18 also contains points from a similar AFFDL quarter-scale model test with the short trunk. Comparison of Fig. 18 and Fig. 19 again shows that roll has a minimal effect on the dynamic responses of the system. The pressures did not cause excessively high g-loads keeping the forces due to impact to a reasonable level. The leveling of pressure after peak conditions may be due to a resurge of power to the fans after the force of initial impact. When load on the fans is relieved after peak conditions, the fans could rotate faster, providing more air to the system and thus more pressure.

Figure 18 also contains points from AFFDL quarter-scale tests at the same initial conditions. Note that peak trunk pressure was 29 psf higher, peak cushion pressure 14 psf higher, and peak g-load about 1 g-load higher than the tenth-scale tests with a longer trunk. Peak pressure conditions also occurred about 0.03 seconds sooner on the

quarter-scale tests as compared to the tenth-scale tests. Quarter-scale results show a quicker decrease in pressure after peak conditions. This fact is attributable to fan stall which occurred on the quarter-scale tests (Ref 3:30). This fan stall was not present in the tenth-scale tests covered in this report; and thus the fans of the two models show different flow characteristics. The quarter-scale model tested by AFFDL used two axial flow fans, while tenth-scale tests used two centrifugal fans. Peak loads on the AFFDL quarter-scale tests occurred 0.100 seconds after peak pressures, while peak loads on tenth-scale tests occurred approximately at the same time as peak pressures.

Figures 20 and 21 show responses at 0.0 degrees roll and 6.0 degrees pitch and -7.5 degrees roll and 6.0 degrees pitch, respectively. No quarter-scale comparisons were available for these tests. Note the effects of pitch creating sharp peaks in cushion and trunk pressure as well as center-of-gravity g-load. Again note pressure leveling after peak conditions probably due to an increase in fan rotation after peak conditions.

Figures 22 and 23 show responses at 0.0 degrees roll and 12.0 degrees pitch, and -7.5 degrees roll and 12 degrees pitch, respectively. The aft portion of the model hard structure next to the rear trunk attachment hit the platform in both cases as is shown by the high value of g-loads (4.6 and 5.1 g-load) at the center of gravity and the erratic behavior of g-loads after the first peak trunk pressure. The hard structure contact has probably sent vibrations through the fuselage to the accelerometer causing this erratic behavior after peak g-load. Unlike previous tests discussed, both 12.0 degree pitch cases showed peak cushion pressure occurring about 0.07 seconds after peak trunk pressure. This

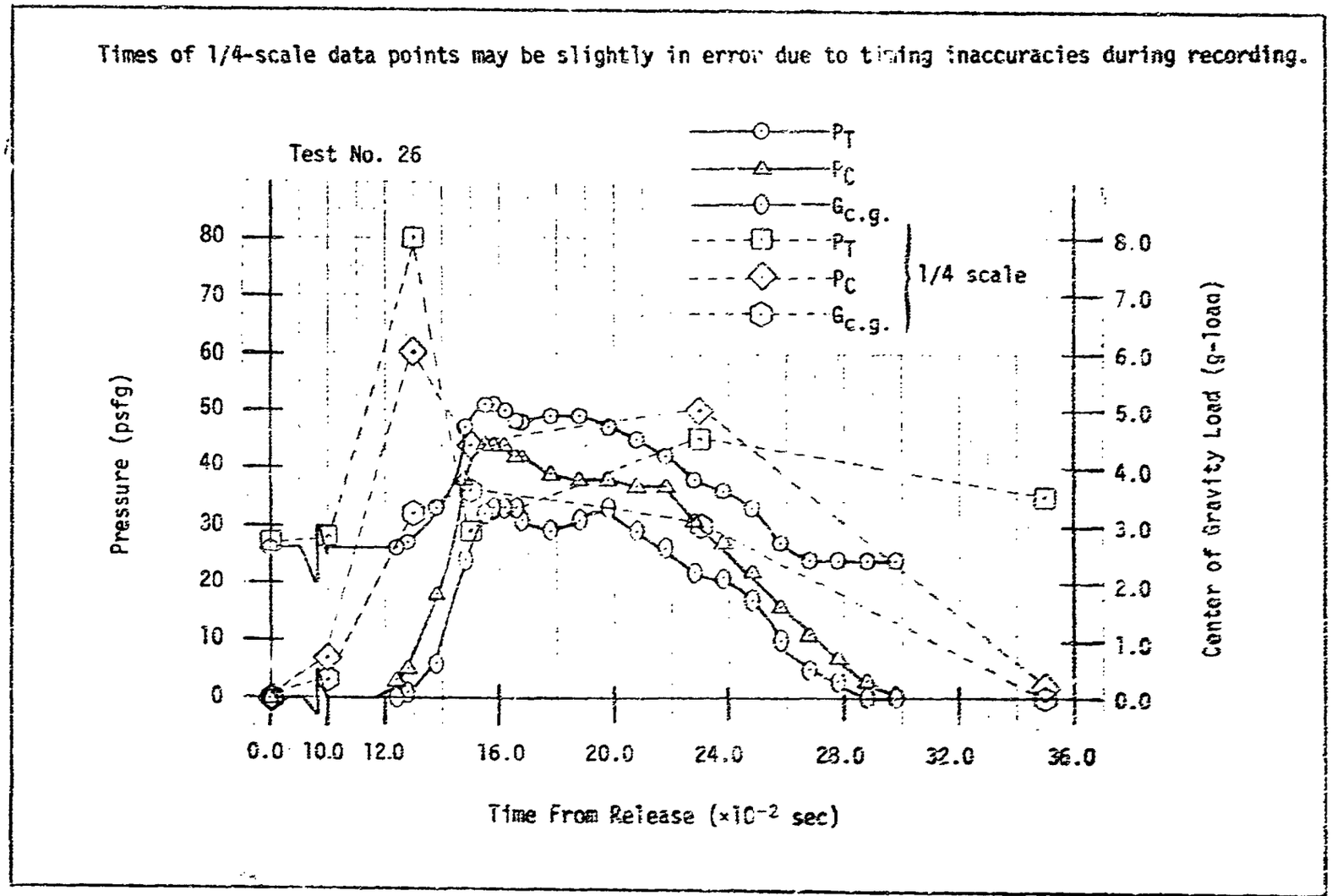

Fig. 18. IGE Dynamic Responses of ACLS, $\theta = 0.0$, $\phi = 0.0$

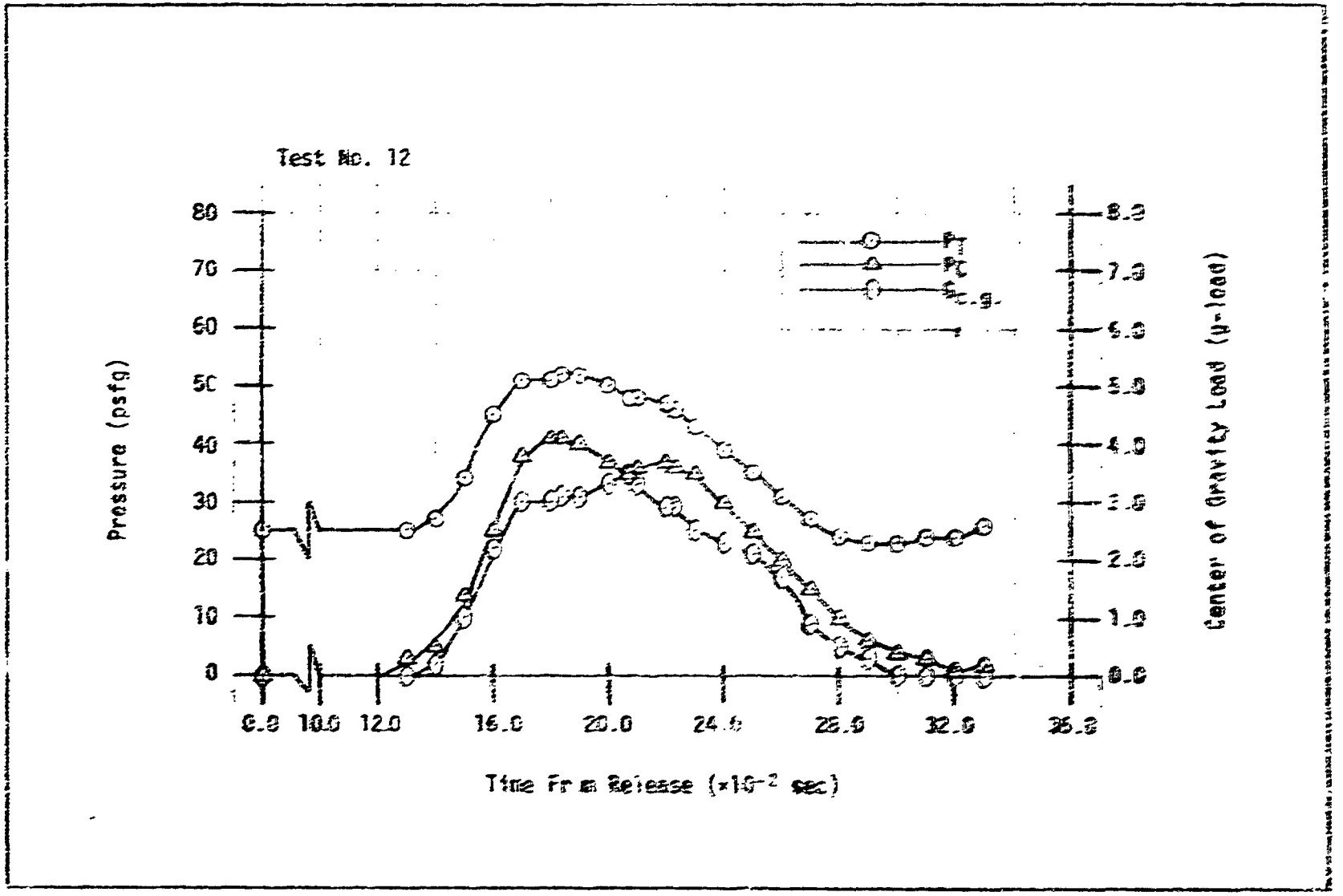

Fig. 19. LEE Dynamic Responses of AOLS, $\theta = 0.0$, $\phi = -7.5$

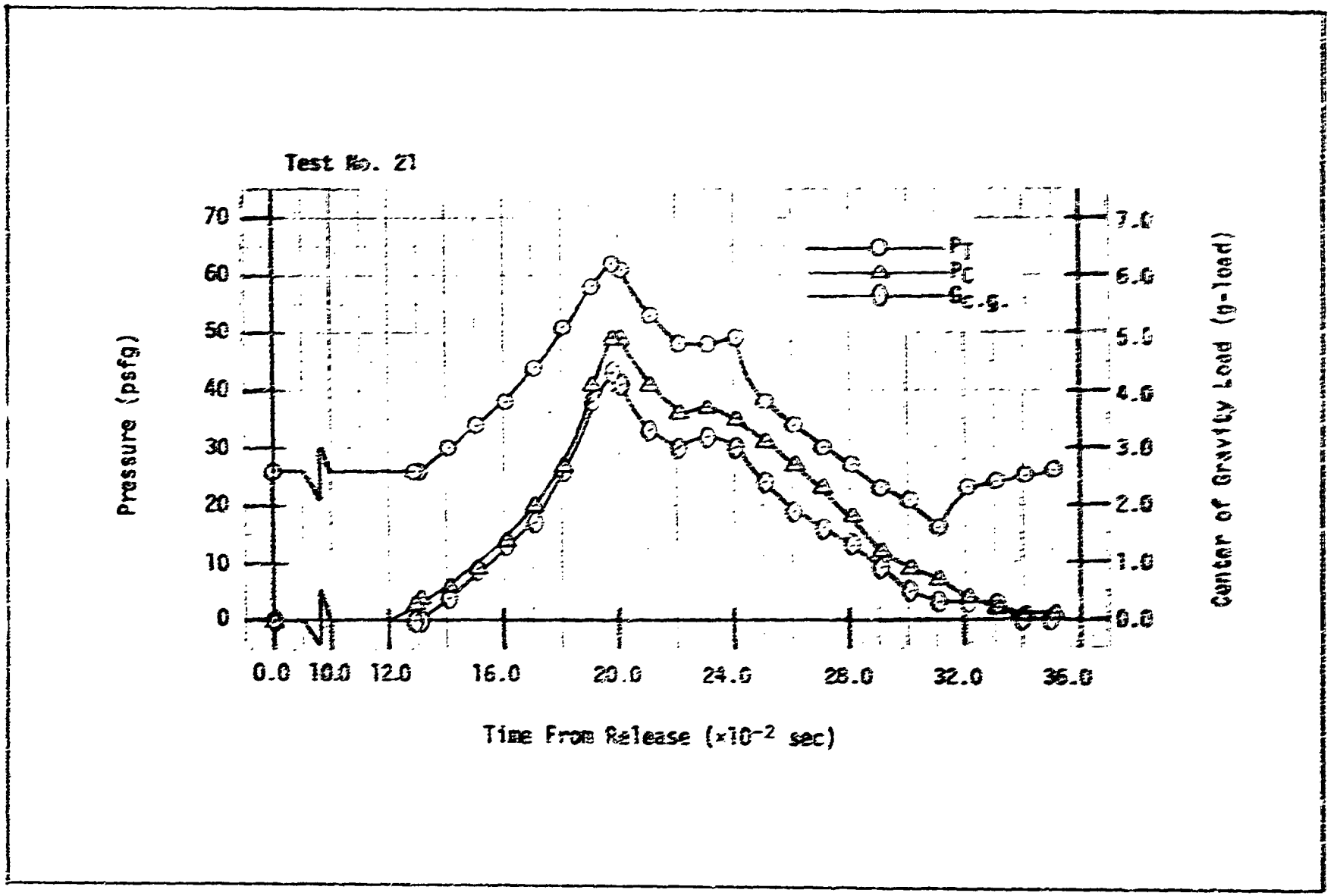

Fig. 20. IGE Dynamic Responses of ACLS, θ = 6.0, ϕ = 0.0

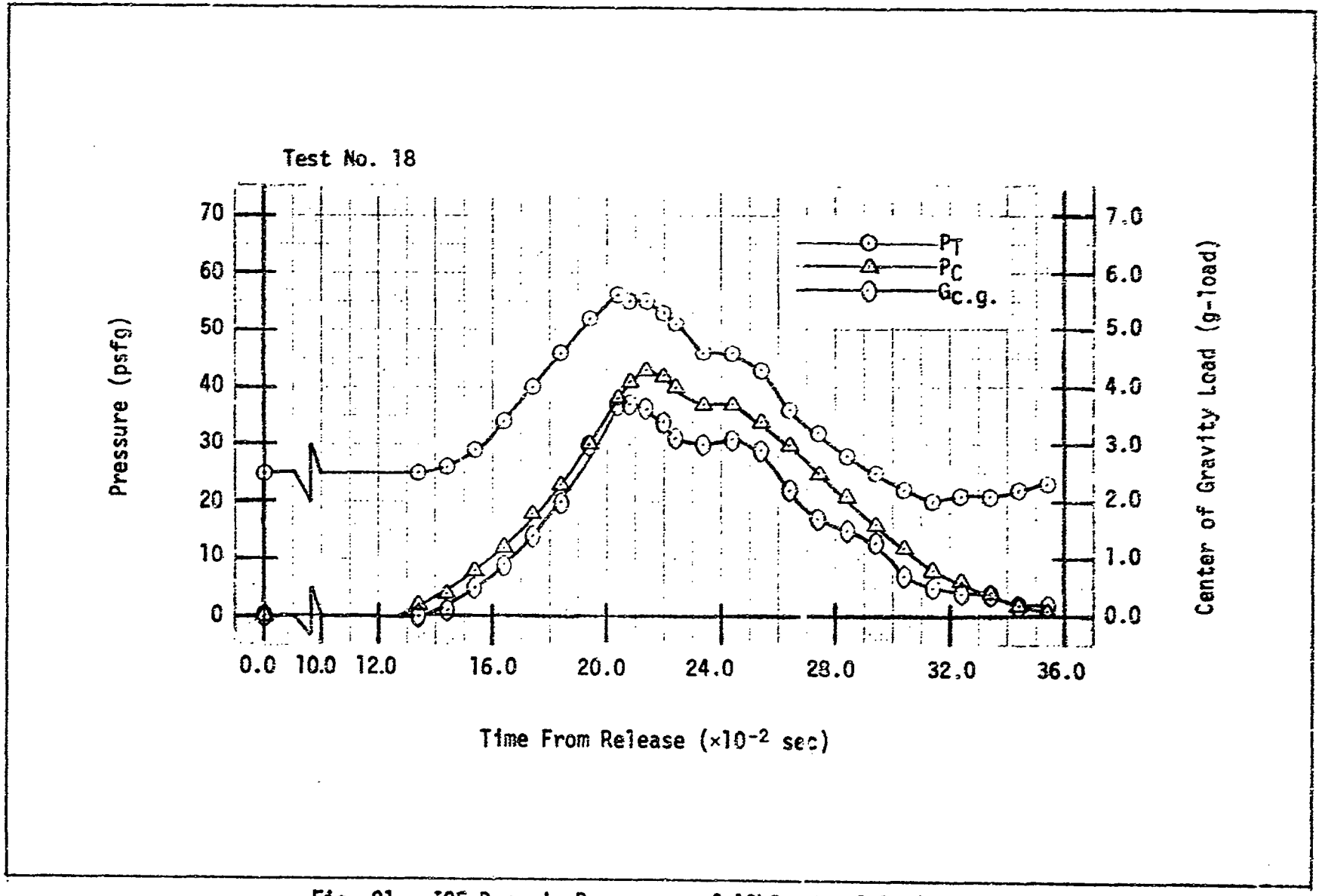

Fig. 21. IGE Dynamic Responses of ACLS, $\theta = 6.0$, $\phi = -7.5$

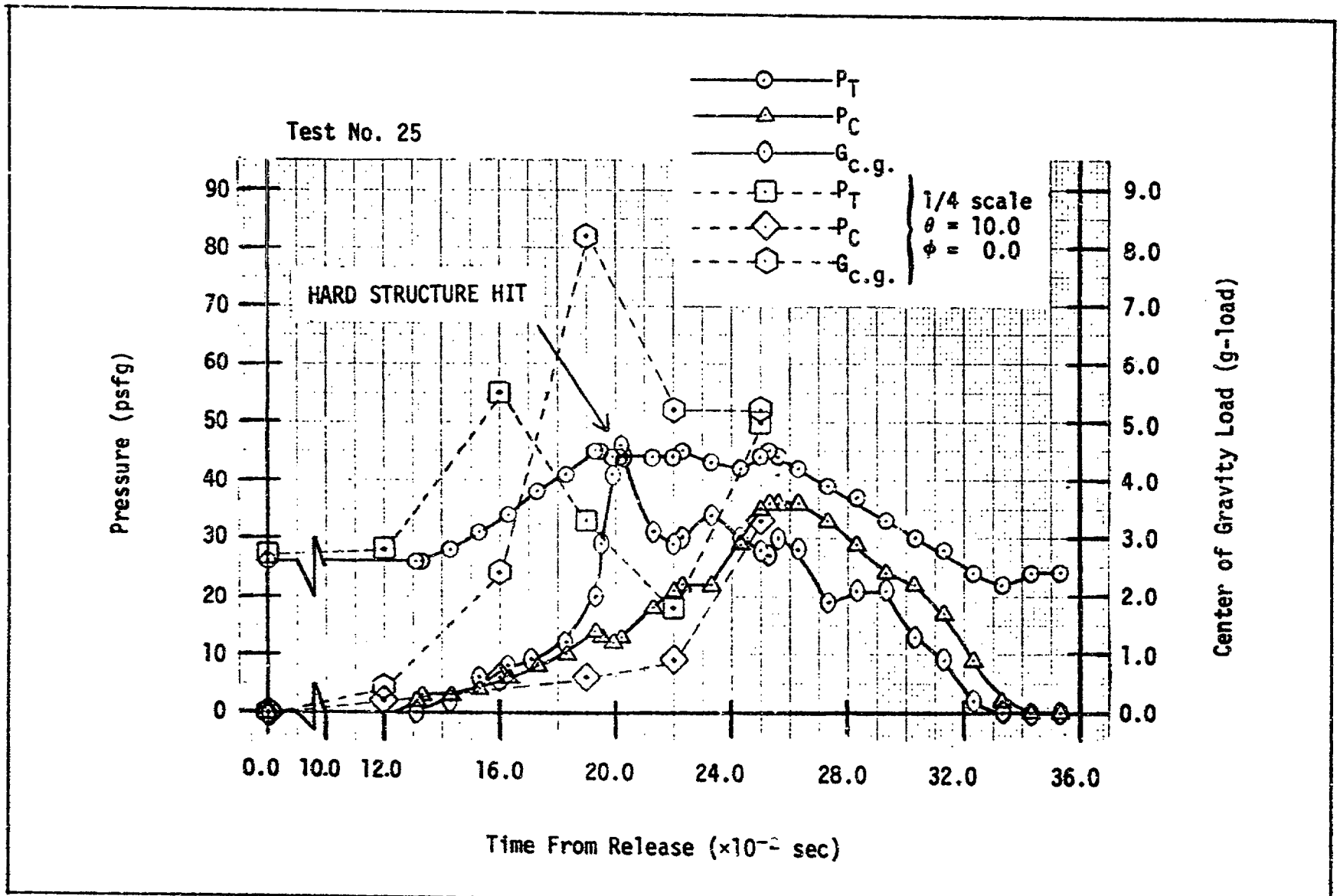

Fig. 22. IGE Dynamic Responses of ACLS, θ = 12.0, ϕ = 0.0

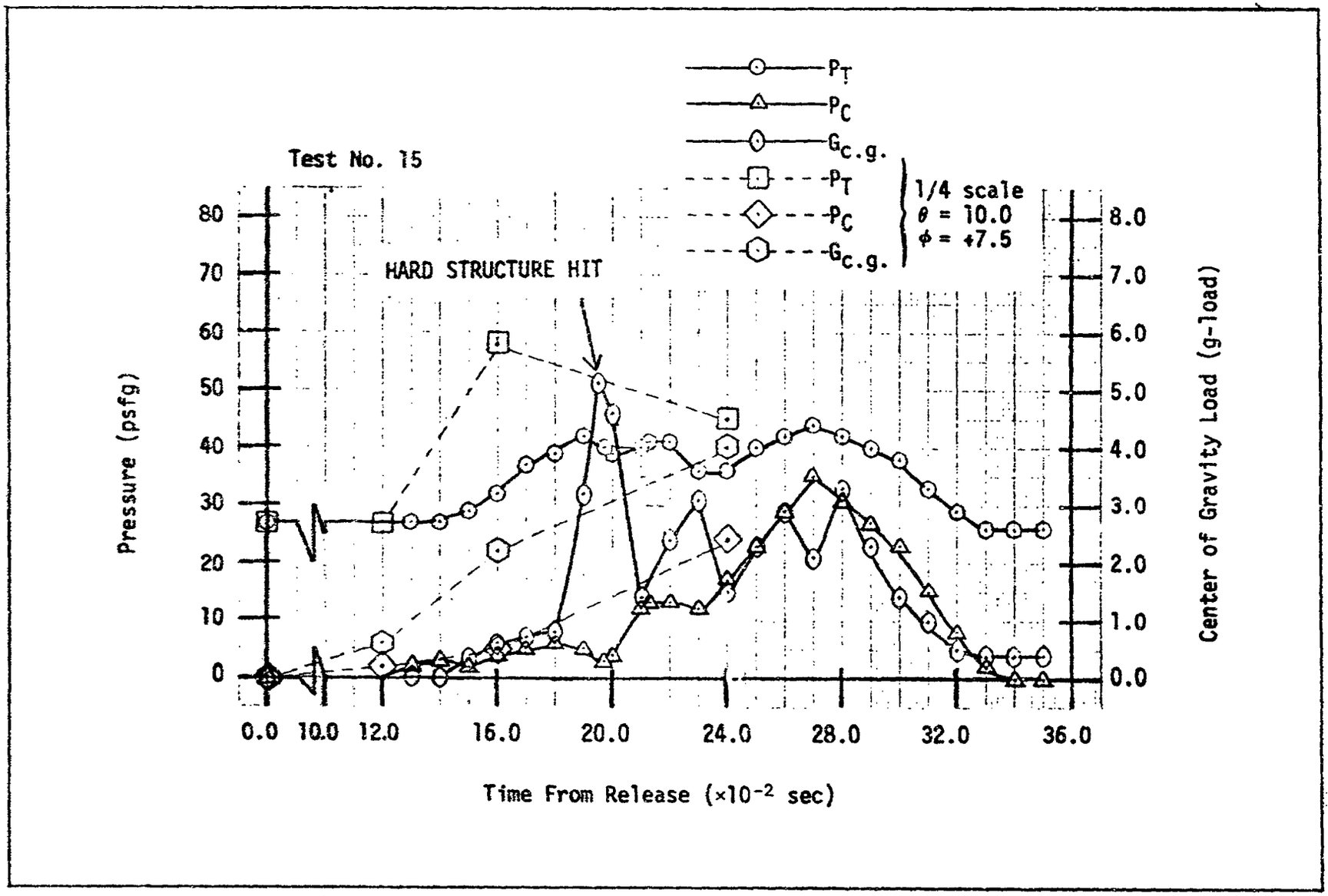

Fig. 23. IGE Dynamic Responses of ACLS, θ = 12.0, ϕ = -7.5

delay is probably attributable to the fact that at 12.0 degrees of pitch there is not enough of the cushion air entrapped to absorb the initial impact. After the initial impact, the model pitches forward entrapping more air in the cushion and causing a late cushion pressure peak. Quarter-scale results are plotted for a 10.0 degree pitch attitude in both graphs instead of 12.0, which was not performed on AFFDL quarter-scale tests. Quarter-scale points appear to show the similar trend for late cushion pressure peak as on tenth-scale, since the quarter-scale model also hit hard structure. Initial peak trunk pressures were 10 to 16 psf higher on quarter-scale short trunk results compared to the longer trunk of tenth-scale tests.

Results of OGE (Out of Ground Effect) Drop Tests

The OGE Design condition drop tests were conducted by using a trunk pressure equal to 32 psfg. When placed in ground effect the trunk pressure rose to 39 psfg and the cushion pressure to 16 psfg. Thus the OGE design point essentially placed the trunk pressure at a higher initial value, as the trunk comes near to the platform, than the IGE tests already discussed.

Since the results of the IGE tests indicated that sink rate only affected peak values, it was decided to conduct OGE tests only at two full-scale sink rates of 12.5 fps and 8.0 fps. Attitudes of the model for both sink rates were as follows:

Pitch (degrees)	Roll (degrees)
0.0	0.0
0.0	-7.5
6.0	0.0
6.0	-7.5
12.0	0.0
12.0	-7.5

The effects of sink rate on peak conditions and the effects of attitude on trunk and cushion pressures were the same as for the IGE tests. The model hard structure again made contact with the platform when the pitch angle was 12 degrees with and without roll.

The dynamic responses of trunk pressure, cushion pressure, and center-of-gravity g-load correspond very closely to those found during the IGE tests except that cushion pressure was about 0 to 7 psf higher and trunk pressure 4 to 10 psf higher over the same interval of time. Center-of-gravity g-loads were about the same for both IGE and OGE tests, and key events also occurred at approximately the same time. The rise in pressures is attributable to the higher initial trunk pressure, which the OGE design mode calls for at the beginning of a drop. An example of the results of a drop at a sink rate of 12.5 fps with no roll or pitch is found in Fig. 24. Plots of the remaining attitudes at the 12.5 fps sink rate as well as tabular listings of key event values for the 8.0 fps OGE drops are contained in Appendix C.

A comparison with the tests conducted by the Bell Aerospace Company on the tenth-scale model with the short trunk is found in Table III. Only peak values were available from the Bell tests as found in the report by Coles (Ref 1). The Bell tests were conducted with the model adjusted to approximately the same dynamic and geometric characteristics as the tests of this report except for the shorter trunk. Bell tests were not performed at exactly the same sink rates and attitudes; and, therefore, comparisons were made to an approximately matching attitude and sink rate. The comparison shows trunk pressure, and center-of-gravity g-loads to be about 0 to 36% higher, depending on sink rate and attitude, with

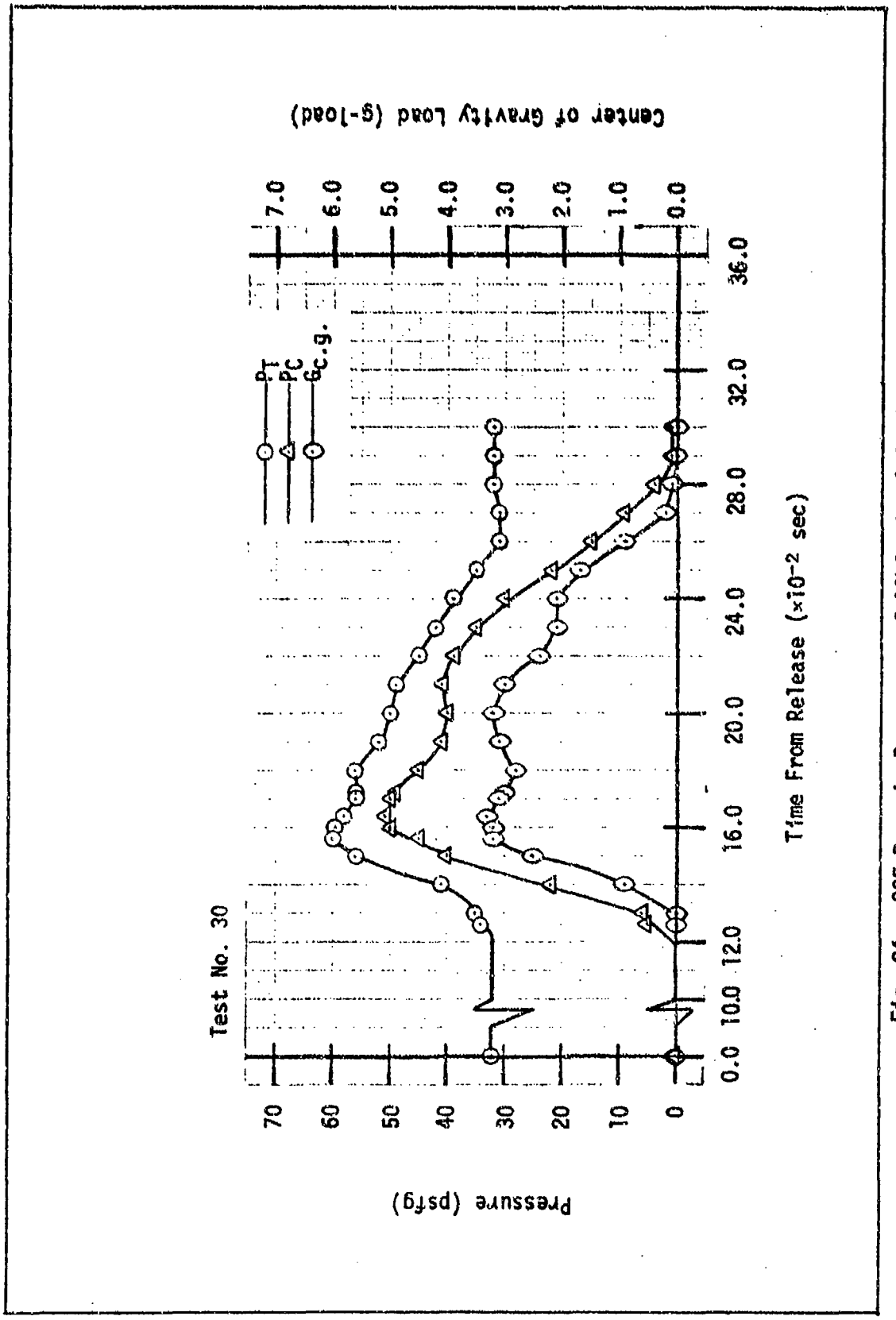

Fig. 24. OGE Dynamic Responses of ACLS, $\theta = 0.0$, $\phi = 0.0$

TABLE III

Comparison of Long and Short Trunk Peak Values

1/16 Scale Model, OGE Design Mode

(Values in parentheses correspond to short trunk. Short trunk values taken from Bell tests (Ref 1).)

Sink Speed (fps)	Pitch (degrees)	Roll (degrees)	P_C (psfg)	P_T (psfg)	$G_{c.g.}$ (g-load)
12.5 (12.7)	0.0 (1.0)	0.0 (-0.5)	51 (54)	60 (81)	3.3 (4.2)
12.5 (12.7)	0.0 (-0.5)	-7.5 (6.0)	46 (55)	58 (76)	3.2 (4.4)
12.5 (12.7)	6.0 (5.5)	0.0 (-0.5)	56 (54)	66 (71)	4.0 (4.5)
12.5 (12.7)	6.0 (6.0)	-7.5 (5.0)	47 (52)	61 (77)	3.7 (4.6)
8.0 (7.4)	0.0 (1.0)	0.0 (0.5)	46 (47)	56 (64)	3.7 (3.0)
8.0 (9.1)	0.0 (-0.5)	-7.5 (6.0)	42 (49)	56 (73)	3.1 (4.1)
8.0 (9.1)	6.0 (6.0)	0.0 (0.0)	48 (47)	60 (70)	3.3 (3.9)
8.0 (9.1)	6.0 (6.0)	-7.5 (5.5)	43 (47)	58 (71)	3.3 (4.0)

Physical Comparison of the Two Models Tested

	Bell Short Trunk	Long Trunk
Gross weight (lbs)	39.3	39.1
Center of gravity (inches)		
X from nose	32.5	32.4
Z from bottom	7.5	7.0
Moments of inertia (slug-ft^2)		
Pitch	3.45	2.71
Yaw	5.01	4.55
Roll	2.49	2.05

the short trunk than with the long trunk as was the case with the same comparison for the IGE quarter-scale and tenth-scale results. Cushion pressures were generally 0 to 20% higher in Bell tests as compared to the tests of this report. Both tenth-scale short trunk and long trunk tests did not exhibit any fan stall during a drop.

IV. Static Tests

Introduction

Static tests were performed on the model to obtain stiffness of the ACLS in level, pitched, and rolled attitudes as it applied to the CC-115 aircraft. In conjunction with the level tests, a static pressure footprint of the system was obtained, and equilibrium relationships of cushion pressure, bag deflection, and area of trunk contact were developed. Equilibrium relationships do not account for dynamic interactions, but these results can be used as a baseline in predicting responses to various dynamic inputs. Level or vertical stiffness tests were conducted with loads, in addition to the model weight, applied over the center of pressure in both the OGE and IGE design mode. The effects of the OGE and IGE design modes will be compared. In addition, load was applied over the center of gravity in the OGE design mode. The results of the center-of-gravity loading will be compared to center-of-pressure loading in the OGE design case. The pressure footprints were obtained with load over the center of gravity in the OGE design mode.

Vertical Stiffness

Procedure and Equipment. A level, or vertical loading, test was conducted by first adjusting trunk pressure to desired OGE or IGE condition. Trunk pressures for each condition were the same as those of the drop tests. Loads on the ACLS from 0.0 pounds up to the weight of the model, 39.1 pounds, were applied by placing a lifting force on the model and thereby decreasing the normal model weight on the ACLS. Beyond 39.1

pounds, load was applied in the form of lead-shot bags weighing approximately 10 pounds each. Thus, above 39.1 pounds, load on the ACLS consisted of the model weight of 39.1 pounds acting at the c.g. plus the additional load over the c.g. or c.p. The center of the bags was placed on top of the model fuselage directly above the center of gravity or center of pressure, whichever case was being tested. At each applied load the model attitude and center-of-gravity height above the platform were measured. Cushion and trunk pressures were also measured using water manometers. The quarter-scale results compared here were obtained from Vaughan (Ref 3). More details on procedure, apparatus, and data reduction are found in Appendix D.

Load Over Center of Pressure, OGE, and IGE. Figure 25 shows a vertical stiffness curve for the OGE and IGE design conditions. The graph depicts how much the ACLS trunk deflects for each load applied on the ACLS. The stiffness increases rapidly up to approximately 20 pounds of load, then up to approximately 75 pounds of load the system stiffness remains constant at about 125 pounds per inch deflection. The quarter-scale tests of AFFDL were conducted from 39.1 to 84 pounds load and showed a stiffness of 89.6 pounds per inch deflection. The difference between the quarter and tenth-scale tests, IGE, was the trunk length. The results seem to indicate a stiffer system by 35 pounds per inch deflection for the longer trunk.

Beyond 75 pounds of load, stiffness began to decrease, decreasing more for each applied load up to 160 pounds or 4.1 g's. Above 75 pounds the tests performed in the OGE condition indicated a greater stiffness than IGE. Increased stiffness is due to the increased trunk pressures of the OGE design condition which work to create a more rigid trunk

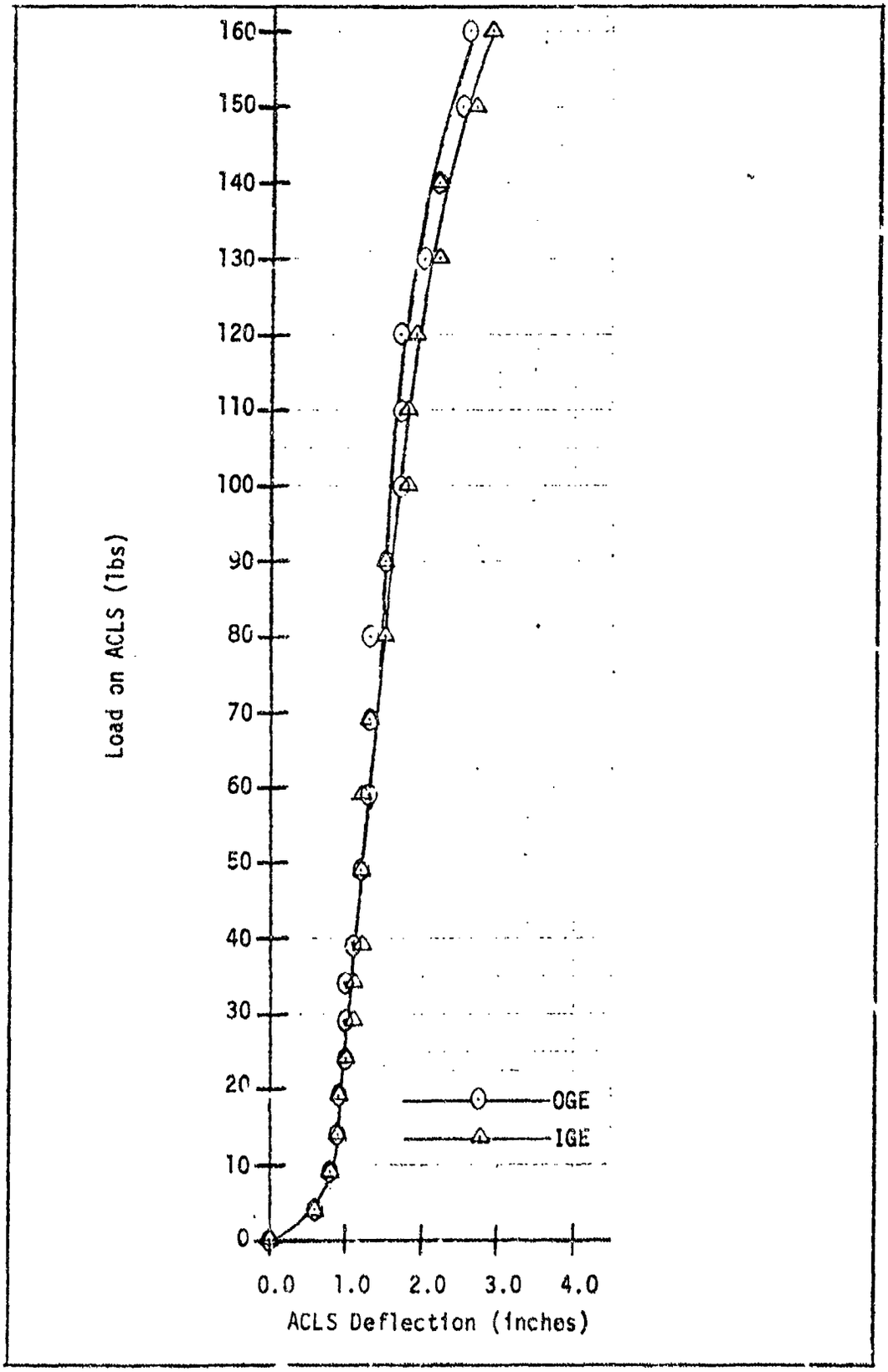

Fig. 25. Effects of Load on ACLS Deflection (OGE and IGE)

structure at the higher loads.

Area of trunk flattening or contact can be obtained using the following relationship for a model in a static condition with no vertical acceleration (Ref 3:15):

$$W_A = P_C A_C + P_T A_T + \text{Aerodynamic lift} + \text{Weight on brakes} \qquad (2)$$

Since there is no weight on the brakes and no air flow over the body, the last two terms are zero. Therefore, by solving for A_T with the remaining terms,

$$A_T = \frac{W_A - P_C A_C}{P_T} \qquad (3)$$

Above 39.1 pounds, the area of the cushion A_C may be assumed constant (Ref 3:15), which for the tenth-scale long trunk was 2.44 square feet. Knowing the load W_A applied on the cushion, cushion pressure, trunk pressure, and area of cushion, one may easily obtain the trunk contact area. Below 39.1 pounds of load on the ACLS, the model is being lifted above the platform and the trunk flattening area is zero. In this case any load being supported by the ACLS is being done solely by the cushion pressure on the cushion area.

Figure 26 demonstrates how area of trunk flattening changes with respect to ACLS deflection and also height of the model center of gravity above the ground. An increase in deflection or decrease in center-of-gravity height corresponds to increased loading. The data gathered from the IGE and OGE tests show a linear relationship between area and deflection or height up to approximately 2.6 inches deflection, 9.4 inches center-of-gravity height. The slope of both curves in the linear region is approximately 0.5 ft^2 per inch of deflection or center-of-gravity height.

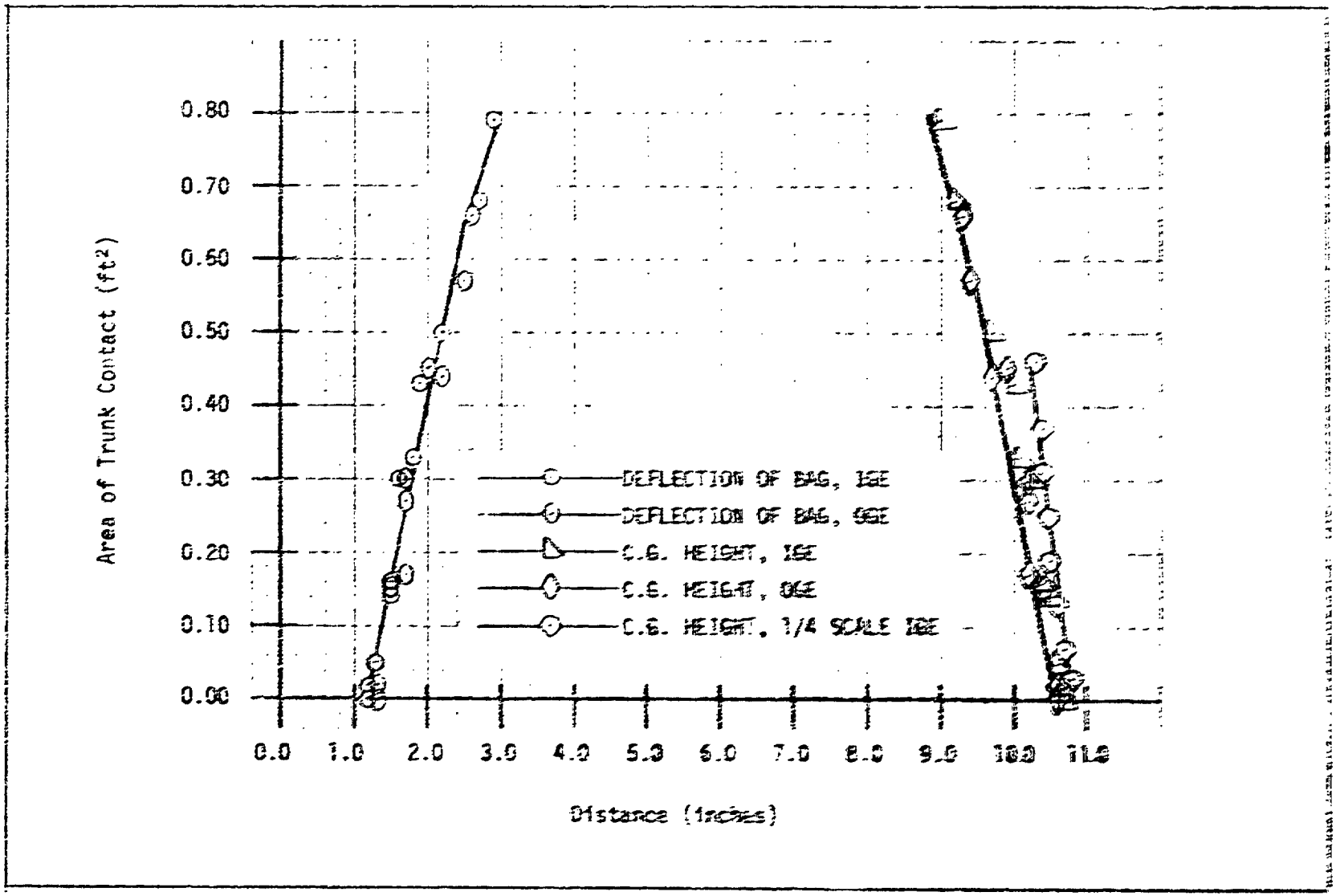

Fig. 26. Area of Trunk Contact Due to ACLS Deflection (OGE and IGE)

The results were the same for both IGE and OGE tests, which seems to indicate that for these pressures the area of trunk contact is a strict function of the deflection of the bag and is independent of trunk pressure. Figure 26 also shows quarter-scale results in the IGE case only (Ref 3:9). In the AFFDL quarter-scale tests, the range of loads was smaller than in the tenth-scale tests but the resulting curve was linear in the same region as for the tenth-scale model. The slope of the quarter-scale line is approximately 0.8 ft^2 per inch of deflection showing more area flattening per inch deflection for the short trunk than the long trunk. This result corresponds to the decrease in stiffness of the shorter trunk as compared to the longer trunk.

Figure 27 shows the variation of trunk pressure with area of trunk contact in the OGE and IGE cases. In addition, results from the AFFDL quarter-scale tests in IGE mode are plotted. Quarter-scale short trunk tests demonstrate more area contact for a specific pressure than do tenth-scale long trunk tests, which corresponds with the results which have been discussed.

Figure 28 demonstrates how much of the total load the trunk supports for each load on the ACLS. The percentage is calculated as follows:

$$\frac{P_T A_T}{W_a} \times 100 = \% \text{ Load on } A_T \qquad (4)$$

The remainder of the load is supported by the cushion. The IGE case, of course, shows the trunk supporting more load than OGE; since OGE load-deflection characteristics are stiffer. Quarter-scale tests with the short trunk show the trunk carrying considerably more load than the long trunk. The long trunk design, therefore, shows an improvement since it

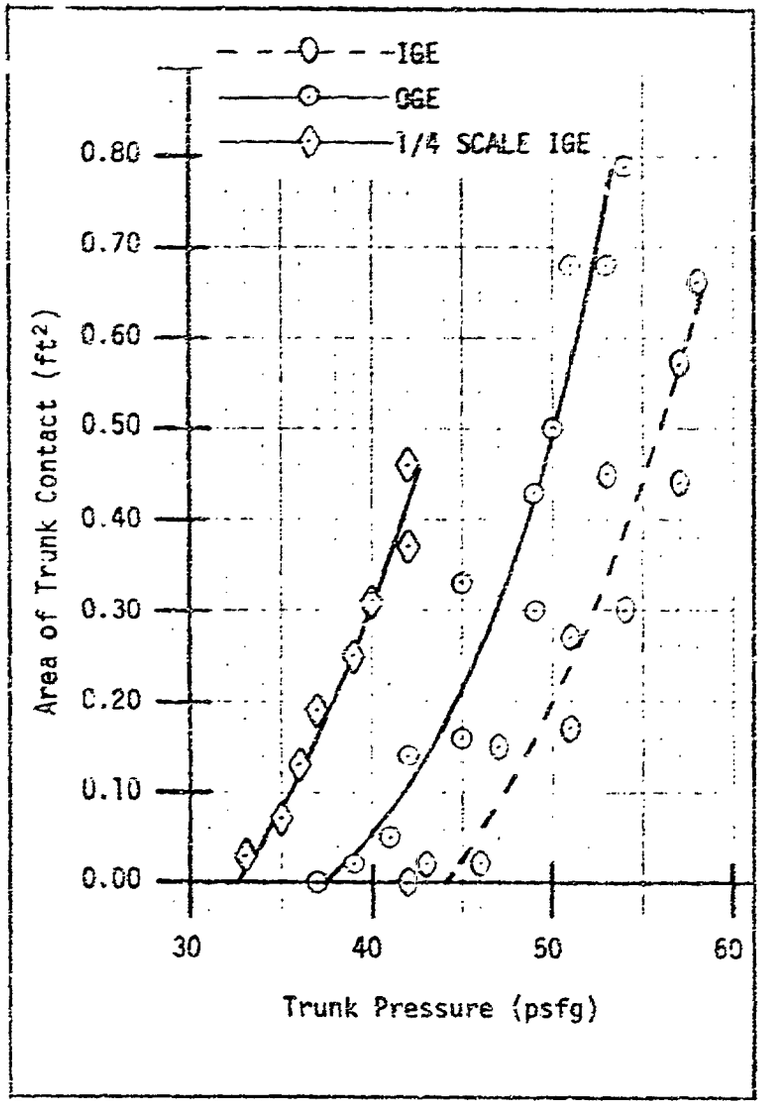

Fig. 27. Variation of Trunk Pressures With Area of Trunk Contact (OGE and IGE)

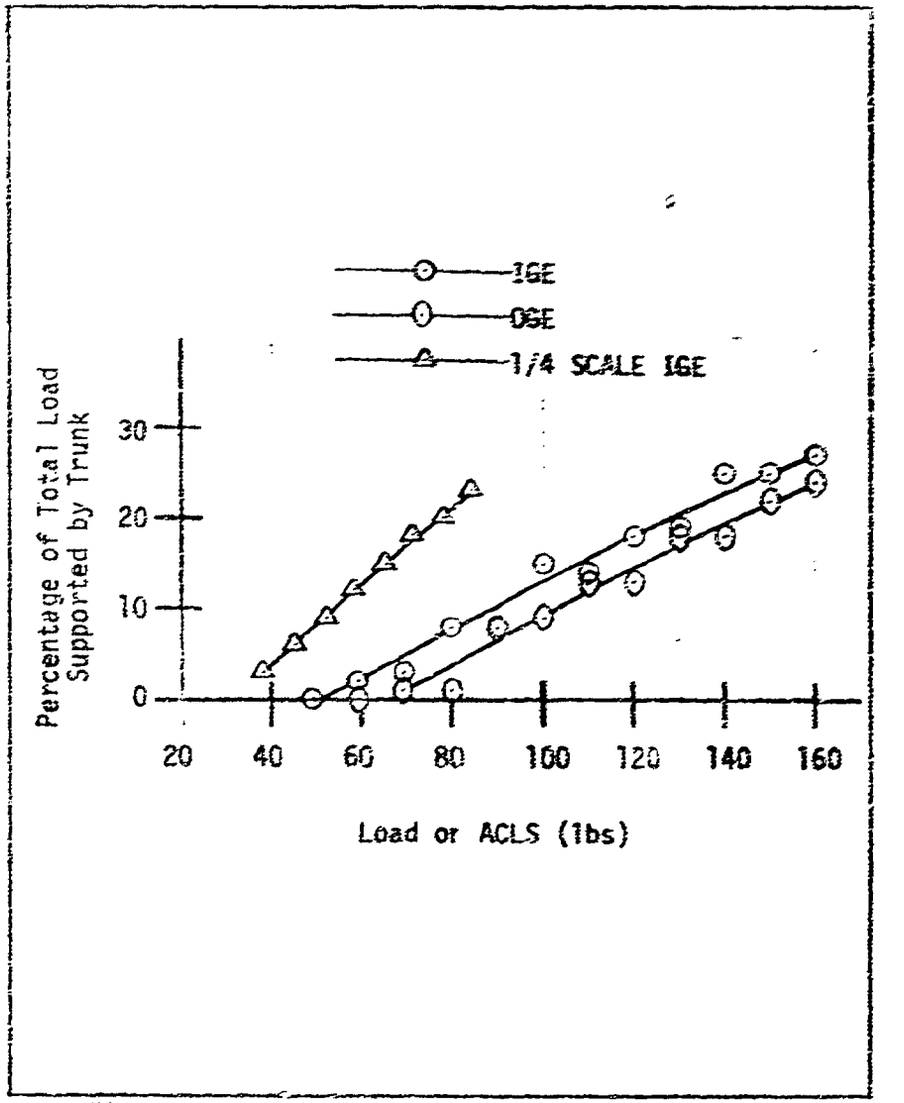

Fig. 28. Percentage of Total Load Supported by Trunk (OGE and IGE)

is more desirable to have the cushion support most of the load and thus keep trunk flattening and possible surface-to-surface contact to a minimum. Note also that trunk flattening did not occur with the long trunk until approximately 60 pounds of load, while the short trunk of the quarter-scale model showed flattening at the normal landing weight of the model. The decrease in long trunk flattening is probably due to the increase in cushion area caused by the longer trunk. As shown in Fig. 29, the quarter-scale trunk and cushion pressures were about the same as those for the tenth-scale at IGE conditions. The increase in cushion area of the long trunk allows more weight to be supported at a given pressure.

Figure 29 also compares OGE to IGE pressures. Trunk pressure in the OGE mode was 4 to 7 psf higher than in the IGE mode as expected, and the cushion pressure was about 2 psf higher above 39.1 pounds. Below 39.1 pounds of load on the ACLS, the cushion pressures were the same for both cases.

Cushion to trunk pressure ratio (P_C/P_T), a dimensionless scaling parameter for the ACLS, increased from 0.5 for 39.1 pounds of load on ACLS to about 0.9 for 160 pounds of load on ACLS as shown in Fig. 30.

Effects of Shifting Load From C.P. to C.G., OGE. In addition to loads over the center of pressure, the model was also loaded over the center of gravity with the design point set in the OGE condition. This section will compare the effects of shifting load concentration from over the center of pressure to over the center of gravity, both in the OGE design condition. No quarter-scale results for load over the center

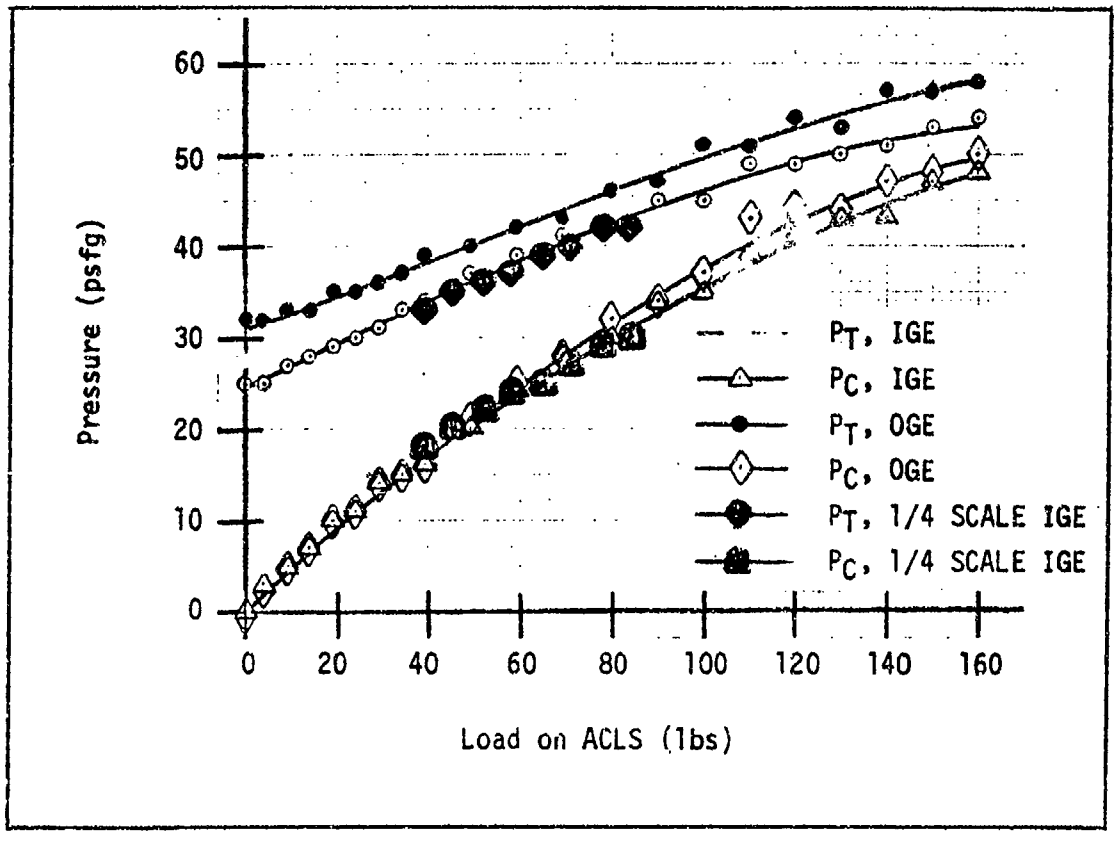

Fig. 29. Variation of Cushion and Trunk Pressure With Load (OGE and IGE)

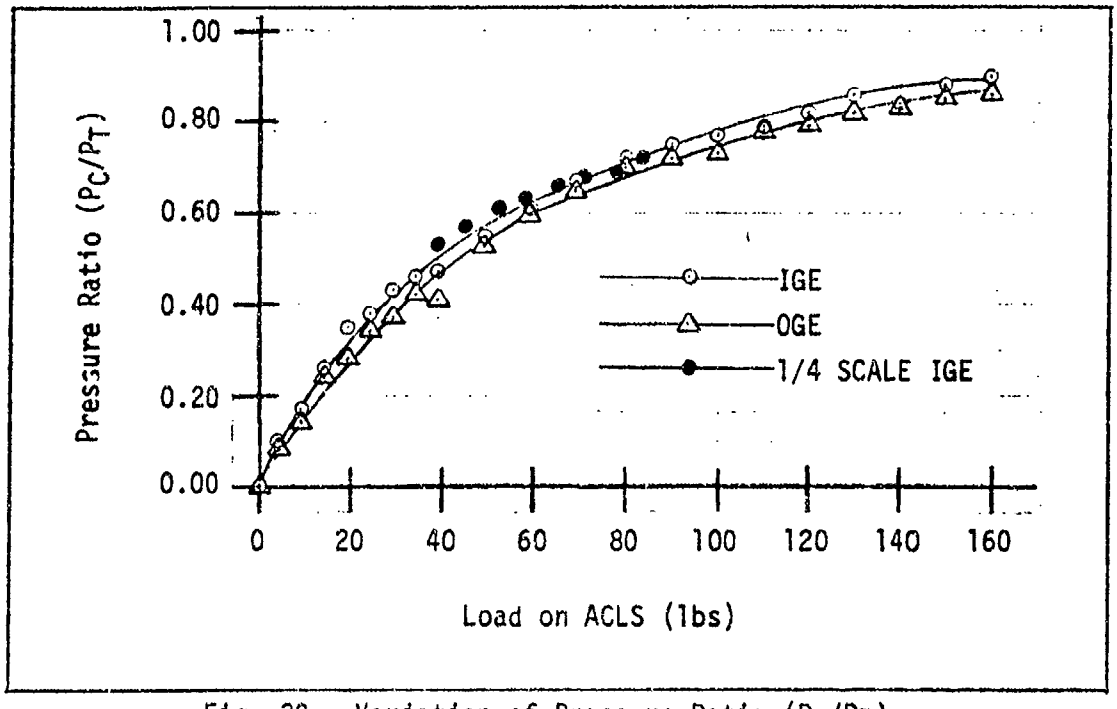

Fig. 30. Variation of Pressure Ratio (P_C/P_T) With Load (OGE and IGE)

of gravity with the center of pressure forward of the center of gravity are available.

Figure 31 shows the model center-of-gravity deflection for each load. When 39.1 pounds, or more, of load is applied over the center of gravity, the stiffness of the ACLS decreases as compared to applying load over the center of pressure. When load is applied over the center of gravity the model begins to pitch and increases that pitch with increasing load as shown by Fig. 32. This pitching is due to the fact that the center of gravity of the model is 2.2 inches aft of the center of pressure of the ACLS. Thus a load at the center of gravity causes the aft portion of the trunk to deflect, which in turn forces the model to pitch. When load is applied over the center of pressure the ACLS deflection is distributed evenly over the whole trunk, preventing a pitching of the model.

Figure 33 shows the variation of trunk area contact with center of gravity deflection for each load. The position of the load does not affect this relationship as the graph in Fig. 33 demonstrates. The graph is linear up to 2.6 inches of deflection with a slope of 0.5 ft^2 per inch deflection, as was the case with a similar graph discussed in the last section. With the load over the center of pressure, the area was evenly distributed fore and aft of the center of pressure; but with the load over the center of gravity that same area is apparently concentrated aft of the center of pressure due to the pitching of the model. Figure 34 shows the variation of trunk pressure with contact area for both load positions.

Figure 35 shows how much of the total load the trunk supports with load over the center of gravity and load over the center of pressure. Due

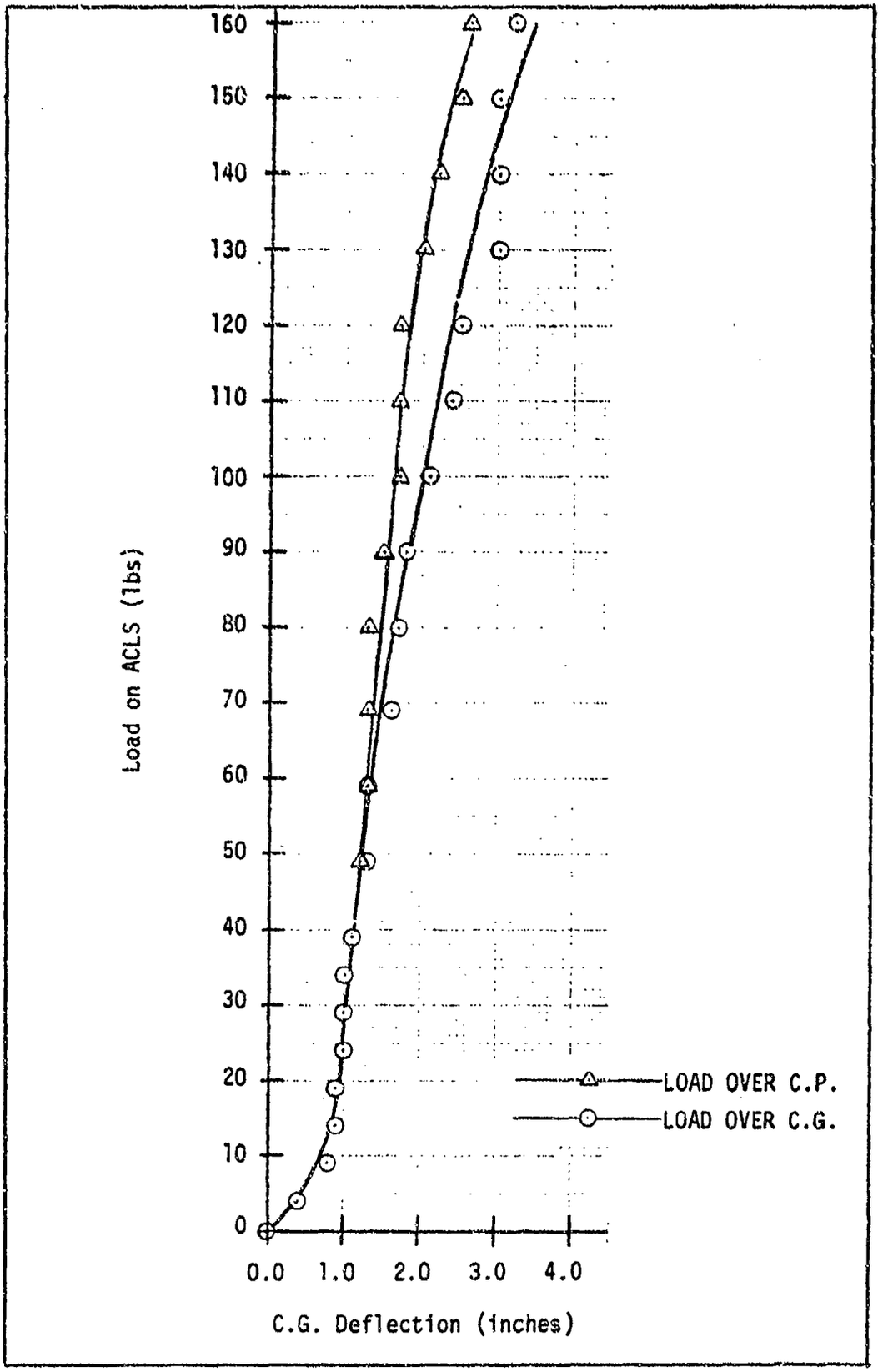

Fig. 31. Load Deflection for C.P. and C.G. Loading

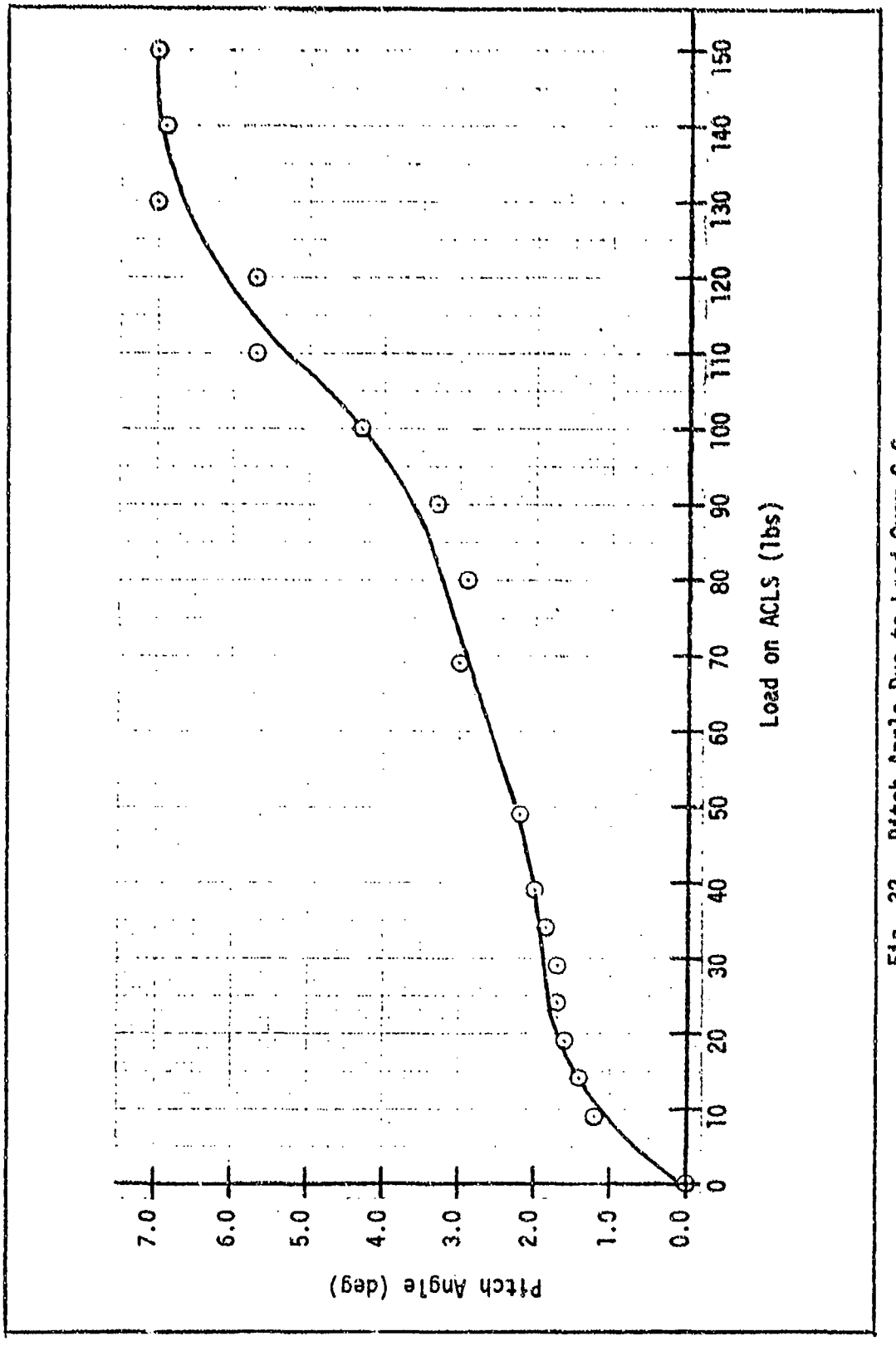

Fig. 32. Pitch Angle Due to Load Over C.G.

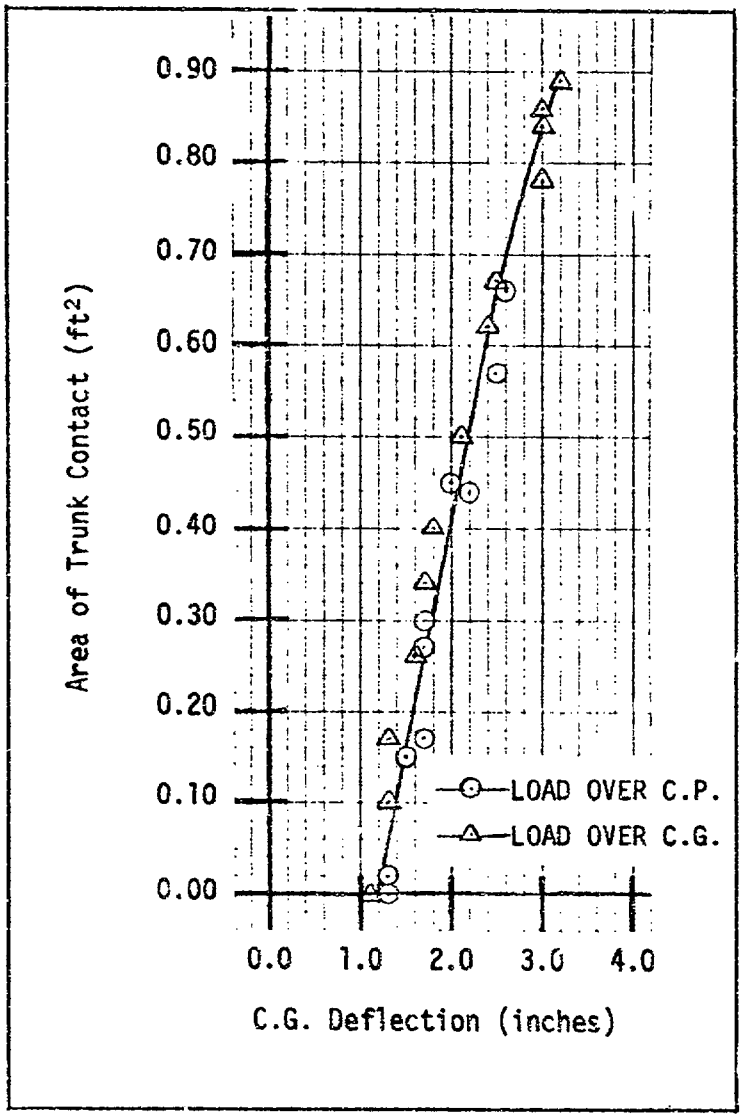

Fig. 33. Area of Trunk Contact Due to C.G. Deflection

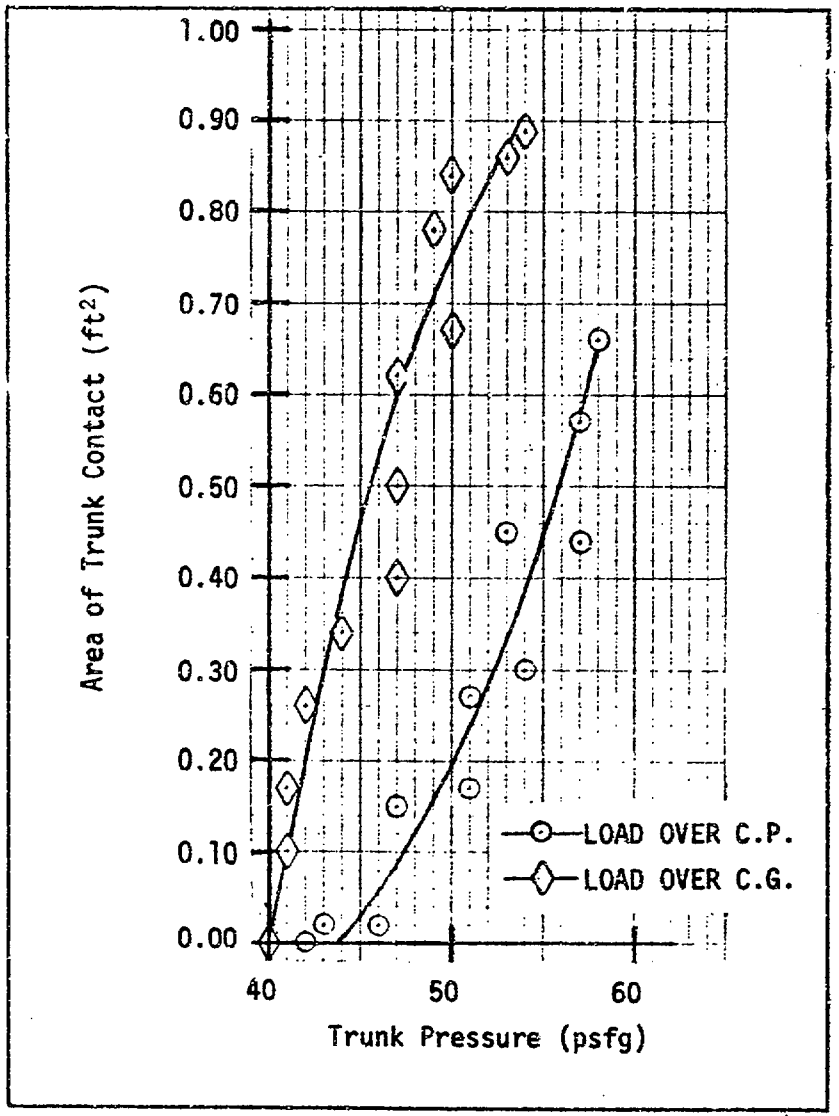

Fig. 34. Variation of Trunk Pressure With Area of Trunk Contact (Load over C.G. and C.P.)

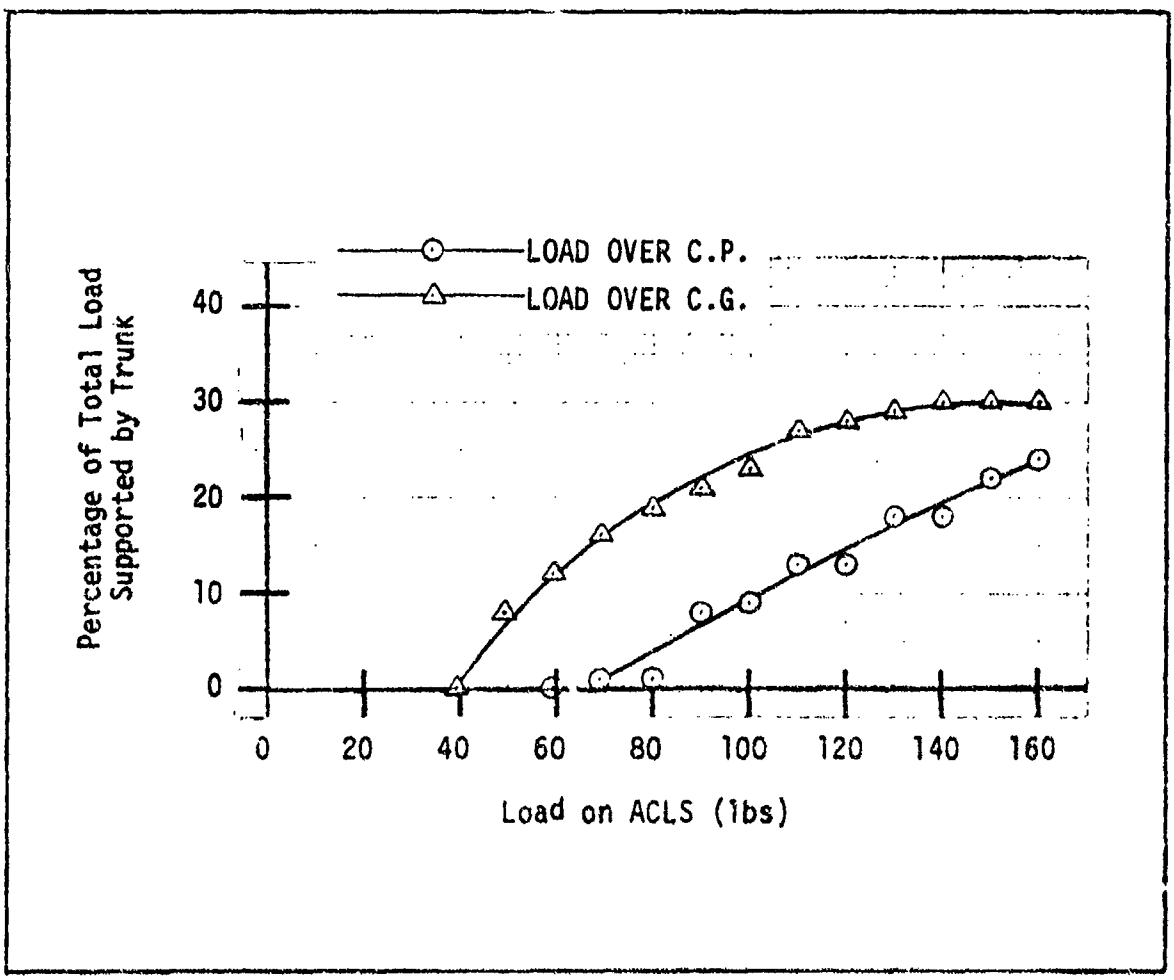

Fig. 35. Percentage of Total Load Supported by the Trunk

to the pitching of the model, more load is being supported by the trunk when the load is over the center of gravity. The trunk began to support load immediately after the load was increased above the normal hover weight of 39.1 pounds and leveled off at 30 percent of the total load from 140 to 160 pounds of load. A load of 160 pounds is equivalent to a 4.1 g-load on the aircraft. These static loading tests show that even at high g-loads most of the force will be absorbed by the air cushion.

Beyond 39.1 pounds slightly less trunk pressure and cushion pressure are required for load support, when that load is applied over the center of gravity as compared to over the center of pressure. This variation of pressure with load is depicted in Fig. 36. The decrease can only be attributable to the pitching of the model due to the load being over the center of gravity. With the model so pitched, the forward portion of the trunk is receiving a smaller portion of the load and is also rising above the floor allowing some air in the cushion cavity to escape to the atmosphere. This flow was felt by hand at the forward part of the trunk. The escape of air would force cushion pressure to decrease due to the pitched attitude as compared to a level attitude where the cushion air is more entrapped by the trunk. The trunk now supports more load, and since trunk contact area is greater with loads over the center of gravity, lower trunk pressures are required with center-of-gravity loading than center-of-pressure loading for the same load. Figure 37 shows the variation of cushion to trunk pressure ratio with load for the two loading positions.

Roll Stiffness

Roll stiffness of the ACLS was obtained by applying a torque about the center of gravity of the model in the roll plane and then measuring

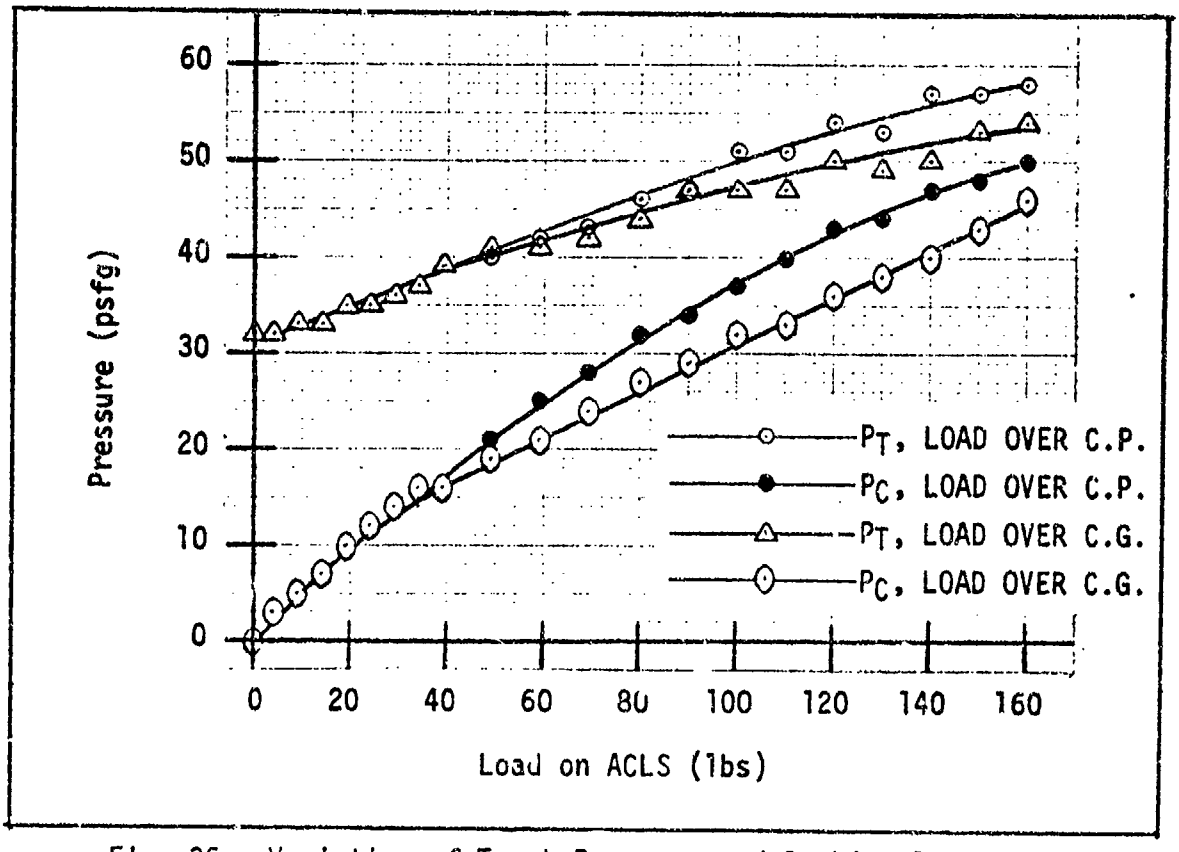

Fig. 36. Variation of Trunk Pressure and Cushion Pressure With Load Over C.G. and C.P.

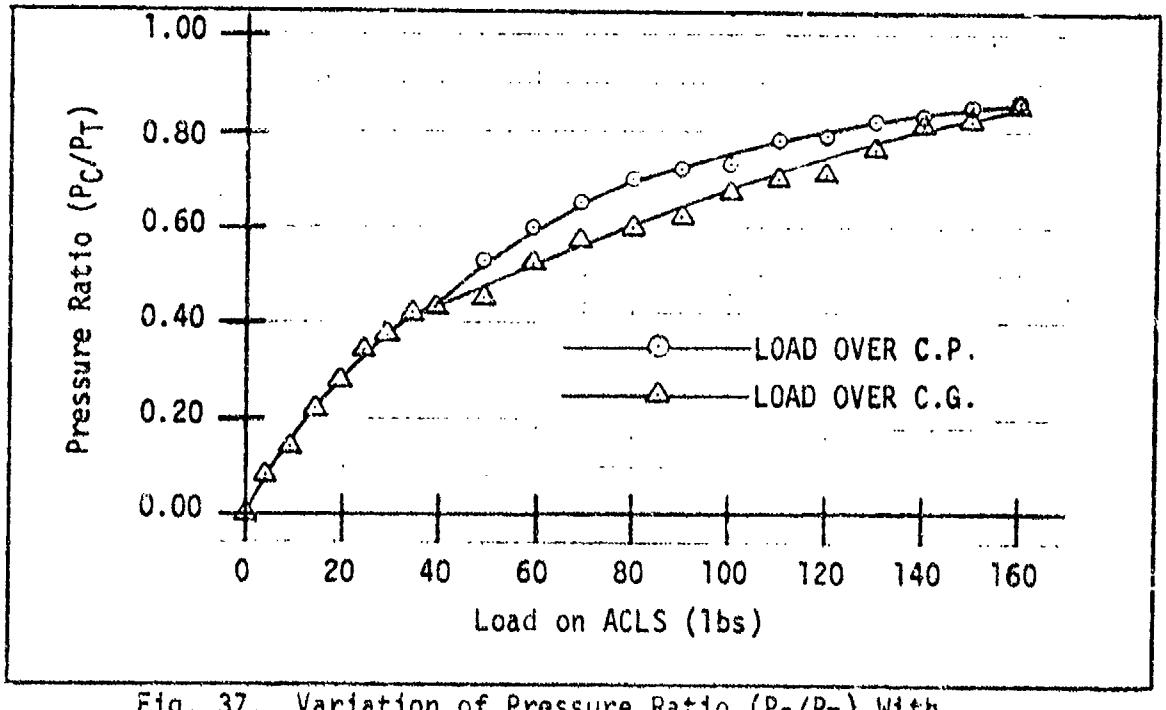

Fig. 37. Variation of Pressure Ratio (P_C/P_T) With Load Over C.G. and C.P.

the roll angle caused for each torque value. Initial trunk pressure was set to the IGE design mode. The torque was created by placing a load at the starboard wing tip of the model and using the wing as a moment arm about the center of gravity. In order to maintain a constant load on the ACLS during torquing, a load equal in magnitude but opposite in direction to the torque load was applied at the center of gravity of the model. More details concerning procedure are found in Appendix D.

The present configuration for the CC-115 with ACLS attached has the center of gravity aft of the center of pressure of the ACLS. As was explained in the vertical stiffness section, this causes the model to pitch in the positive direction. In the hover condition, 39.1 pounds of load on ACLS, the model is pitched at an angle of 2 degrees (see Fig. 32). In order to simulate an actual rolling situation the model was left in this initial pitched condition during roll stiffness tests. This pitch angle did not change during the tests. The model was torqued in roll until the wing touched the platform.

The results of the rolling stiffness tests are presented as a stiffness curve in Fig. 38. The stiffness curve shows that as roll angle increases, stiffness in roll (inch-lbs/degree) decreases.

Pitch Stiffness

To obtain pitch stiffness of the ACLS, the model was torqued about its center of gravity in the pitching plane, and the pitch angle was measured for each torque value applied. The trunk pressure was adjusted to the IGE design condition. Positive and negative torque were obtained by placing a load at the tail of the fuselage and using the fuselage as

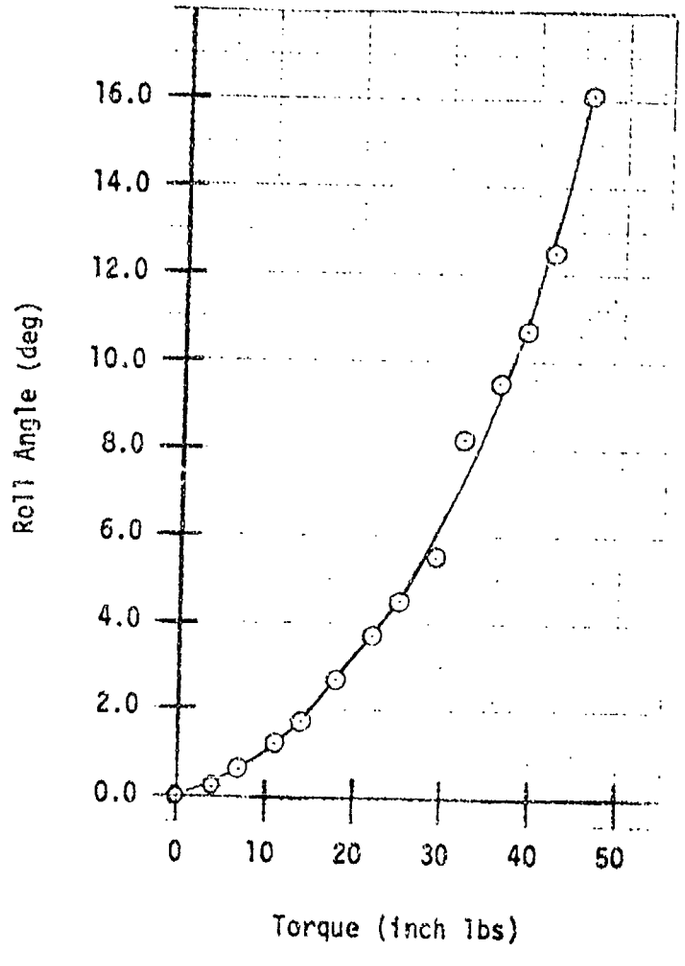

Roll Stiffness

the moment arm. As in roll, the load on the ACLS was kept at a constant 39.1 pounds, the model weight, by applying equal and opposite loads at the center of gravity. More details on procedure and data reduction are found in Appendix D.

As explained above, the model has an initial 2 degree pitch angle at the zero torque condition about the center of gravity. The pitch stiffness results are depicted in a stiffness curve shown in Fig. 39. The curve is quite linear from -2.0 degrees to 5.2 degrees of pitch; however, the slope of positive torque is different than negative torque. From 2.2 degrees to 5.2 degrees, pitch stiffness is approximately 3.3 foot-pounds per degree pitch, while from -2.0 degrees to 2.2 degrees, pitch stiffness increases to 6.2 foot-pounds per degree of pitch. This variation in stiffness is again due to the center of gravity location being aft of the center of pressure. More torque was necessary to force the model to pitch forward than aft of its nominal 2 degree pitch hover attitude. Aft hard structure of the model touches the floor at 11.2 degrees of pitch, while forward hard structure touched at -6.0 degrees pitch. Stiffness decreases quickly beyond both linear regions of the curve.

Pressure Footprint

To examine the pressure being felt by a landing surface beneath an aircraft equipped with ACLS, it was necessary to obtain a pressure footprint of the model. These tests were accomplished for the case of the load over the center of gravity and with initial trunk pressure set at 32 psfg in the OGE design condition.

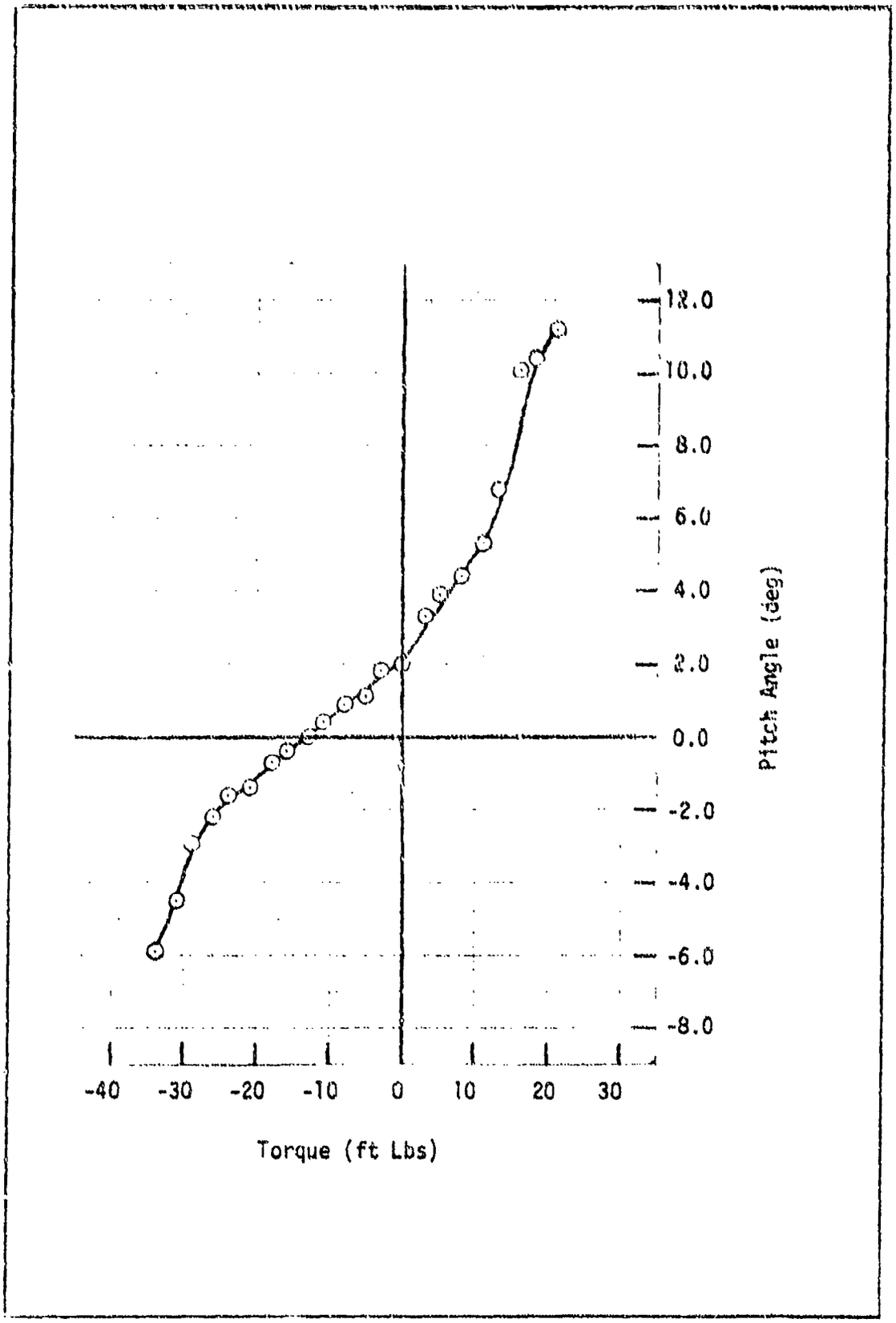

Fig. 39. Pitch Stiffness

The pressure footprint was obtained by imbedding a plate with 48 pressure taps which were 1 inch apart on the test platform as shown in Fig. 40. An overlay of the trunk and cushion as it would appear in its normal hover condition is also shown in Fig. 40, with 36 taps running directly beneath the model longitudinal centerline and 12 additional taps running perpendicular to the longitudinal axis out to the port side of the model. The model was placed on the plate so that the ACLS center of pressure would be directly above the intersection of the two lines of taps. Taps were placed only on the port side due to the symmetry of the system along the roll plane of the model. Tubing was run from the taps to a Scanivalve which measured all 48 pressure points in 20 seconds. The Scanivalve is a special pressure transducer whose operation is explained in Appendix D. The pressure signals from the transducer were collected in the same manner as was done for the pressure transducer of the drop tests with final data appearing as traces on photosensitive paper. A typical test run consisted of adjusting trunk pressure, applying desired load over the center of gravity, recording pressure tap signals, and recording trunk and cushion pressures from water manometers. Pressure footprints were obtained for each of nine loads on the ACLS: 0, 5, 39.1, 59, 80, 100, 120, 140, and 160 pounds. Loads were applied using the same procedure as in the vertical stiffness tests. More details on the equipment used, the procedures followed, and data reduction are found in Appendix D.

The pressure footprint was plotted on graphs as pressure versus pressure tap location from the center of pressure of the ACLS for each load applied. The case for zero load resulted in no pressure on the floor,

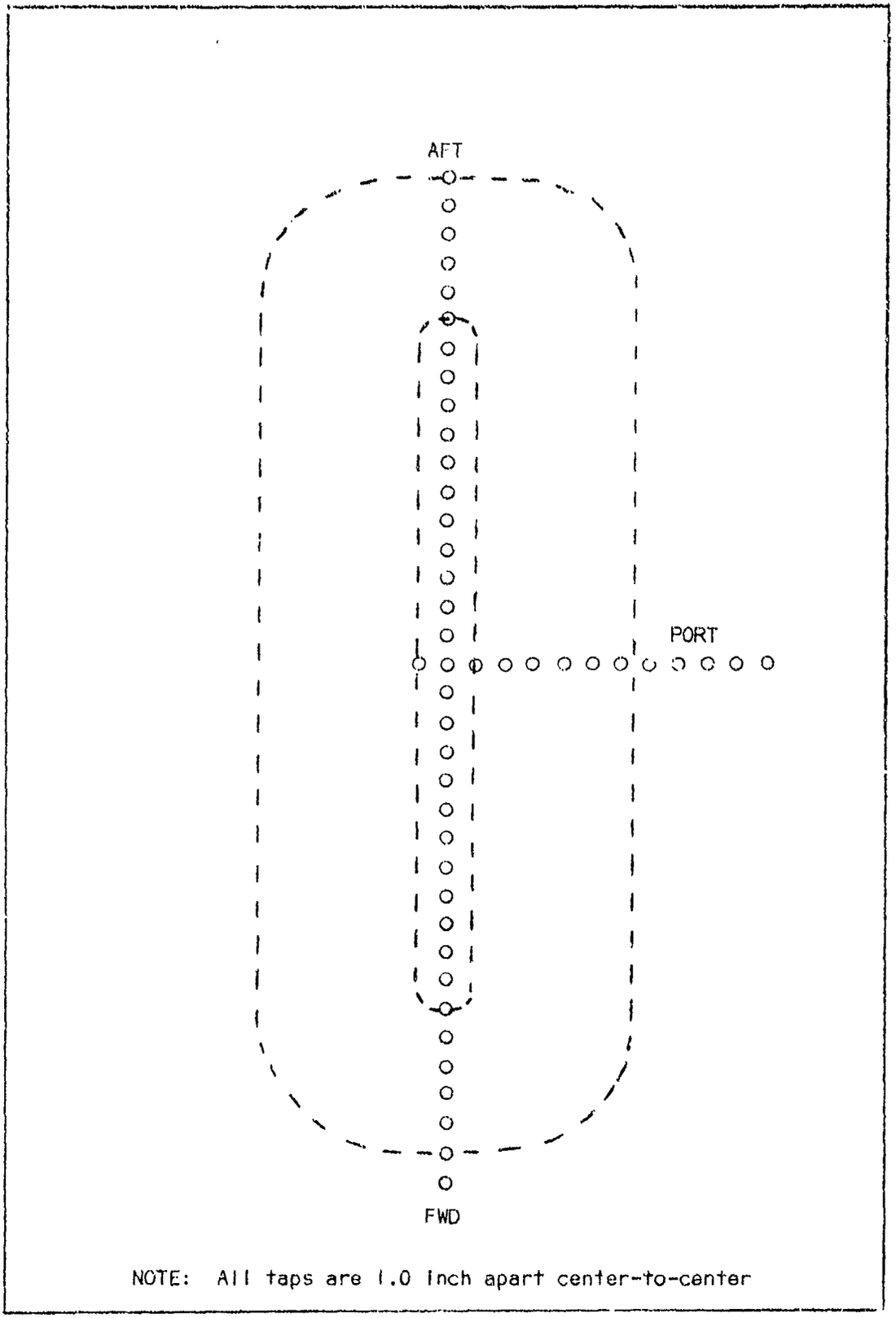

Fig. 40. Pressure Footprint Plate

as was expected, and was not plotted. Figures 41 to 48 show the pressure profiles for each of the loads tested as well as the trunk and cushion pressure during the test. Negative pressures result from the flow of air from the cushion cavity beneath the trunk passing over taps directly outside of the trunk periphery. Since it was difficult to maintain the model in its desired positon over the taps as more load was applied, some points on the plots often vary from one position to the next. The curve drawn through these points gives an average value of the pressure at those approximate locations.

Figure 42 shows the floor pressure with the model at its normal landing weight and hover condition. Containment of air in the cushion by the trunk is obvious from the increased pressure near the center, which drops off slightly as the forward portion of the trunk is approached. Floor pressure beneath the cushion was the same or at most 1 psf higher than the cushion pressure. This difference is probably due to some air flow from the vent holes in the trunk directly onto the pressure taps beneath them. With the center of gravity aft of the center of pressure, the model becomes pitched, as has been explained; and this pitching allows more air flow out of the forward cushion area than anywhere else. This last fact can probably account for the decreased pressure under the forward portion of the trunk as compared to the rear portion.

Figures 43 to 48 show pressure footprints with loads above normal hover weight. Note that pressures beneath the forward trunk and cushion are about 1 to 2 psf higher than aircraft cushion pressure; and the additional load is now causing part of the rear trunk to flatten out, which

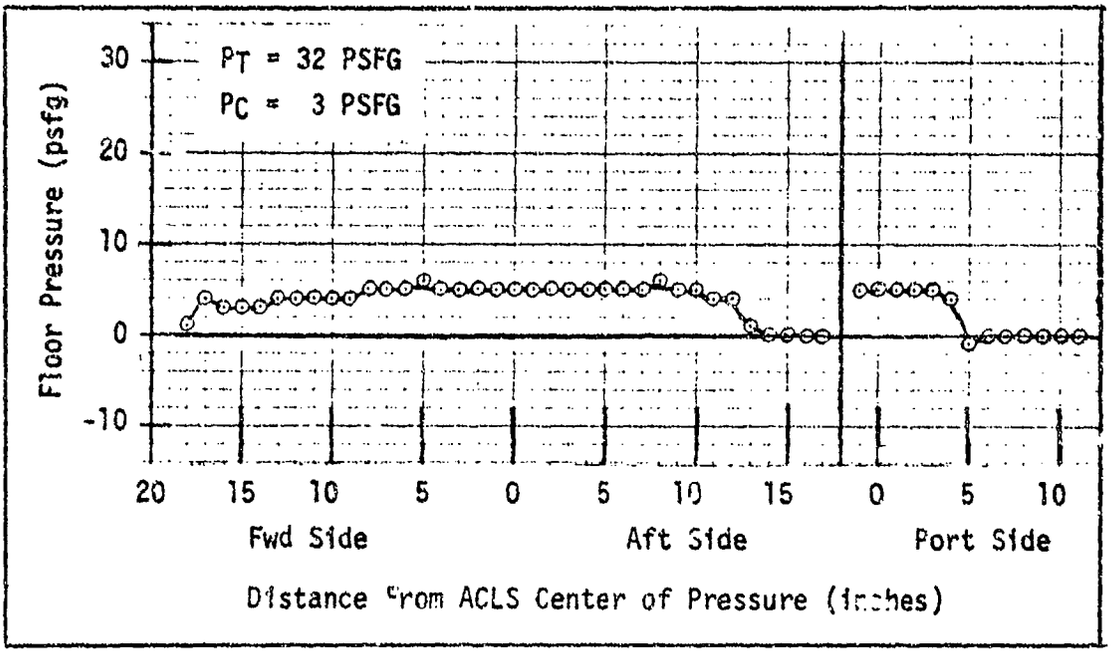

Fig. 41. Pressure Footprint, 5 lbs Load on ACLS

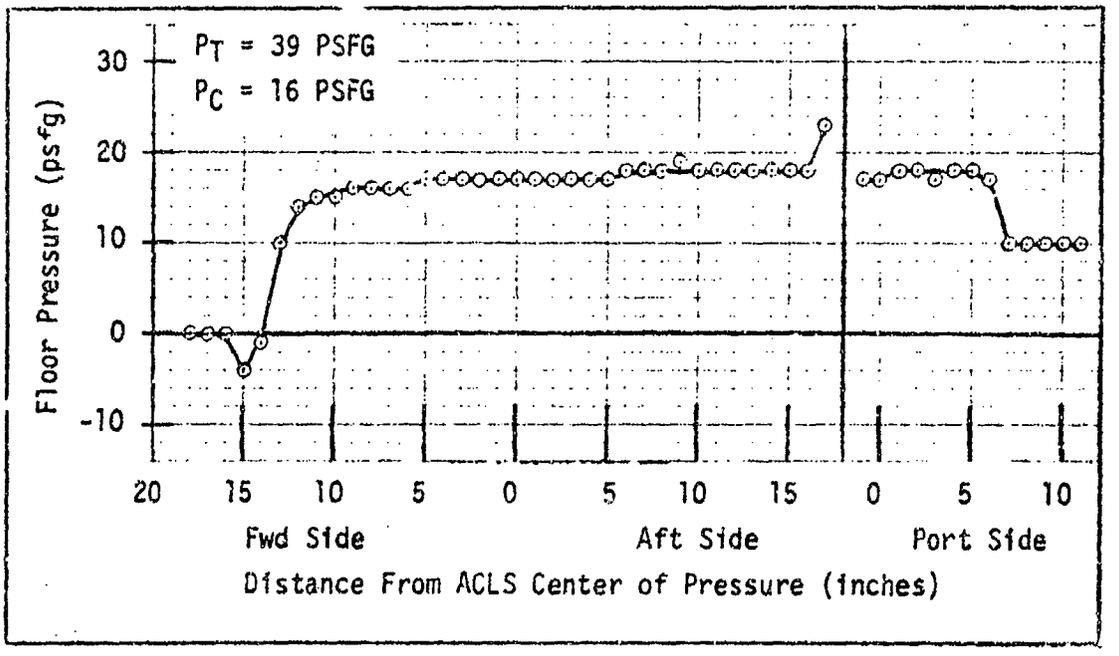

Fig. 42. Pressure Footprint, 39.1 lbs Load on ACLS

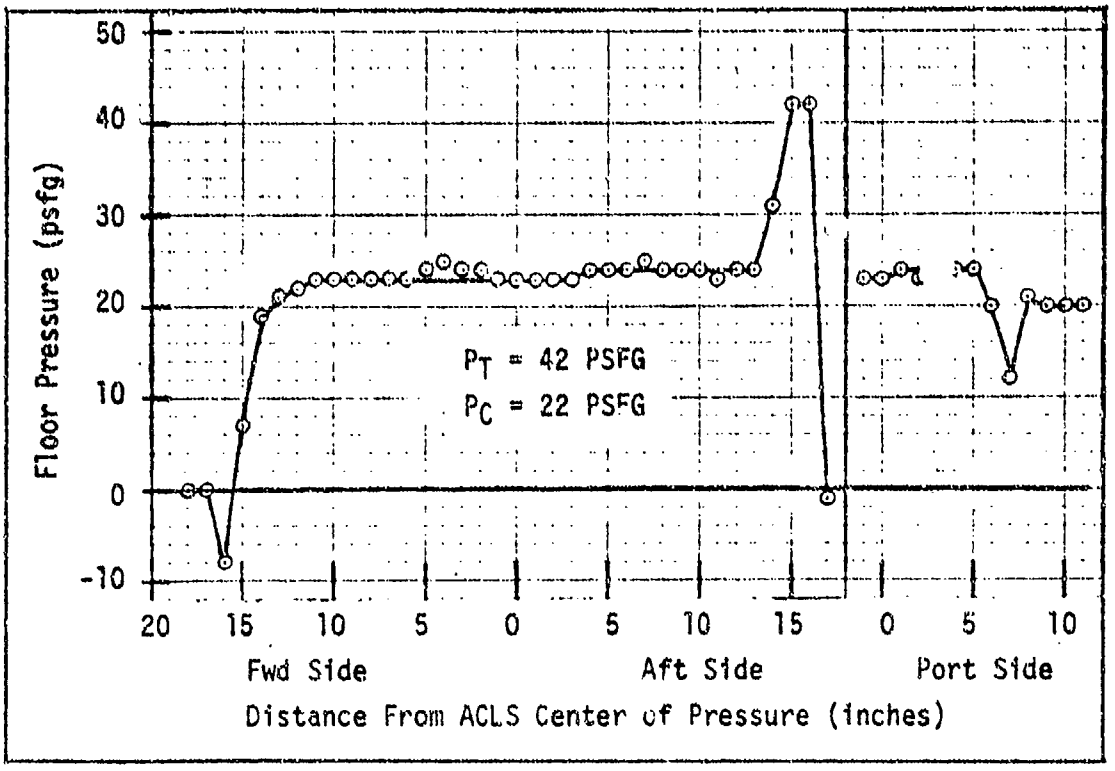

Fig. 43. Pressure Footprint, 59 lbs Load on ACLS

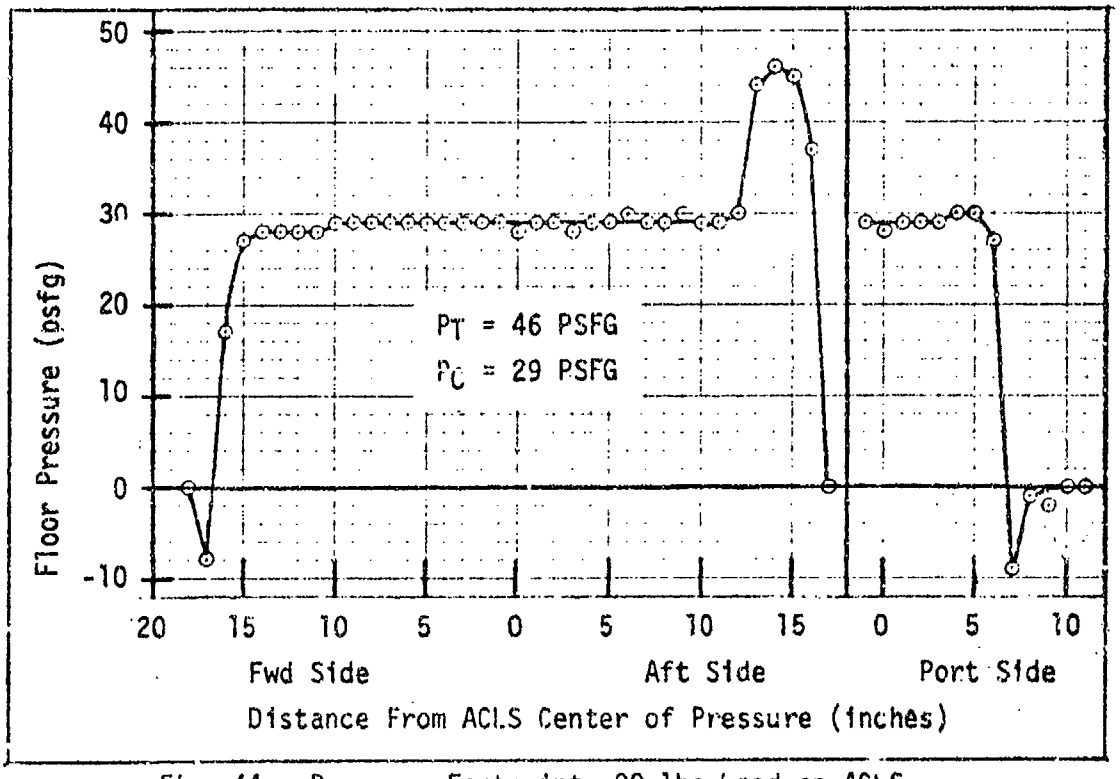

Fig. 44. Pressure Footprint, 80 lbs Load on ACLS

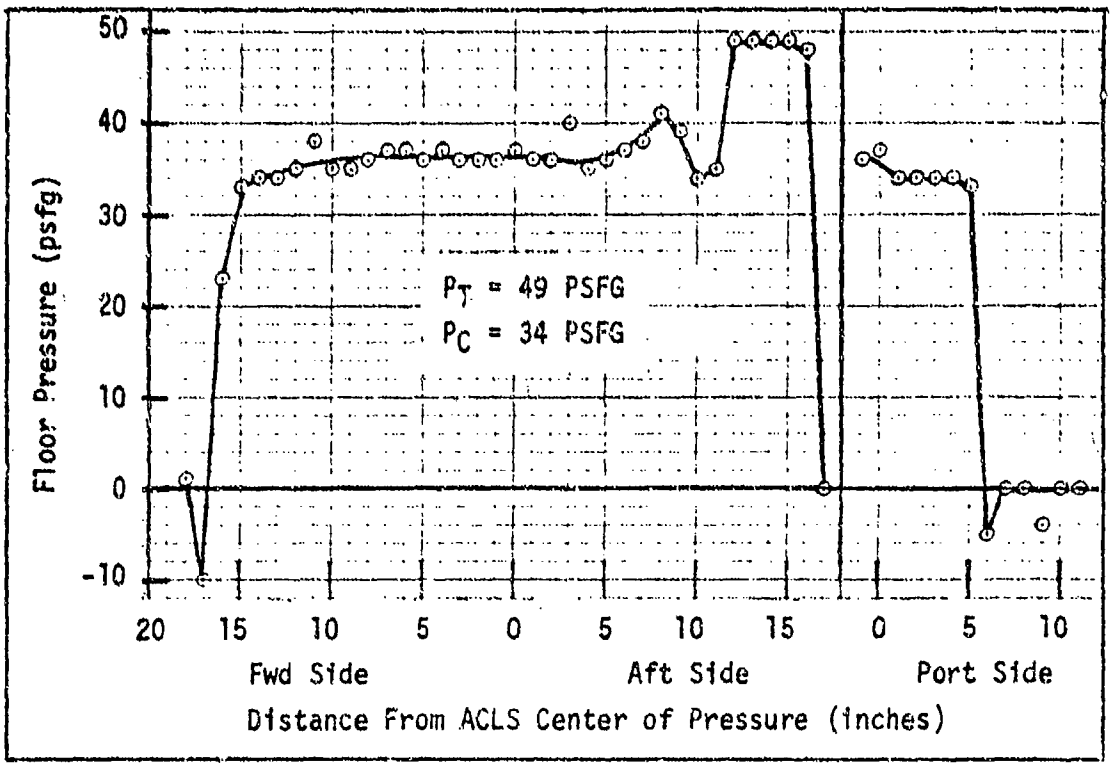

Fig. 45. Pressure Footprint, 100 lbs Load on ACLS

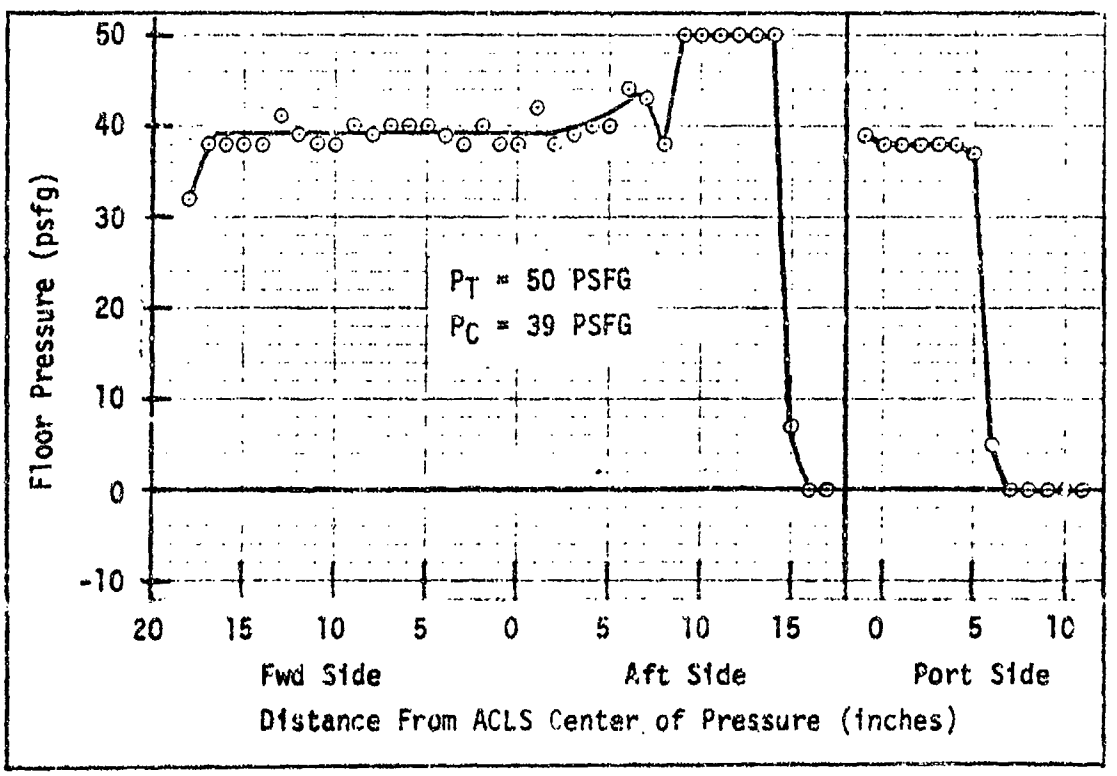

Fig. 46. Pressure Footprint, 120 lbs Load on ACLS

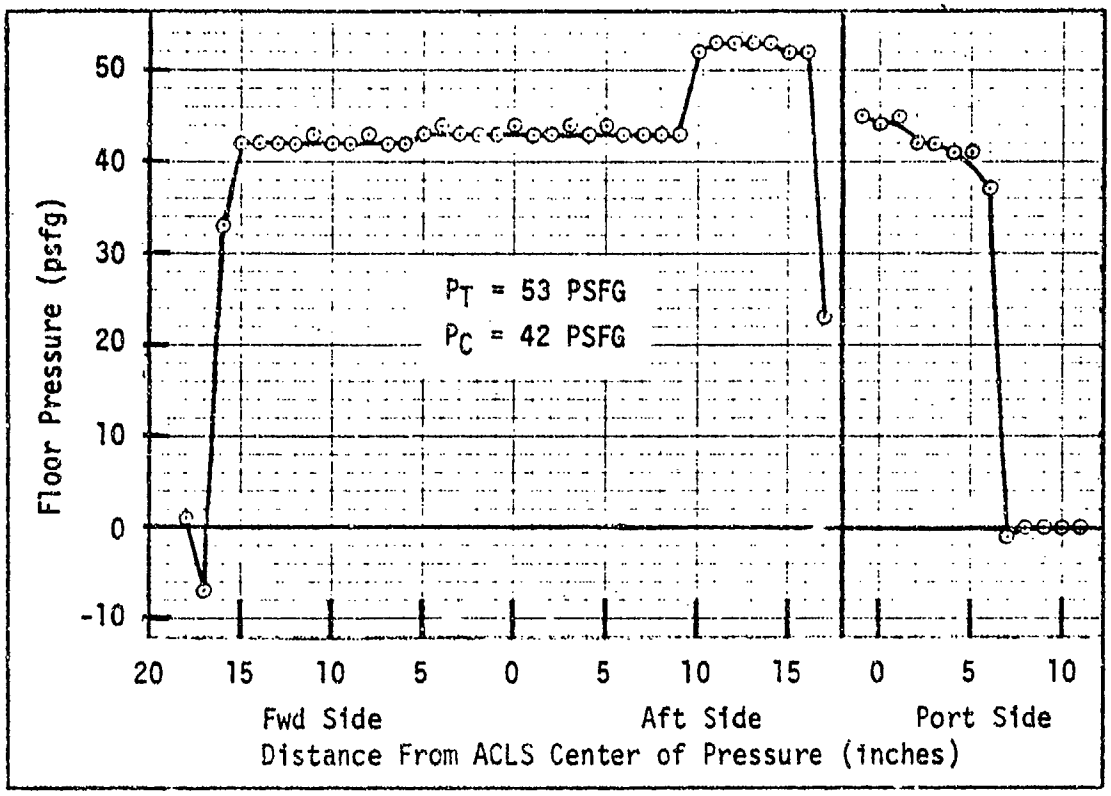

Fig. 47. Pressure Footprint, 140 lbs Load on ACLS

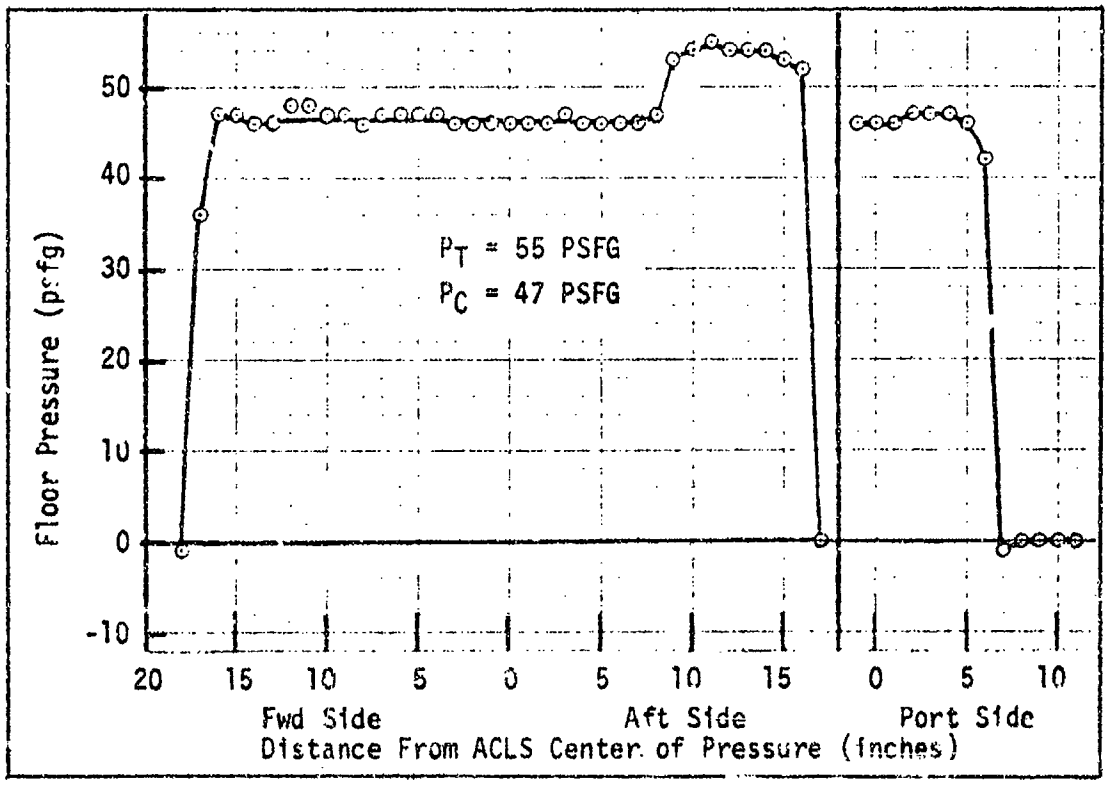

Fig. 48. Pressure Footprint, 160 lbs Load on ACLS

is demonstrated by a sharp increase in pressure on the floor to a point very near or equal to trunk pressure. As more load is applied, the trunk flattening area becomes larger, and the distance over which the increased pressure on the floor is being felt also increases. This distance is a measure of the width of the rear trunk flattening. Note that the port side of the floor pressure is near cushion pressure, indicating no trunk contact for all loads. In general, the floor pressure was slightly higher than aircraft cushion pressure, unless the trunk flattened, in which case floor pressure approached or equalled trunk pressure.

If enough taps were available to measure around the entire surface beneath the model, one could obtain an approximate shape of the trunk flattening or contact area by noting the distance over which the floor pressures approach the trunk pressure. A plot could then be laid out showing the approximate trunk flattening or contact area where high pressures were recorded. A measurement of this nature would require more equipment and a more elaborate pressure recording procedure. Based on data gathered from pressure footprint tests of this report, the trunk contact area, for model loading over the center of gravity, probably takes on an approximate shape as shown in Fig. 49. The aft portion of the trunk from the center of pressure location aft, begins contact with increasing area towards the rear. This total area increases with increasing load.

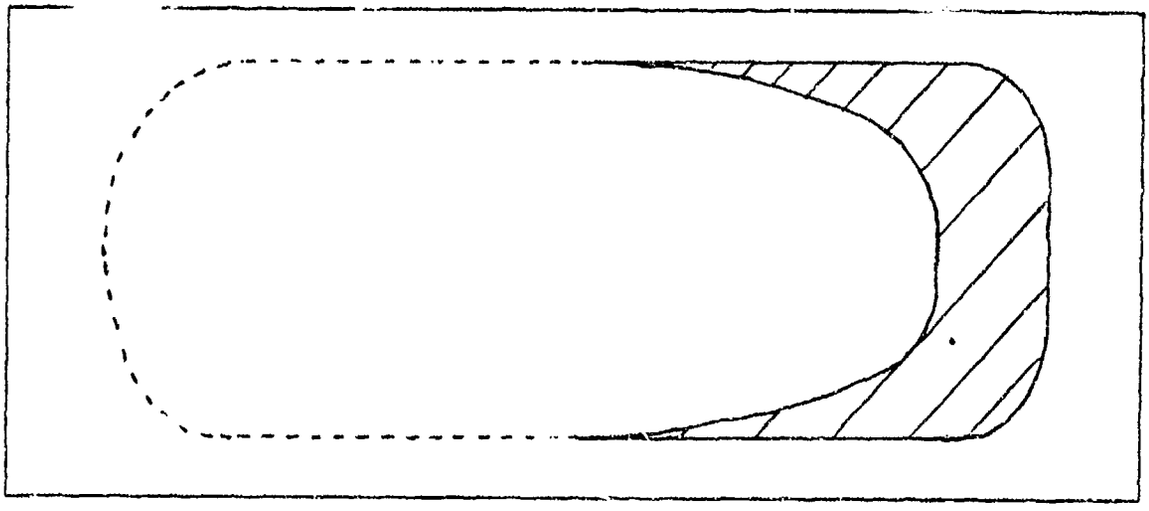

Fig. 49. Shape of Trunk Contact Area

V. Static Braking Tests

Introduction

Braking of an ACLS equipped aircraft was briefly described in the introduction of this report. In order to brake the aircraft, cushion pressure must be decreased allowing a portion of aircraft weight to be shifted onto the brakes. The cushion pressure is decreased by inflating brake pillows which increase in height from the ground. Raising the trunk allows more cushion air to escape, thus decreasing cushion pressure. Cushion pressure can then be thought of as a function of brake height, and it is important to know how much brake height is necessary to achieve a cushion pressure which will allow the aircraft to decelerate at a desirable rate when brakes are applied. To determine this relationship of brake height to cushion pressure and deceleration, braking tests were conducted on the tenth-scale model. Data discussed in this report up to this point have shown the responses and effects of the ACLS to a landing or hovering attitude. The braking data enhance the previous results by showing the static responses and effects of the ACLS in a braking or decelerating mode. The braking tests conducted were of a static nature which demonstrate the effects of brake height on cushion pressure, trunk pressure, and drag or deceleration.

Equipment and Procedures

Brakes were simulated with wooden blocks and rubber pads for each brake height according to dimensions shown in Fig. 50. The ACLS is designed

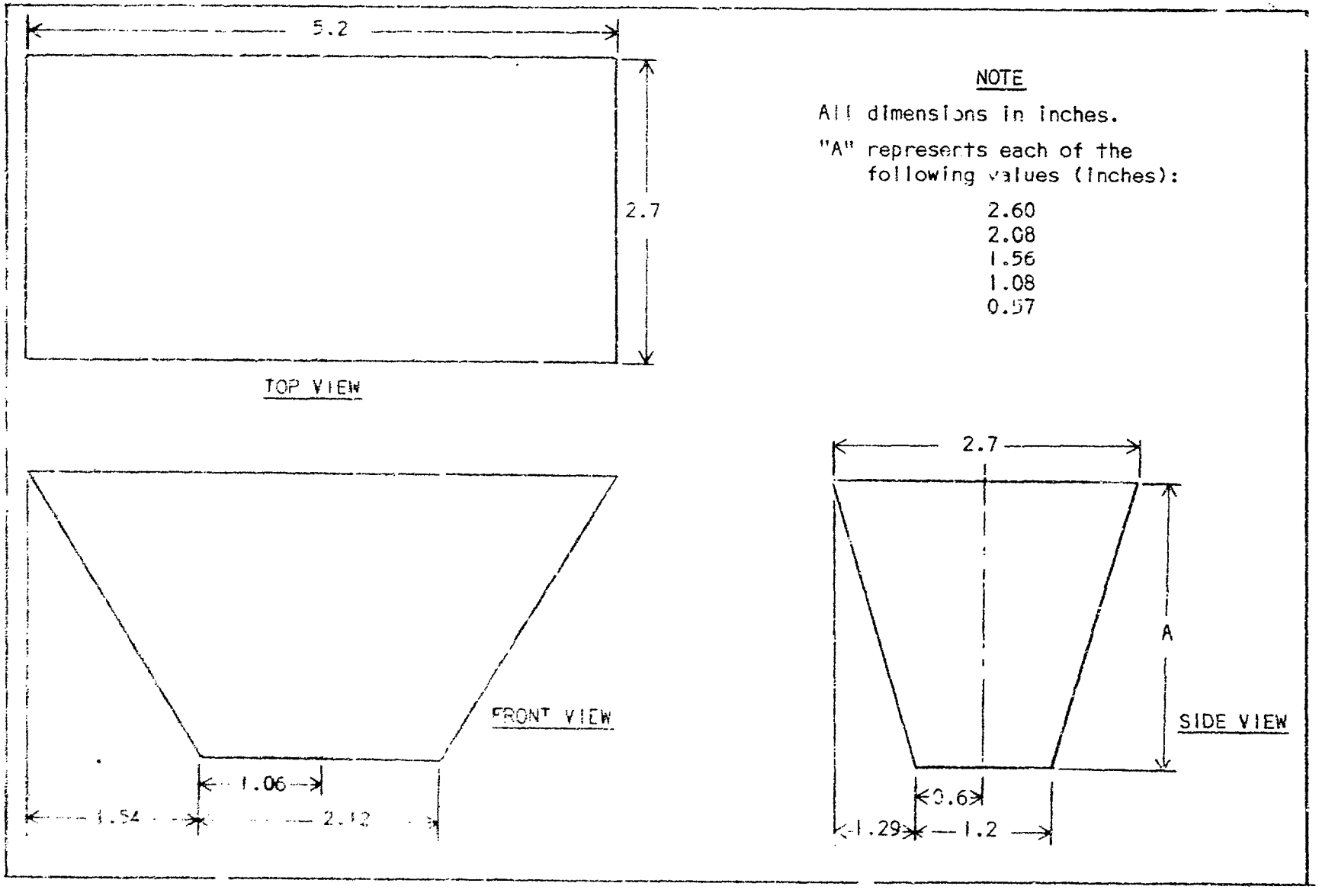

Fig. 50. Brake Pillows

to use six of these brake pillows attached to the aft portion of the trunk, as was shown in the introduction to this report (see Fig. 1). Tests were conducted at six brake heights: 0.0, 0.57, 1.08, 1.56, 2.08, and 2.60 inches, including rubber pads. An explanation of the brake simulation and attachment is found in Appendix I.

Before brakes are applied, the full-scale aircraft would have an IGE trunk pressure equal to 342 psfg. Applying brakes would change trunk and cushion pressures. To simulate a similar situation the model had to be set into an IGE design mode with trunk pressure equal to 34 psfg, IGE, without brakes. Brake blocks had to be attached to the inflated trunk while the model was above the platform, out of ground effect. Previous tests had shown that whenever the model was raised out of ground effect from the hover condition at a trunk pressure of 34 psfg, IGE, the trunk pressure would drop to 26 psfg, OGE. Therefore, for braking tests the model was set at 26 psfg, OGE. If brakes were not attached, raising the trunk above the platform floor, trunk pressure would have returned to 34 psfg when the model was lowered to the hover condition, IGE. With this procedure, the proper IGE design mode could be easily obtained with the brakes attached. For each brake height tested, cushion pressure and trunk pressure were measured from the water manometers. In addition, the model was pulled at its center of gravity, and the force required to make the model just begin to move was measured by use of a spring scale with a range from 0 to 25 pounds. The force measured was a static drag or frictional force. The coefficient of friction between the rubber pads of the brakes and the brown paper surface on the platform was found to be 0.8, which is a typical coefficient of friction between a normal runway

and the ACLS. A typical test run consisted of attaching brake blocks, adjusting trunk pressure, lowering the model onto the platform, measuring trunk and cushion pressures, pulling the model, and measuring drag or force of that pull. More details on procedures, equipment, and data reduction are found in Appendix L.

Results

During initial pull tests on brake heights of 2.60 and 2.08 inches, it was noticed that the two most forward brakes would pivot around their forward edge as shown in Fig. 51. This tilting prevented the proper area

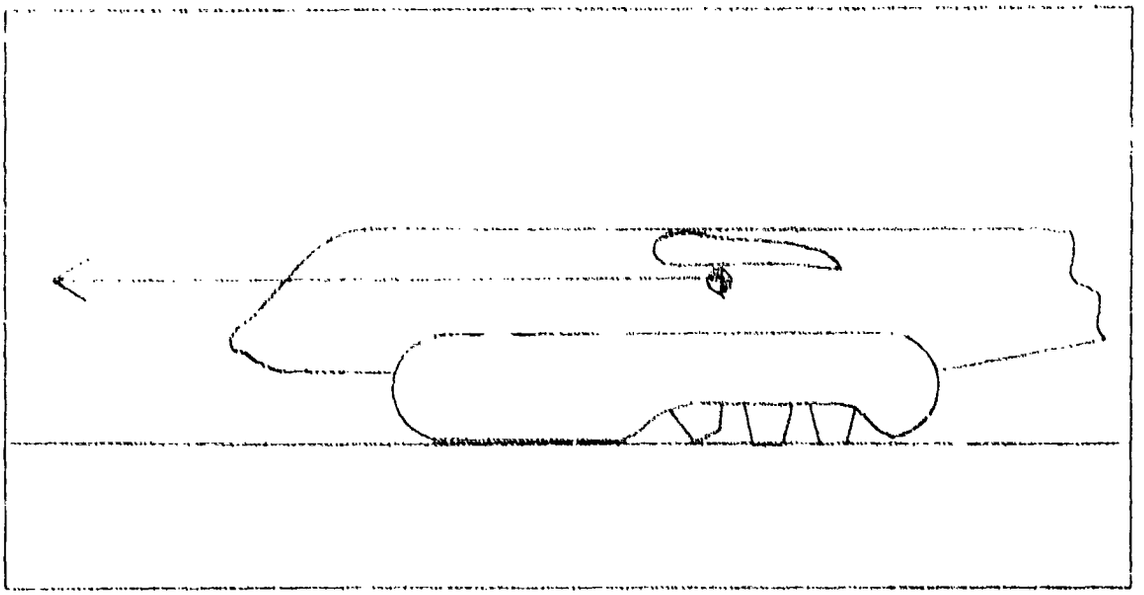

Fig. 51. Forward Brake Tilting

from being in contact with the surface. The tilting is due to the solid construction of the simulated brake pillows. Full-scale brake pillows, constructed of an elastic material, would compress. In order to simulate that compression, the forward wooden blocks for each of the two heights mentioned were modified as shown in Fig. 52. The edge of the block was sanded down until proper contact area of 2.54 square inches was obtained.

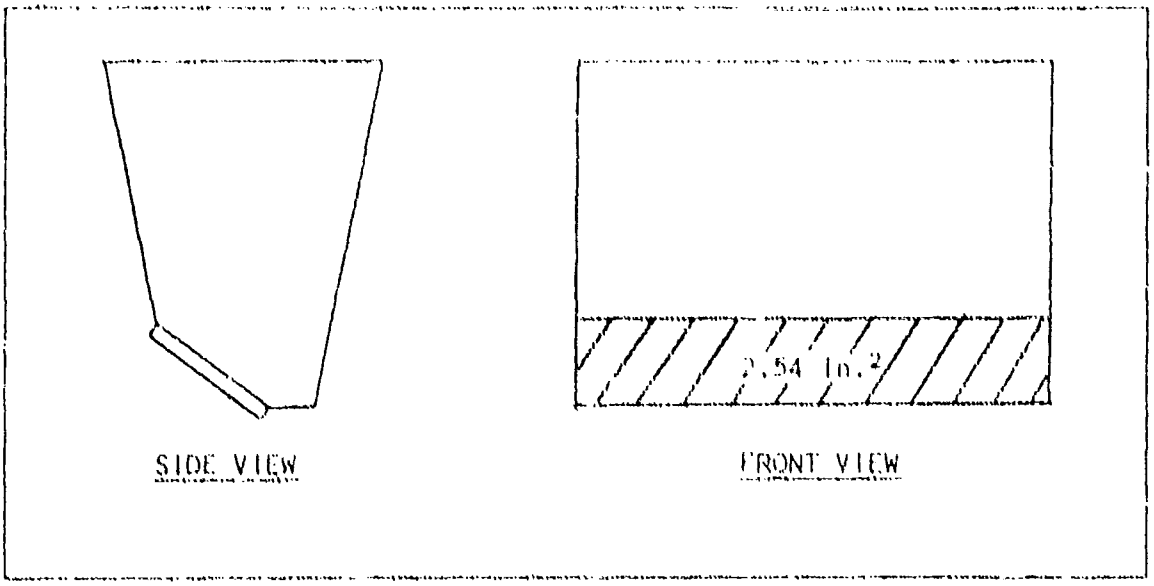

Fig. 52. Forward Brakes Modification

The blocks were placed in this condition only for pull tests to obtain a proper drag value on a required contact area. The overall height of the six brakes at 2.60 inches and 2.08 inches was not altered during the pull by this adjustment. Cushion and trunk pressures were obtained before and after the adjustment, and these also did not change. The blocks of the lower brake heights did not exhibit this compressing effect at the first motion of the model and were not altered.

Figure 53 shows how brake height affects trunk and cushion pressure. Cushion pressure decreased most rapidly between 0.57 and 1.08 inches of brake height, indicating a possible transition point between these two brake heights which greatly affects the cushion pressure. This transition is probably attributable to a critical distance above which the jet curtain around the trunk periphery ceases to provide a seal to maintain a high cushion pressure. When the jet curtain is broken in this manner, the cushion pressure is decreased. Trunk pressure decreased as brake

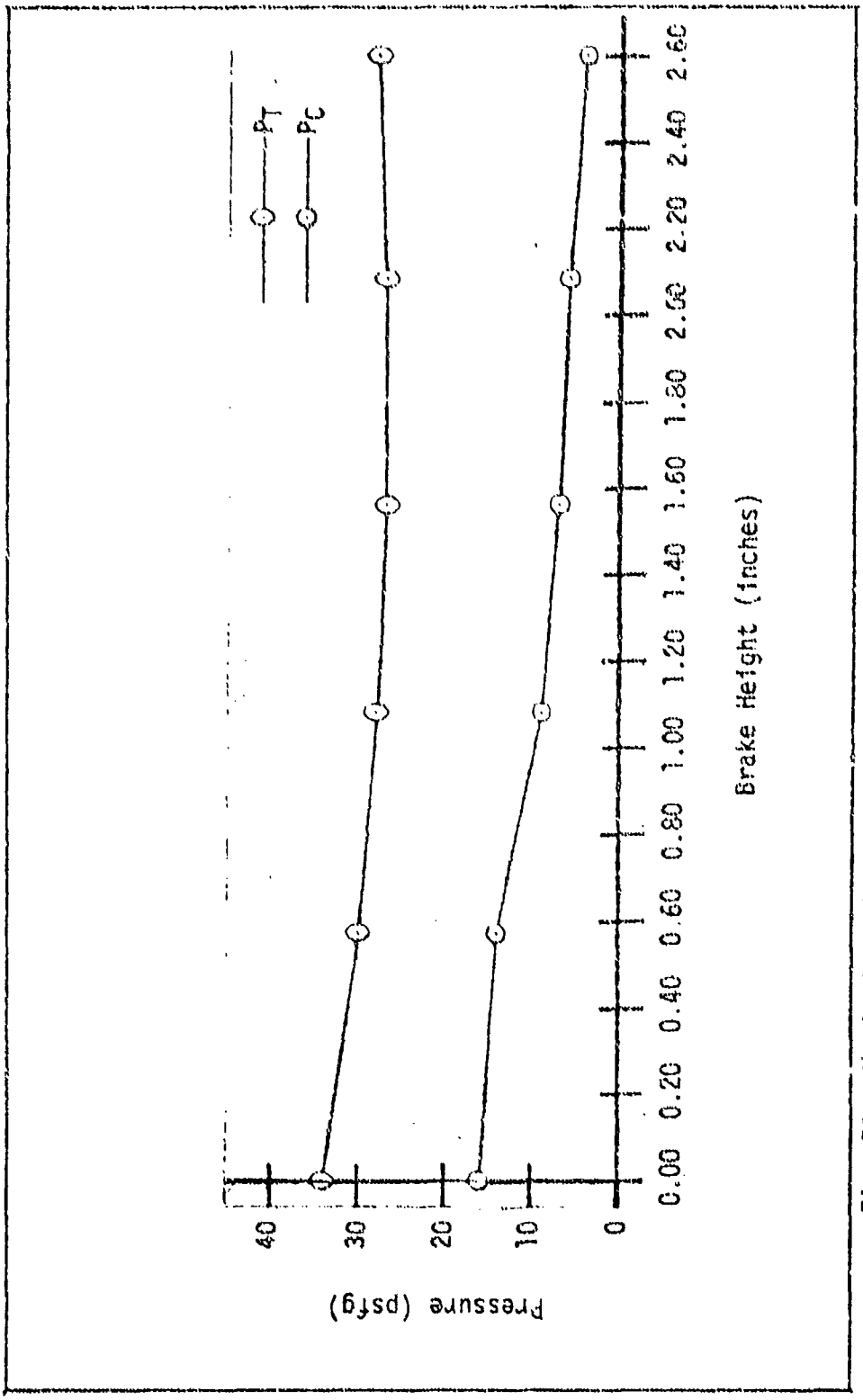

Fig. 53. Variation of Trunk and Cushion Pressures With Brake Height

height was increased to 1.56 inches and then leveled off and gradually increased with increasing brake height. As brake height was increased the model began pitching forward; and above 1.56 inches of brake height the forward portion of the trunk began to compress and flatten, causing the increase in trunk pressure.

The effects of brake height on static drag are shown in Fig. 54. Note the sharp increase in drag for brake heights from 0.57 inches to 1.08 inches. The rapid decrease in cushion pressure within this region has placed more load on the brakes, forcing the brake drag of the model to increase. Additional brake height above 1.08 inches does not increase drag appreciably.

Deceleration rates for each brake height were calculated from the drag data. The method of calculation is found in Appendix E. Figure 55 shows the effects of brake height on deceleration in terms of g_e's ($1\ g_e = 32.2\ ft/sec^2$). Deceleration, being a function of drag, follows the same pattern as drag, showing a rapid increase up to 1.08 inches of brake height. Above that point deceleration is almost constant at approximately 0.34 g_e. The increase in brake height had no substantial effect on the deceleration rate above 1.08 inches of brake height, and thus brake heights above that point provide no worthwhile improvement in braking.

Figures 56 to 60 are photographs of the starboard side of the model showing the brakes attached to the trunk. Figures 59 and 60 show the rear portion of the trunk above the floor for brake heights of 2.60 and 2.08 inches, respectively (numbers shown on model are approximate brake heights). The rear trunk was raised by the brakes approximately

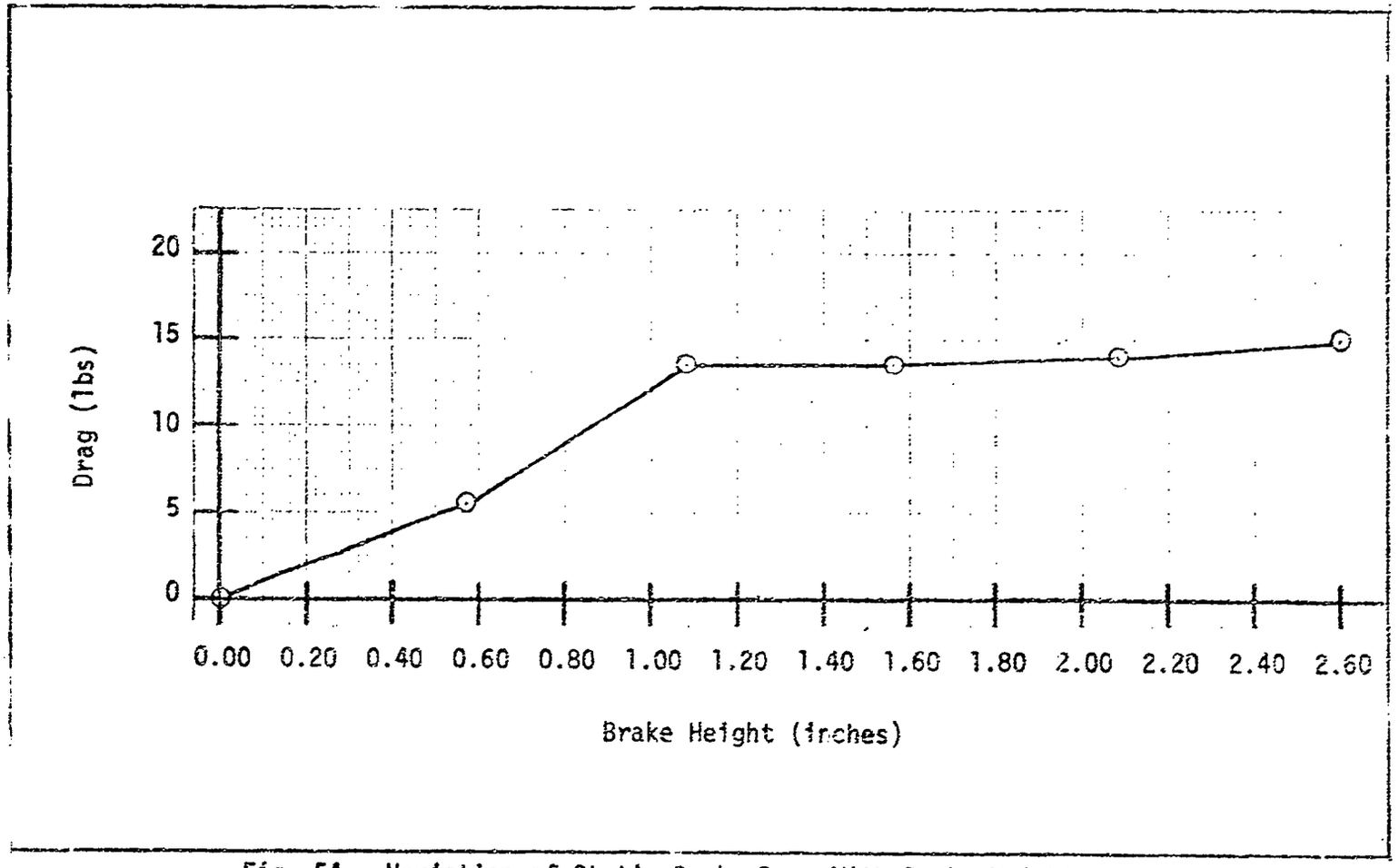

Fig. 54. Variation of Static Brake Drag With Brake Height

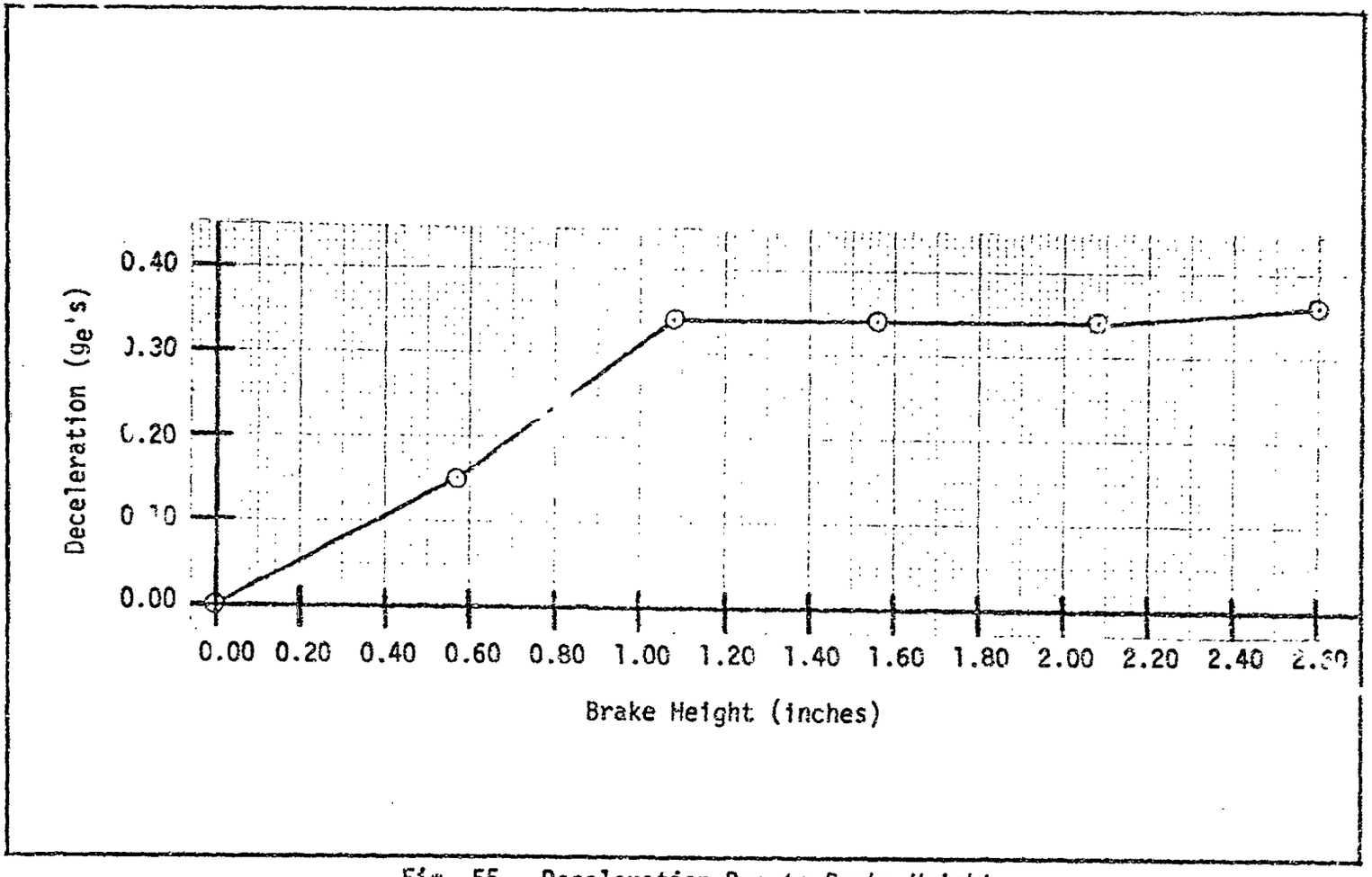

Fig. 55. Deceleration Due to Brake Height

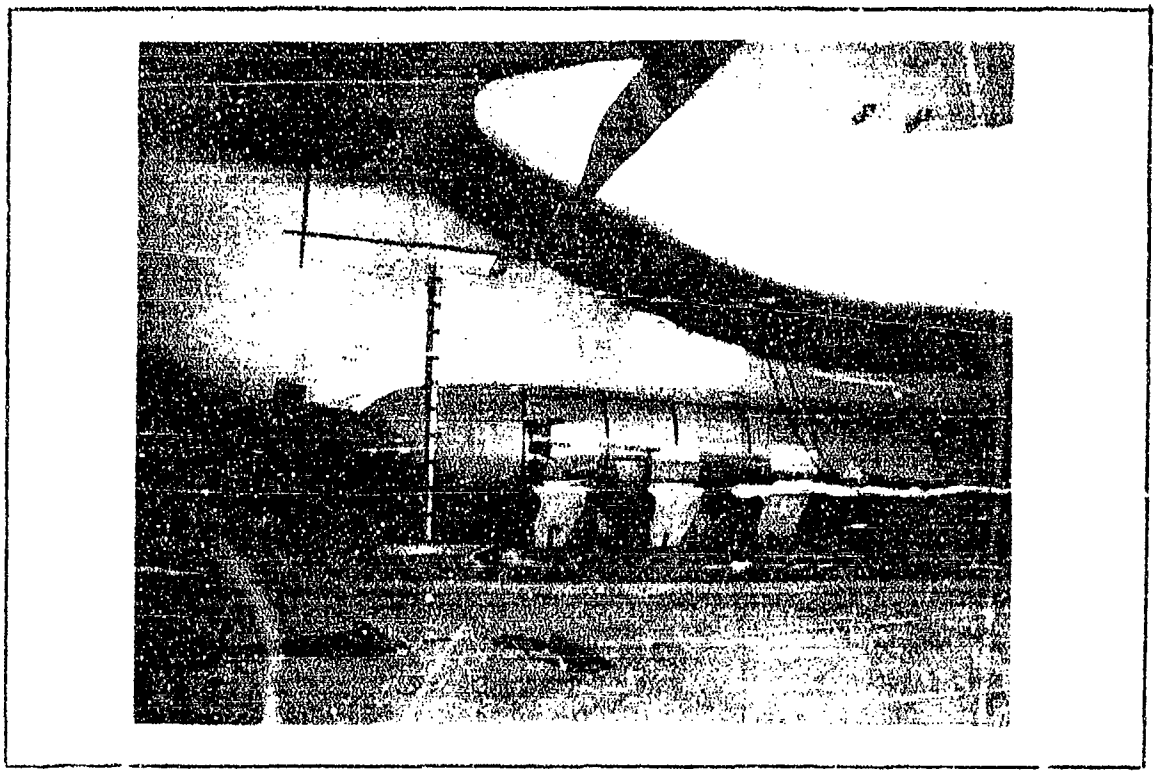

Fig. 56. Starboard View of Brakes, 2.60 inches

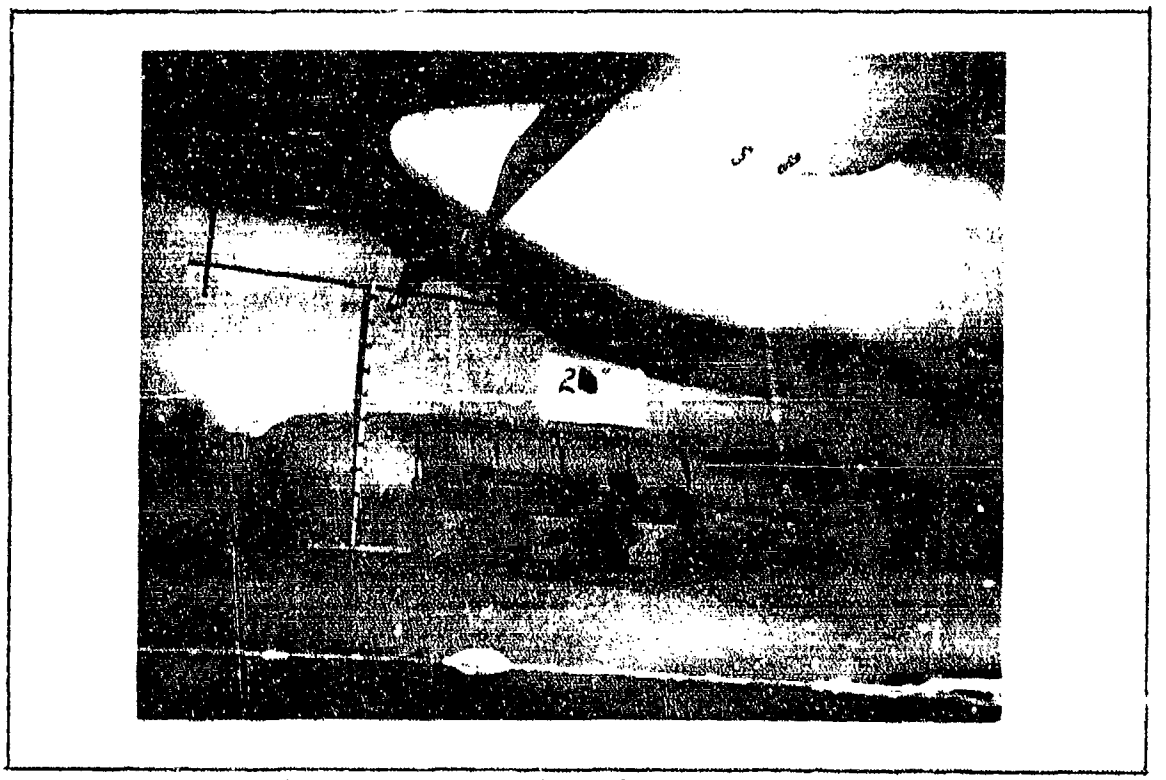

Fig. 57. Starboard View of Brakes, 2.08 inches

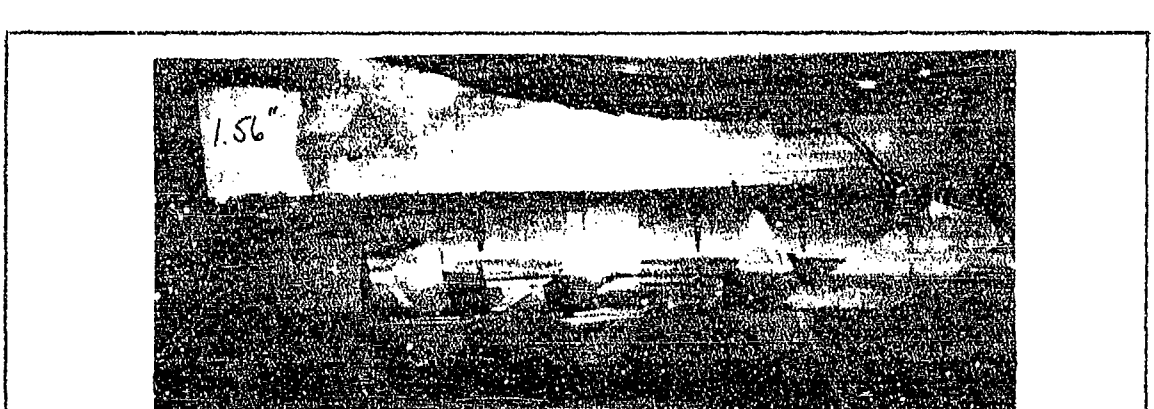

Fig. 58. Starboard View of Brakes, 1.56 inches

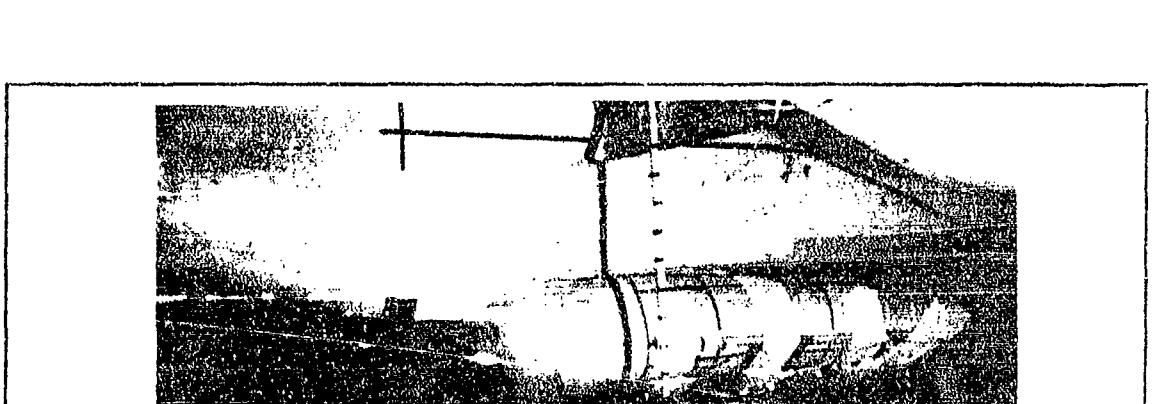

Fig. 59. Starboard View of Brakes, 1.08 inches

Fig. 60. Starboard View of Brakes, .57 inches

1.5 inches above the floor for the 2.60 inches brake height and approximately 3/4 inch for the 2.08 inches brake height. At other brake heights, the rear portion of the trunk maintained its normal hover attitude.

The amount of load being carried by the brakes can be calculated if the trunk area contact is assumed to be zero. With trunk area being zero the equilibrium equation discussed in Chapter IV becomes

$$W_a = P_c A_c + F_b$$

where F_b is the vertical load on the brakes. The air cushion provides negligible friction; therefore, the drag on the system during braking is entirely due to the brakes, and

$$F_b = \text{Drag}/\mu \qquad (5)$$

From the braking data, it was apparent that trunk contact area only began above 1.56 inches of brake height. This fact was observed in increased trunk pressure above 1.56 inches as was discussed. Thus, up to 1.56 inches, the load on the brakes may be calculated as shown above. This calculation reveals that the [illegible]pport as much as 42% of the total load at 1.56 inches of [illegible]bove that height the trunk begins to support a portion [illegible]reased brake height offers no advantage to braking or dece[illegible] discussed.

VI. Conclusions and Recommendations

Conclusions

An experimental investigation of the Air Cushion Landing System has been conducted with a one-tenth scale model of the CC-115 ACLS equipped aircraft. The collected data have revealed the following conclusions:

1. The cushion absorbs most of the impact load due to the vertical velocity at all full-scale sink rates from 0.0 to 12.5 fps except for a 12.0 degree initial pitch attitude with and without roll. Pitch attitudes of 12.0 degrees caused the hard structure of the model to make contact with the floor. A comparison of the long and short trunk tests revealed that trunk pressures and center-of-gravity loading were as much as 36% higher in the AFFDL and Bell short trunk drop tests as compared to the long trunk tests of this report. Cushion pressures of the AFFDL and Bell short trunk tests were as much as 20% higher than long trunk tests.

2. Vertical stiffness of the tenth-scale long trunk was approximetel, 125 pounds per inch of trunk deflection between 20 and 75 pounds of load on the ACLS.

3. Forward, or positive, pitch stiffness was found to be about 88% greater than the aft pitch stiffness of 3.3 foot-pounds per degree of pitch. Roll stiffness increased with increasing angle up to 46 inch-pounds of required torque for a 16-degree roll angle.

4. Up to loads of 4.1 times the model weight the pressure footprint of the ACLS never exceeded the trunk pressure at that loading. The trunk pressure of the model at 4.1 times the model weight was 55 psfg.

5. Braking tests revealed that brake pillows above 1.08 inches of tenth-scale brake height did not increase deceleration rates beyond about 0.34 g.

Recommendations

Based on the results of this study the following recommendations are made:

1. Data from the drop tests revealed differences in ACLS responses between the tenth-scale model and the quarter-scale model due to the different fan characteristics of the two models. An investigation should be made to observe how the ACLS is affected by the use of a centrifugal flow fan air supply as opposed to an axial flow fan air supply. The investigation should also reveal the benefits and disadvantages to ACLS of the one system as compared to the other.

2. Theoretical computer models of the ACLS should be developed incorporating the results gathered from this study.

Bibliography

1. Coles, A. V. Air Cushion Landing System CC-115 Aircraft. Technical Report AFFDL-TR-72-4, Part I. Wright-Patterson Air Force Base, Ohio: Air Force Flight Dynamics Laboratory, May 1972.

2. Digges, K. H. Theory of an Air Cushion Landing System. Technical Report AFFDL-TR-71-50. Wright-Patterson Air Force Base, Ohio: Air Force Flight Dynamics Laboratory, June 1971.

3. Vaughan, John C., III, Shade Campbell and David J. Pool. Static and Drop Tests of a Quarter-Scale Model of the CC-115 Aircraft Equipped With an Air Cushion Landing System. Technical Memorandum AFFDL-TM-72-01-FEM. Wright-Patterson Air Force Base, Ohio: Air Force Flight Dynamics Laboratory, September 1972.

APPENDIX A

Determination of Model Similarity and Equipment Installation

Introduction

This appendix describes how the tenth-scale model was checked and adjusted to suit desired geometric and dynamic similarity to its full-scale counterpart. In addition, specifications and locations of all equipment installed in the model are provided.

Physical Dimensions of the Model and Trunk

All physical dimensions such as wingspan, fuselage length and width, and trunk length were checked and verified as being equivalent to full-scale dimensions by using the scaling parameters found in table I of Chapter I. The trunk was constructed by the Bell Aerospace Company, and its specifications for the OGE inflated condition (trunk pressure = 32 psfg) are found in Fig. 61.

Equipment Installation

Before adjusting the model center of gravity location, all necessary equipment was installed in the model. This equipment consisted of the centrifugal fans, the motor to rotate the fans, two pressure transducers, and four accelerometers. The fans and the motor were described in Chapter II. Specifications on the pressure transducers and the accelerometers are as follows:

Pressure Transducers (2):

Statham Differential Pressure, Bellows Transducer
Model PL 283TC-0.5-350
Range: ±0.5 psi
Low side vented to atmosphere

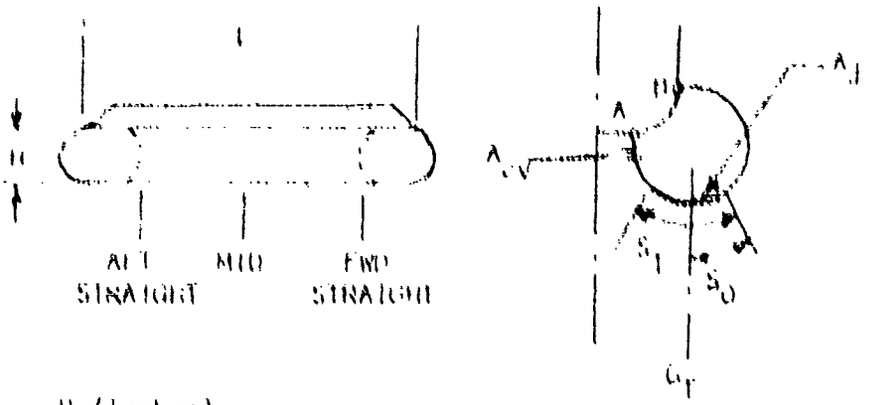

H (inches)

Forward centerline	3-3/4
Forward straight	4-3/8
Mid	4-1/4
Aft straight	4-1/8
Aft centerline	3-1/2

Girth from A to B (inches)

Forward centerline	11-5/8
Forward straight	14-1/4
Aft straight	14-1/4
Aft centerline	11-1/4

Jet nozzles, A_j

Diameter of each (inches)	0.034
Total A_j area (sq inches)	3.32
Distance S_T (inches)	3.075
Distance S_0 (inches)	0.615

Cushion vent orifices, $A_{i:v}$

Number of holes	34
Diameter of each hole (inches)	0.5

Trunk length, L (inches) 38-1/16

Fig. 61. Trunk Specifications of Tenth-Scale Model (From Ref 1:351)

Accelerometers (4).

Consolidated Electrodynamics Corporation

Model 4-202-0001

Range: ±5 g's

The location of this equipment on the model is found in Fig. 62. In addition to this equipment, plastic tubing was led from the model to the manometers to measure static trunk and static cushion pressure directly when the model was in an equilibrium condition. This tubing arrangement is also shown in Fig. 62. Although taps for cushion pressure measured by the transducer and the manometer were at two different locations, the resulting values of the two locations were equal. The center of gravity accelerometer was placed as close to the model center of gravity as possible. The fan motor location prevented the accelerometer from being exactly at the center of gravity.

Weight and Center of Gravity Determination

After all equipment, excluding plastic tubing, was installed, the model was weighed on a Toledo scale which has a range from 0 to 800 pounds in 1/2-pound increments. The model weighed 38.0 pounds. The model was left at this weight to adjust the center of gravity location. The model center of gravity was fixed and checked in each of three axes as shown by Fig. 63. First, the location in the x-axis was adjusted by balancing the model on two pivot points on the port and starboard sides of the fuselage at the desired center of gravity location. Small weights were added and subtracted at various locations on the model until it was perfectly balanced on the pivoting stand as shown in Fig. 63. To establish the center of gravity location in the y and z directions, the model was suspended by an eyelet hook in its tail via parachute cable from a beam

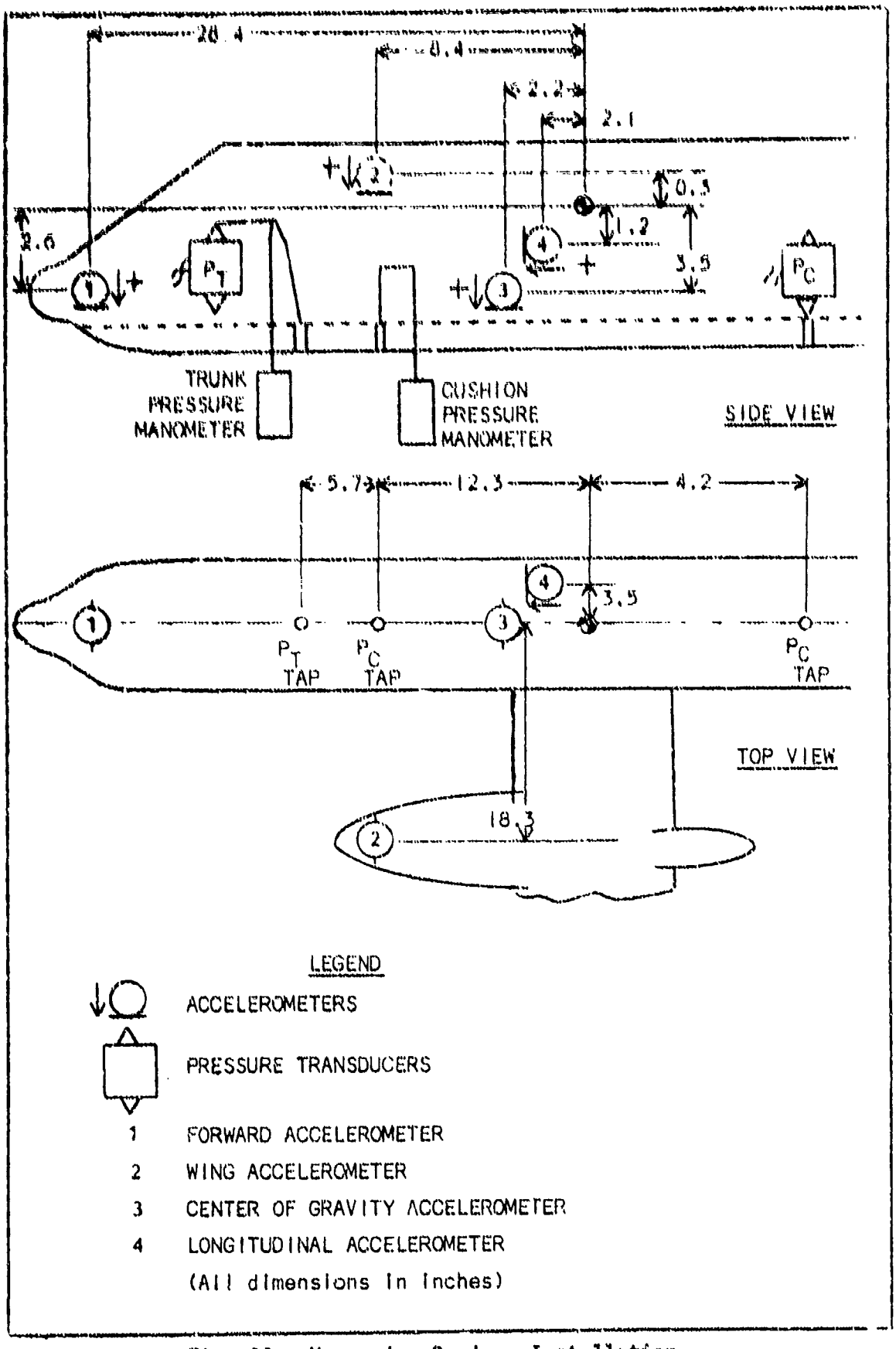

Fig. 62. Measuring Devices Installation

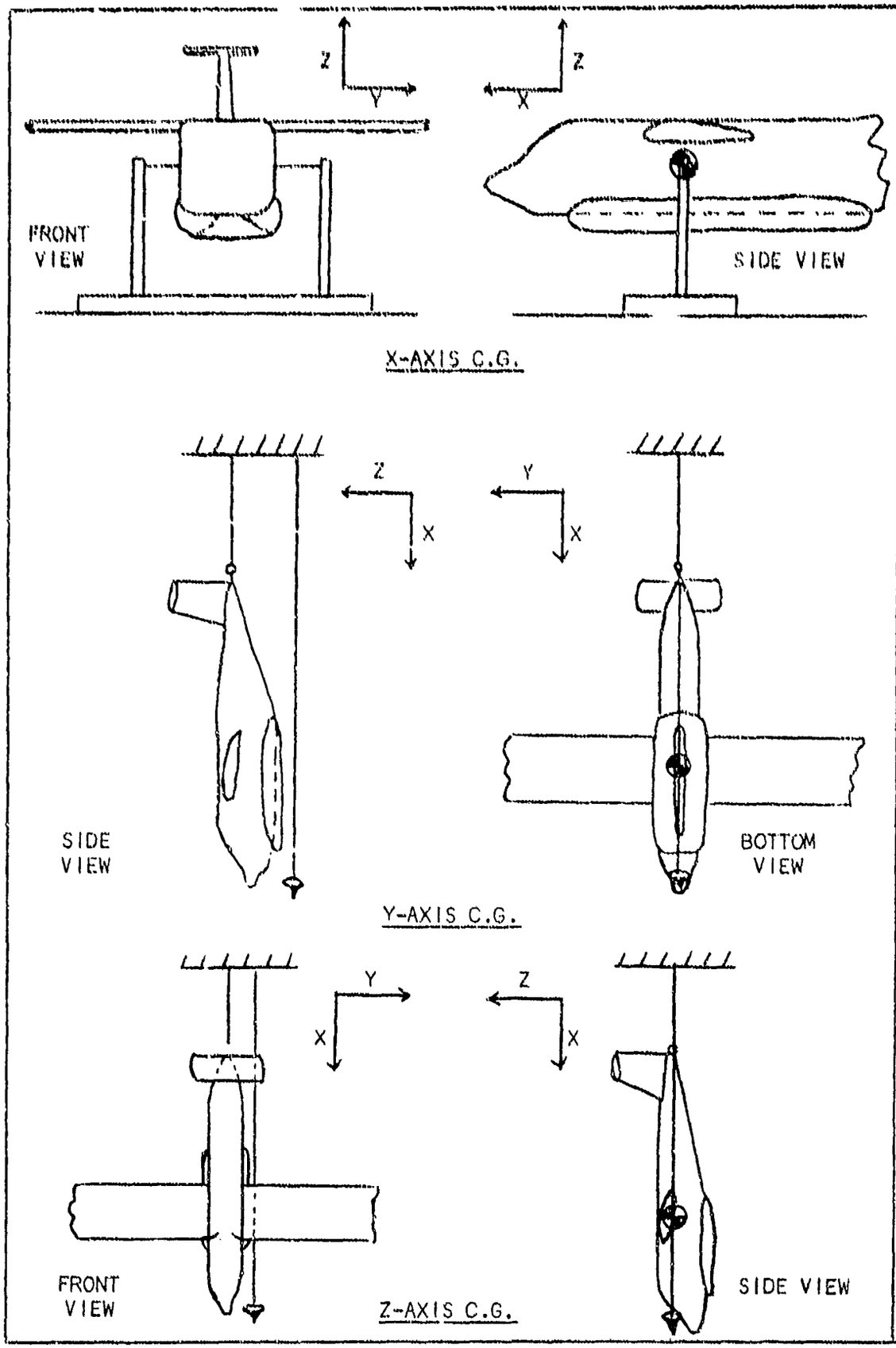

Fig. 63. Center of Gravity Adjustment

above the floor, and the model was allowed to hang freely. Next, a string with a plumb bob was dropped along planes parallel to the y and z plane directions as shown in Fig. 63. For the z direction, it was desired that the plumb bob line would intersect the already fixed x center of gravity point, as it so did. In the y direction, it was desired that the plumb line would fall along the longitudinal centerline of the model, as it also did. The model was again weighed, and additional weight was added to the model center of gravity location to bring the model weight up to the desired 39.1 pounds. To insure that the center of gravity had not changed, the procedure to adjust the center of gravity was repeated, and no changes were found to be necessary.

Moments of Inertia

After the weight and the center of gravity were fixed, the moments of inertia of the model were experimentally obtained in roll, pitch, and yaw. To accomplish this measurement the model was hung from a support as shown in Fig. 64 in each of the roll, pitch, and yaw planes. Hung in this manner, the model was deflected from its equilibrium position in each case and allowed to freely oscillate in the roll, pitch, and yaw planes. The model was allowed to oscillate for a specific number of cycles, one cycle consisting of the swing from one side of an arc to the other and back to its initial position. While the number of cycles was counted, an electric timer was used to measure the duration of the specified number of cycles. In this manner the frequency of oscillation was obtained, the inverse of which is the period of oscillation T. Once the period, the weight or mass of the model, and the pivot point distance from the

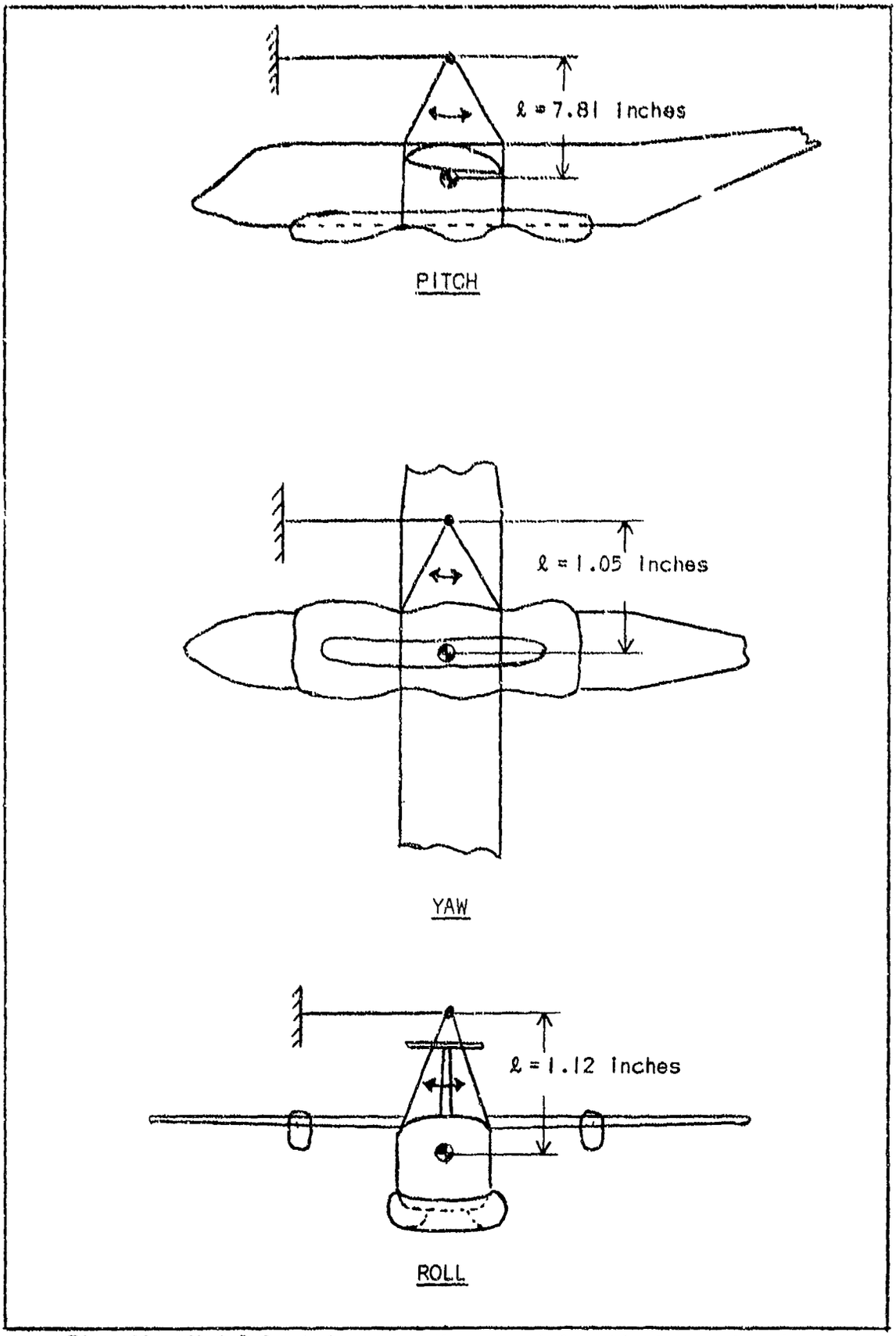

Fig. 64. Model Positions for Moment of Inertia Determination

center of gravity were known, the moments of inertia about the three axes of pitch, yaw, and roll could be calculated using the following equation for each plane:

$$I = \frac{Mg_e \ell T^2}{4\pi^2} - M\ell^2 \qquad \text{(A-1)}$$

In order to obtain the period by this method, it was assumed that drag on the model during oscillation was negligible. This experimental procedure was performed several times in each plane in order to verify the results. The moments of inertia of the model were found to be:

Pitch: 2.71 slug ft^2

Roll: 2.05 slug ft^2

Yaw: 4.55 slug ft^2

APPENDIX B

Equipment, Procedures, and Data Reduction For Drop Tests (OGE and IGE)

Introduction

This appendix discusses the electronic equipment, the procedures, and the data reduction used to conduct the drop tests of Chapter III. The discussion applies to both OGE and IGE drop tests.

Recording Equipment

In order to gather pressure and g-load data during a drop test, two pressure transducers and four accelerometers had to be installed in the model as was explained in Appendix A. The signals from these devices were calibrated and then transmitted as shown by the schematic in Fig. 65.

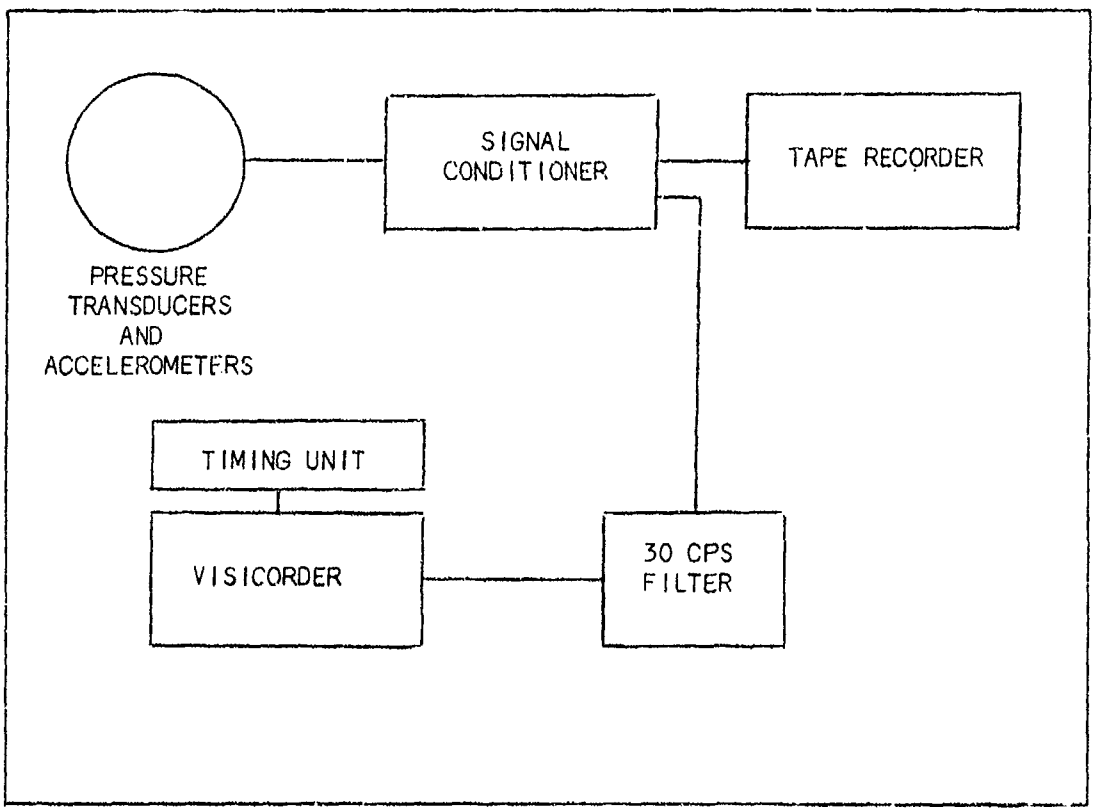

Fig. 65. Electronic Signal Path

The calibrated signals from these devices were fed into a Bell and Howell Datatape recorder and signal conditioning unit where they were converted into electronic impulses. These impulses were then recorded on magnetic tape for later reproduction, if desired. At the same time the conditioned signal was also fed into a 30 cycles per second filter to eliminate undesirable noise in the signal. From that point the filtered signal was fed into a Honeywell Visicorder model 906A1680GH. Filters with frequencies above and below 30 cps were tried and were found to either include too much noise due to fan rpm or to eliminate data peaks that were considered important. The visicorder transformed the filtered signal into traces on Kodak Linagraph Direct Print Paper, which was 6 inches wide. All six signals or traces were recorded on the 6 inch wide paper but were easily discernible for data reduction. Attached to the Visicorder was a Honeywell Timing unit which provided timing lines across the width of the paper every 0.01 seconds. The paper was run in the Visicorder at 50 inches per second for each drop test. Data reduction was performed directly from the traces of the Visicorder. The process of data reduction and accuracy will be explained shortly.

Model Support Cables

The model was supported by three points as shown in Fig. 66. Parachute cord was used to attach the three points at one central point. This arrangement allowed pitch attitude to be adjusted by use of the forward or nose cable and roll adjustment by use of the port and starboard cable. From the central point another parachute cord was tied and fed through an overhead pulley held up by an overhead hoist. The cable through the pulley was fed onto a shaft of a Boston gear reduction unit with a 30

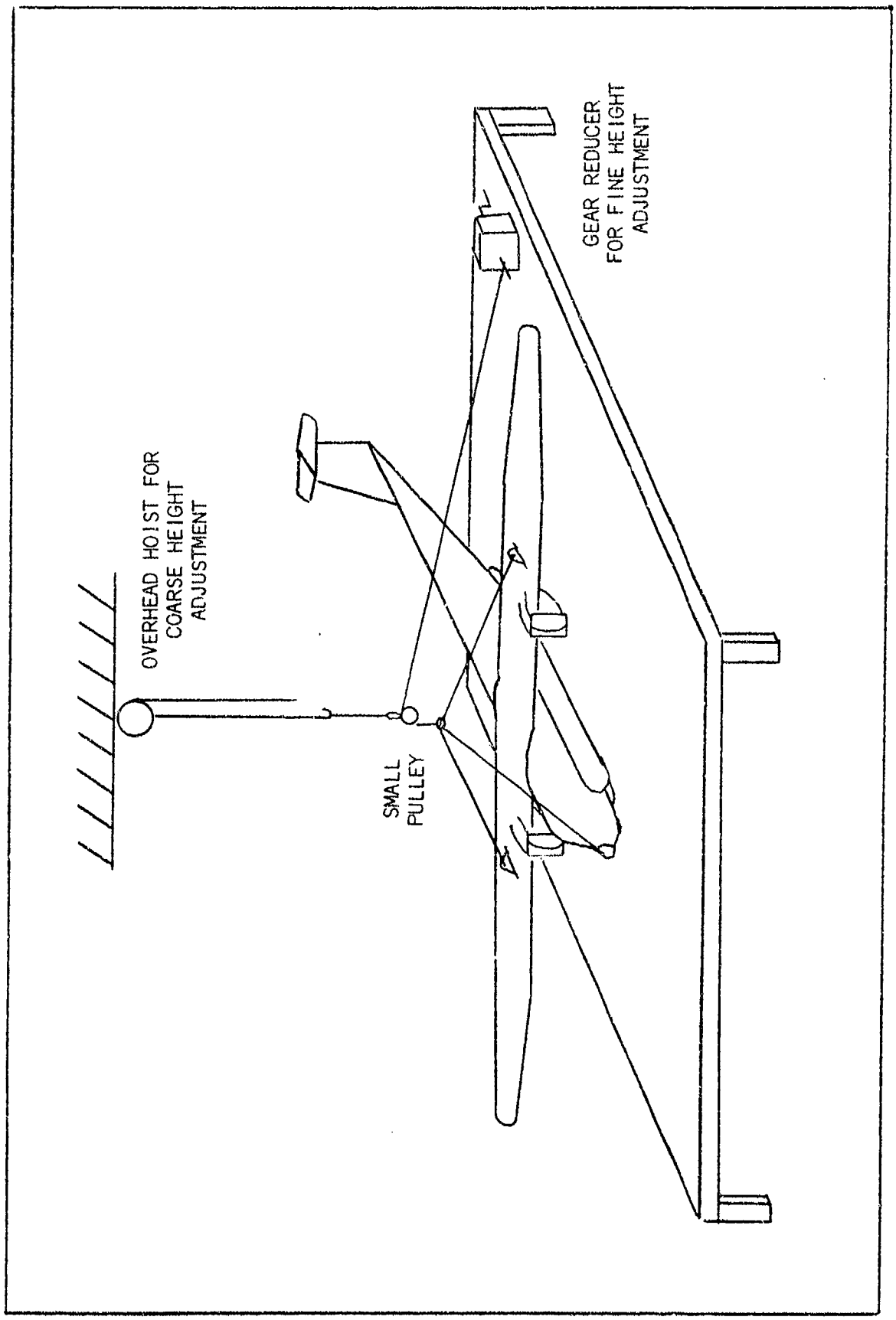

Fig. 66. Model Support and Cable Attachment

to 1 ratio. The gear reducer was located on the floor of the platform. In this manner the overhead hoist was used for coarse height adjustment and the gear reducer for fine adjustment. Cabling and pressure tubing to the model was supported by the overhead hoist in such a way as not to interfere with the model motion or weight during a drop test. The model was released at the desired time by cutting the cable tied to the gear reducer with a pair of scissors.

Photography

Two high-speed cameras (500 frames per second) were situated as shown in Fig. 67 for the drop tests. Cameras 1 and 2 were used for IGE tests, and cameras 1 and 3 for OGE tests. Position of the cameras was changed for the OGE tests merely to provide a different view of a drop test.

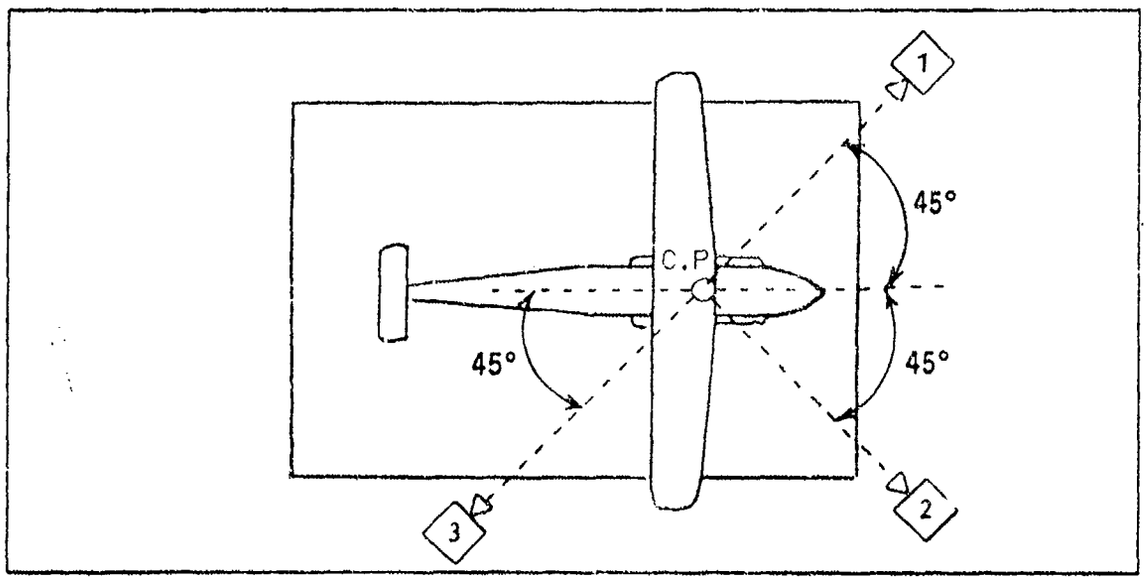

Fig. 67. Camera Positions

Transducer and Accelerometer Calibration

At the beginning of each day of drop tests, all instrumentation was calibrated. The two pressure transducers were calibrated simultaneously

by placing a known air pressure, measured by a water manometer, directly to the measuring port of each transducer. At each pressure of 0, 5, 10, and 12 inches of water the corresponding signal was recorded on the Visicorder paper and its pressure value noted. The accelerometers were calibrated using the normal force of gravity due to the earth, and the fact that the accelerometers measure acceleration only in the plane in which they are mounted. When the model was level, all accelerometers except that on the longitudinal axis were considered at +1 g-load due to the 1 g_e of gravity. The longitudinal accelerometer was considered at 0 g_e acceleration. To obtain a -1 g-load deflection on all but the longitudinal axis accelerometer, the model was turned upside down; and to record a +1 g_e acceleration on the longitudinal axis and 0 g-load on the remaining accelerometers, the model was placed on its nose perpendicular to the base of the longitudinal accelerometer. This method is effective, since the accelerometers only measure loads or accelerations along the perpendicular axis to which they are mounted. Thus when this axis is placed perpendicular to the g_e vector through the floor the accelerometer will read zero. At each position mentioned, the output signal was recorded; and its g-load or acceleration value noted. Thus for each value of pressure and g-load or acceleration a corresponding deflection of the line trace on the Visicorder paper was measured and a calibration factor developed in terms of the amount of pressure or g-load per inch deflection. The calibration factors for each series of drop tests are listed on the next page.

Test Number	P_T (psfg/inch)	P_C (psfg/inch)	G_n (g/inch)	G_w (g/inch)	G_ℓ (g/inch)	$G_{c.g.}$ (g/inch)
1 - 9	32	21	2.0	2.0	2.0	2.0
10 - 11	32	21	2.0	2.0	2.0	2.0
12 - 15	32	20	1.9	2.0	1.8	2.0
20 - 29	31	20	1.9	2.0	1.9	2.0
30 - 43	32	22	2.1	1.9	1.9	2.2

Note: G_n--nose accelerometer; G_w--port nacelle accelerometer; G_ℓ--longitudinal accelerometer.

Trunk Pressure, Cushion Pressure, Fan rpm, and Barometric Pressure

Initial trunk pressure had to be adjusted to 34 psfg (6.6 inches of water) for IGE tests and 32 psfg (6.05 inches of water) for OGE tests. In each case the desired trunk pressure was obtained by covering the vent holes in the cushion cavity as shown in Fig. 68. These holes were covered using masking tape. Fourteen holes were covered for the OGE mode and two holes for the IGE mode. Covering the holes restricts air flow out of the trunk, thereby increasing trunk pressures and decreasing air supply to the cushion. The desired trunk pressures were obtained with fans rotating at 8600 rpm simulating a 640 full-scale horsepower supply. Trunk pressure in the equilibrium condition was measured by a Meriam Type W water manometer with a range from 0.0 to 40.0 inches of water. Cushion pressure was measured in the same condition using a 15

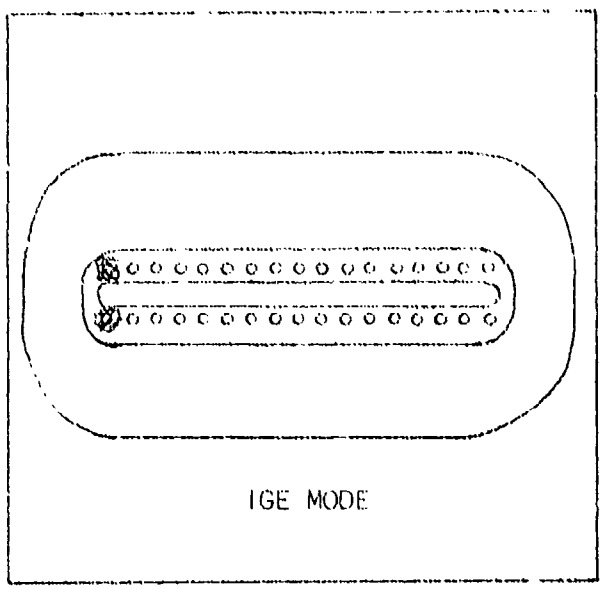

Fig. 68. Trunk Vent Holes

inch CDDC water manometer. Both manometers were vented to the atmosphere to give gauge pressure.

Fan rpm was measured by means of a General Radio Company stroboscope with a range from 100 to 25,000 rpm and accurate to the nearest 100 rpm. The stroboscope light was directed onto the fan blades and the light frequency adjusted until the fan blades appeared stationary. At that time the fan rpm was recorded from the stroboscope. Barometric pressure was recorded from a Hass Brothers Instrumentation Company mercury-filled barometer. The barometer provided atmospheric pressure to the nearest 0.1 mm of mercury. In addition a thermometer was attached to the barometer to give temperature in degrees centigrade to the nearest 0.5 degrees.

Roll and Pitch Attitude Adjustment

Roll and pitch angles were obtained as shown in Fig. 69. The model was first set so that it was perfectly level above the floor, i.e., its roll and pitch axes were parallel to the floor of the platform. For a roll of -7.5 degrees, a height difference of 1.47 inches for the center of gravity markers on the fuselage was necessary.

The model was rolled by adjusting the port and starboard support cables until this height difference was reached within ±.005 inches. A 19-inch Brown and Sharp steel vernier equipped ruler accurate to 0.001 inches was used to make these measurements in roll and pitch. For pitch, a distance of 1.00 feet from the center of gravity was measured along the port fuselage on a line parallel to the longitudinal center-of-gravity axis. Then for 6.0 degrees and 12.0 degrees of pitch, a required height difference of 1.25 inches and 1.18 inches, respectively, was measured. The forward cable was adjusted until this height difference was within ±.005 inches. For

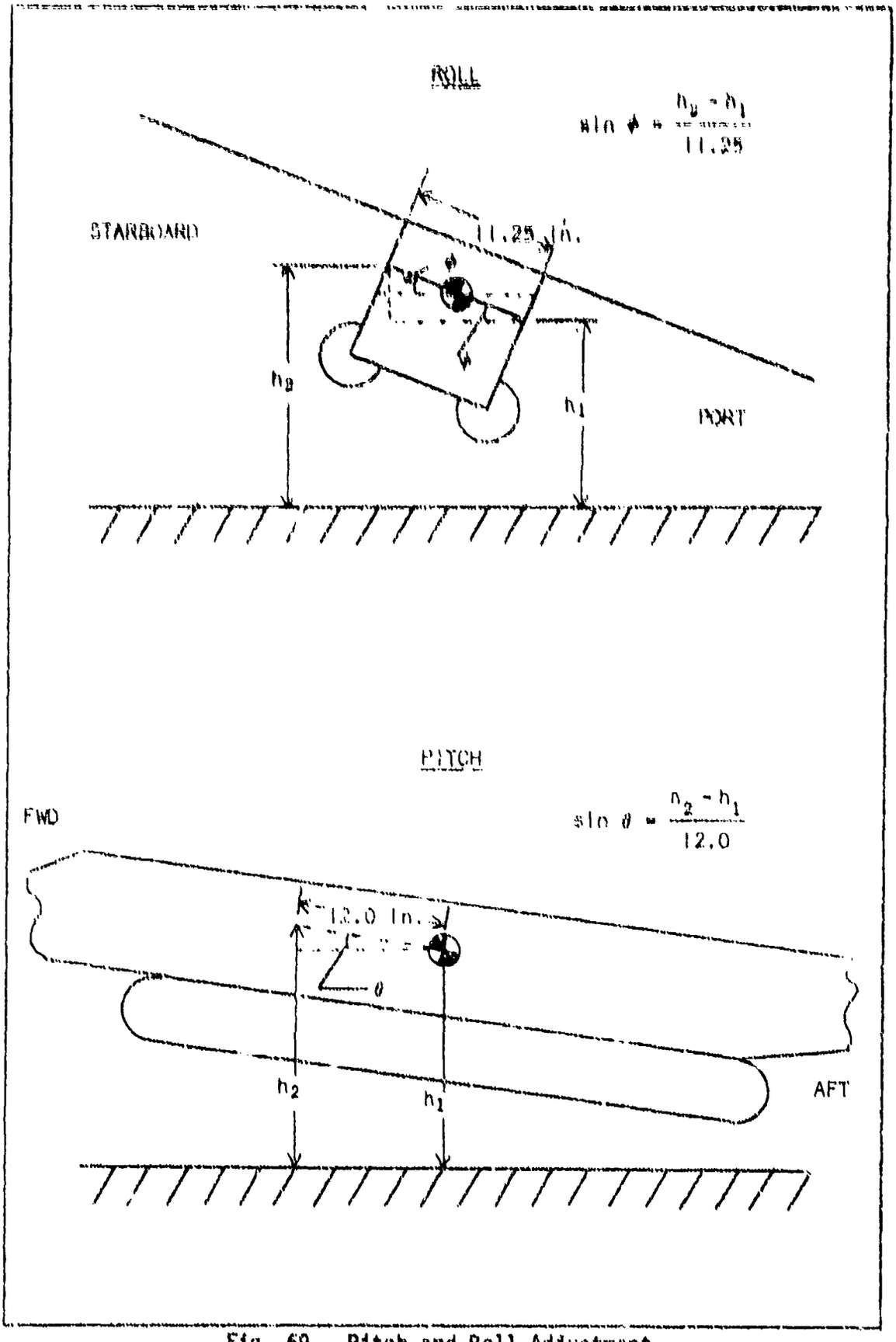

Fig. 69. Pitch and Roll Adjustment

combined pitch and roll, the desired attitude of the model was that the longitudinal center-of-gravity axis be at a specific pitch angle with the platform and that the model also be rolled about the inclined longitudinal axis. To obtain this desired position, it was necessary to roll the model first around the longitudinal axis as was mentioned above for pure roll. Then with the desired roll angle adjusted, the longitudinal axis was inclined, or pitched, vertically away from the floor of the platform (see Fig. 70) using the method for obtaining pure pitch as previously described. Thus pitch was obtained without disturbing roll.

Sink Rate

In order to simulate the desired full-scale sink rate, the scaled value of sink velocity was calculated using the scaling parameters. Then by use of Eq 1, Chapter III, the necessary drop heights were determined. The drop heights for each full-scale sink rate were:

Full Scale Velocity (fps)	Drop Height (inches)
12.5	2.92
11.0	2.27
8.0	1.20
5.0	0.47
3.0	0.17

Wooden blocks were constructed to the required dimensions and were used as gauges to obtain desired drop height between the floor of the platform and the lowest point on the inflated trunk. The model was considered at the required drop height when the trunk just touched the top of the wooden block.

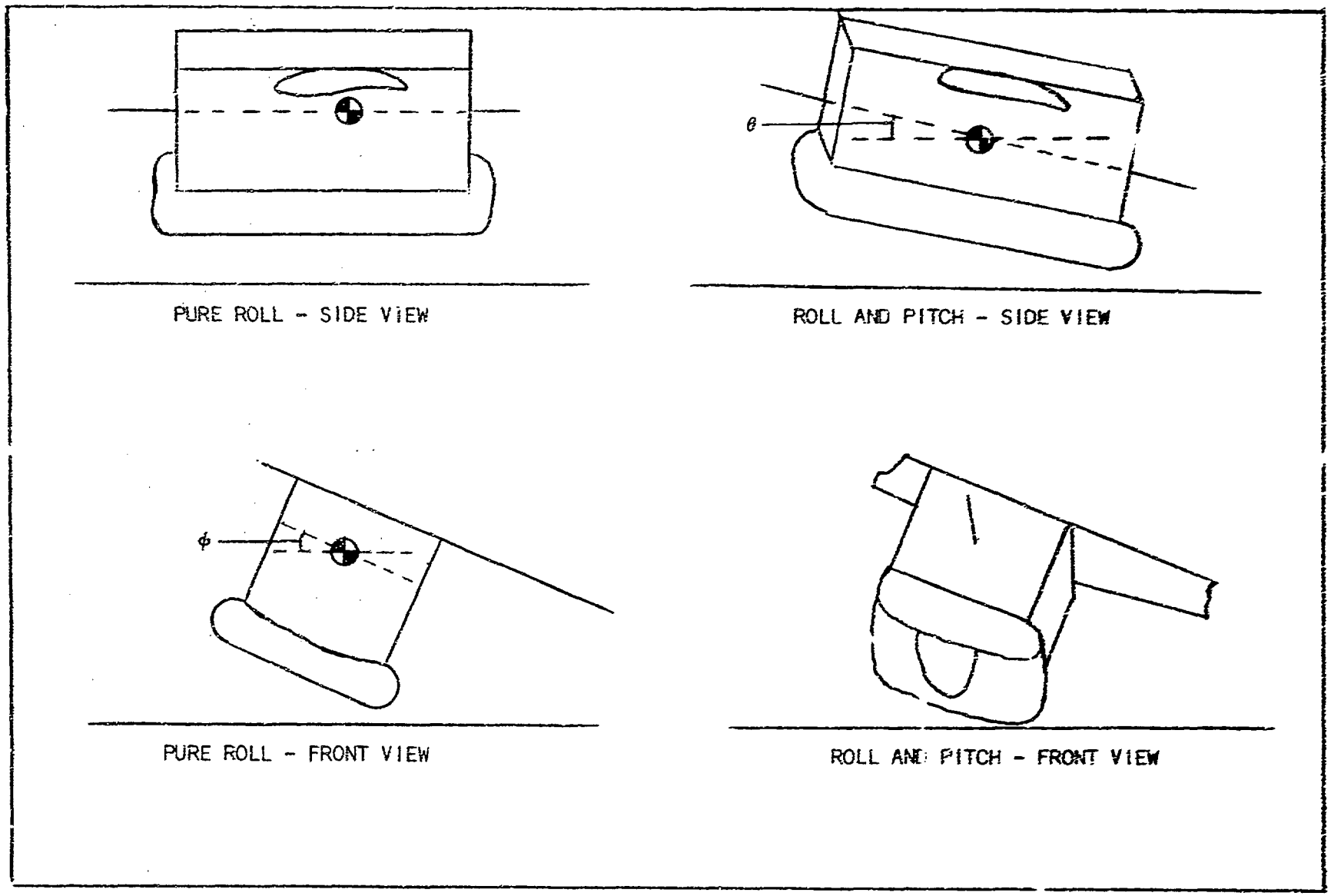

Fig. 70. Combined Roll and Pitch Adjustment

Checklist

The following checklist was used for each drop test run:

I. Design Condition Check

A. Check fan rpm

B. Check trunk pressure and cushion pressure

OGE _____

IGE _____

C. Shut power off

II. Attitude Adjustment

A. Check cable support

B. Tie cable to gear reducer pulley

C. Adjust pitch

D. Adjust roll

III. Test Run

A. Turn power on

B. Check trunk pressure (OGE or IGE)

C. Raise model with hoist to approximate drop height

D. Place model at desired height with wooden spacer bar and gear reducer pulley

E. Check trunk pressure OGE _____

F. Turn on magnetic tape recorder

G. Turn on cameras

H. Turn on Visicorder at 50 inches per second

I. Cut cable support

J. Shut off Visicorder at +3 seconds after release

K. Shut off cameras at +5 seconds after release

L. Shut off magnetic tape recorder

M. Measure following while model is IGE

Fan rpm _____

Trunk pressure _____

Cushion pressure _____

N. Shut off all power

O. Measure barometric pressure and temperature of atmosphere

Data Reduction

Data reduction was accomplished directly from pressure readings off the manometers in the case of initial equilibrium trunk and cushion pressure measurements and from the line traces of the Visicorder in the case of the dynamic pressures and g-loads. Initial trunk and cushion pressures were recorded in inches of water to the nearest 0.1 inch, but this reading was converted to pounds per square foot to the nearest psfg (1 inch H_2O = 5.2 psfg). When calibrations on the electronic equipment were performed, the zero point of each pressure transducer and accelerometer was noted. To reduce the traces to final data, the deflection of each data trace from the zero point was measured with a ruler graduated with tick marks every 0.02 inches. Data points were recorded at every 0.01 seconds and also at peak points between the 0.01 second marks. The deflections were recorded and then multiplied by the appropriate calibration factors listed previously to obtain final data. Final data contain the same number of significant figures as that of the multiplying factor with the least number of significant figures. Thus final data are accurate to ±0.5 psfg and ±0.05 g-loads for pressure transducers and accelerometers, respectively.

The zero time from release point was determined from the accelerometer traces. Before release the model is supported above the platform in a stable condition, and the center-of-gravity accelerometer was at a +1 g-load level. When the model is released, the downward acceleration of -1 g_e changes the accelerometer trace to 0 g-load during free fall. Thus the zero time from release point was noted as the first deflection of the center-of-gravity accelerometer from the +1 g-load position.

Trace readings were usually made on the 0.01 second marker. The distance between each marker was 0.5 inches, since the paper travel was 50 inches per second. Thus to obtain time between the 0.01 second markers, the distance from the previous marker was measured in inches and multiplied by 0.01 seconds/0.500 inches or 0.020 seconds per inch, and that value was added to the time measured at the last marker. Time was thus recorded to the nearest 0.001 seconds.

APPENDIX C

IGE and OGE Drop Test Data

This appendix contains data from the IGE and OGE drop tests not specifically discussed in Chapter III. The data from the IGE mode are only taken from the key events of release, touch, peak pressures, peak loads, and top of the first bounce for the full-scale sink rates of 11.0, 8.0, 5.0, and 3.0 fps. Data from the OGE mode consist of graphs of the 12.5 fps, full-scale drops at the attitudes not discussed in Chapter III as well as data at the key events of the 8.0 fps, full-scale, drops.

Data presented at key events are placed in tabular form from Table IV to Table XXV, while graphs are found from Fig. 71 to Fig. 75. The time in the tables is that from time of release of the model.

TABLE IV

IGE Drop Test Data, 11.0 fps, θ = 0.0, ϕ = 0.0
(Test No. 27)

Time (sec)	Event	P_T (psfg)	P_C (psfg)	$G_{c.g.}$ (g-load)
0.000	Release	26	0	0.0
0.100	Touch	26	2	0.0
0.140	Peak trunk pressure	49	40	2.6
0.149	Peak cushion pressure	48	41	2.9
0.180	Peak $G_{c.g.}$-load	47	38	3.2
0.290	Top of first bounce	25	1	0.2

TABLE V

IGE Drop Test Data, 11.0 fps, θ = 0.0, ϕ = -7.5
(Test No. 13)

Time (sec)	Event	P_T (psfg)	P_C (psfg)	$G_{c.g.}$ (g-load)
0.000	Release	25	0	0.0
0.114	Touch	25	3	0.0
0.165	Peak cushion pressure	47	39	3.1
0.174	Peak trunk pressure	50	38	2.9
0.196	Peak $G_{c.g.}$-load	49	36	3.3
0.345	Top of first bounce	27	2	0.3

TABLE VI

IGE Drop Test Data, 11.0 fps, θ = 6.0, ϕ = 0.0
(Test No. 22)

Time (sec)	Event	P_T (psfg)	P_C (psfg)	$G_{c.g.}$ (g-load)
0.000	Release	26	0	0.0
0.113	Touch	26	2	0.0
0.192	Peak trunk pressure and $G_{c.g.}$-load	58	44	3.8
0.196	Peak cushion pressure	56	45	3.8
0.366	Top of first bounce	28	1	0.0

TABLE VII

IGE Drop Test Data, 11.0 fps, θ = 6.0, ϕ = -7.5
(Test No. 19)

Time (sec)	Event	P_T (psfg)	P_C (psfg)	$G_{c.g.}$ (g-load)
0.000	Release	27	0	0.0
0.120	Touch	27	2	0.0
0.190	Peak trunk pressure	56	3	3.4
0.194	Peak $G_{c.g.}$-load	56	37	3.5
0.206	Peak cushion pressure	54	41	3.4
0.375	Top of first bounce	31	1	0.2

TABLE VIII

IGE Drop Test Data, 11.0 fps, θ = 12.0, ϕ = 0.0
(Test No. 24)

Time (sec)	Event	P_T (psfg)	P_C (psfg)	$G_{c.g.}$ (g-load)
0.000	Release	27	0	0.0
0.120	Touch	27	2	0.0
0.188	Peak trunk pressure	45	13	2.7
0.197	Peak $G_{c.g.}$-load	43	13	4.4
0.258	Peak cushion pressure	41	35	2.5
0.378	Top of first bounce	28	1	0.0

TABLE IX

IGE Drop Test Data, 11.0 fps, θ = 12.0, ϕ = -7.5
(Test No. 16)

Time (sec)	Event	P_T (psfg)	P_C (psfg)	$G_{c.g.}$ (g-load)
0.000	Release	26	0	0.0
0.116	Touch	26	1	0.0
0.183	First peak trunk pressure and peak $G_{c.g.}$-load	39	4	4.8
0.259	Peak cushion pressure and second peak trunk pressure	43	33	2.5
0.440	Top of first bounce	30	0	0.6

TABLE X

IGE Drop Test Data, 8.0 fps, $\theta = 0.0$, $\phi = 0.0$
(Test No. 28)

Time (sec)	Event	P_T (psfg)	P_C (psfg)	$G_{c.g.}$ (g-load)
0.000	Release	28	0	0.0
0.070	Touch	28	3	0.0
0.137	Peak cushion pressure	52	41	2.8
0.138	Peak trunk pressure	53	40	2.9
0.144	Peak $G_{c.g.}$-load	52	39	3.0
0.250	Top of first bounce	28	3	0.2

TABLE XI

IGE Drop Test Data, 8.0 fps, $\theta = 0.0$, $\phi = -7.5$
(Test No. 14)

Time (sec)	Event	P_T (psfg)	P_C (psfg)	$G_{c.g.}$ (g-load)
0.000	Release	25	0	0.0
0.088	Touch	25	2	0.0
0.164	Peak pressure	50	37	2.8
0.174	Peak $G_{c.g.}$-load	49	36	3.1
0.324	Top of first bounce	28	4	0.3

TABLE XII

IGE Drop Test Data, 8.0 fps, θ = 6.0, ϕ = 0.0
(Test No. 23)

Time (sec)	Event	P_T (psfg)	P_C (psfg)	$G_{c.g.}$ (g-load)
0.000	Release	26	0	0.0
0.092	Touch	26	4	0.0
0.174	Peak trunk pressure and $G_{c.g.}$-load	53	39	3.2
0.178	Peak cushion pressure	53	41	3.2
0.338	Top of first bounce	27	2	0.0

TABLE XIII

IGE Drop Test Data, 8.0 fps, θ = 6.0, ϕ = -7.5
(Test No. 20)

Time (sec)	Event	P_T (psfg)	P_C (psfg)	$G_{c.g.}$ (g-load)
0.000	Release	27	0	0.0
0.095	Touch	27	2	0.0
0.189	Peak trunk pressure	54	35	3.2
0.201	Peak cushion pressure and $G_{c.g.}$-load	52	39	3.3
0.342	Top of first bounce	28	1	0.2

TABLE XIV

IGE Drop Test Data, 8.0 fps, θ = 12.0, ϕ = 0.0
(Test No. 11)

Time (sec)	Event	P_T (psfg)	P_C (psfg)	$G_{c.g.}$ (g-load)
0.000	Release	26	0	0.0
0.097	Touch	26	2	0.0
0.184	First peak trunk pressure	42	11	3.0
0.194	Peak $G_{c.g.}$-load	41	13	3.4
0.257	Peak cushion pressure and second peak trunk pressure	43	35	2.4
0.334	Top of first bounce	24	0	0.0

TABLE XV

IGE Drop Test Data, 8.0 fps, θ = 12.0, ϕ = -7.5
(Test No. 17)

Time (sec)	Event	P_T (psfg)	P_C (psfg)	$G_{c.g.}$ (g-load)
0.000	Release	25	0	0.0
0.093	Touch	25	1	0.0
0.169	First peak trunk pressure	39	5	3.4
0.174	Peak $G_{c.g.}$-load	37	4	3.8
0.250	Peak cushion pressure and second peak trunk pressure	41	29	1.2
0.360	Top of first bounce	27	0	0.5

TABLE XVI

IGE Drop Test Data, 8.0 fps, θ = 0.0, ϕ = 0.0
(Test No. 49)

Time (sec)	Event	P_T (psfg)	P_C (psfg)	$G_{c.g.}$ (g-load)
0.000	Release	26	0	0.0
0.047	Touch	26	4	0.0
0.109	Peak $G_{c.g.}$ load and peak cushion pressure	47	36	2.6
0.120	Peak trunk pressure	40	35	2.5
0.224	Top of first bounce	28	6	0.2

TABLE XVII

IGE Drop Test Data, 8.0 fps, θ = 12.0, ϕ = 0.0
(Test No. 10)

Time (sec)	Event	P_T (psfg)	P_C (psfg)	$G_{c.g.}$ (g-load)
0.000	Release	26	0	0.0
0.063	Touch	26	1	0.0
0.172	First peak trunk pressure and $G_{c.g.}$-load	39	12	2.8
0.242	Peak cushion pressure and second peak trunk pressure	43	35	2.4
0.347	Top of first bounce	25	1	0.0

TABLE XVIII

IGE Drop Test Data, 3.0 fps, $\theta = 0.0$, $\phi = 0.0$
(Test No. 27)

Time (sec)	Event	P_T (psfg)	P_C (psfg)	$G_{c.g.}$ (g-load)
0.000	Release	25	1	0.0
0.036	Touch	26	6	0.0
0.100	Peak pressure	44	32	1.8
0.106	Peak $G_{c.g.}$-load	44	31	2.2
0.200	Top of first bounce	27	9	0.3

TABLE XIX

IGE Drop Test Data, 3.0 fps, $\theta = 10.0$, $\phi = 0.0$
(Test No. 8)

Time (sec)	Event	P_T (psfg)	P_C (psfg)	$G_{c.g.}$ (g-load)
0.000	Release	25	0	0.0
0.031	Touch	25	0	0.0
0.184	First peak trunk pressure	39	18	2.3
0.220	Peak $G_{c.g.}$-load and second peak trunk pressure	43	30	2.7
0.235	Peak cushion pressure	43	35	2.5
0.370	Top of first bounce	26	0	0.0

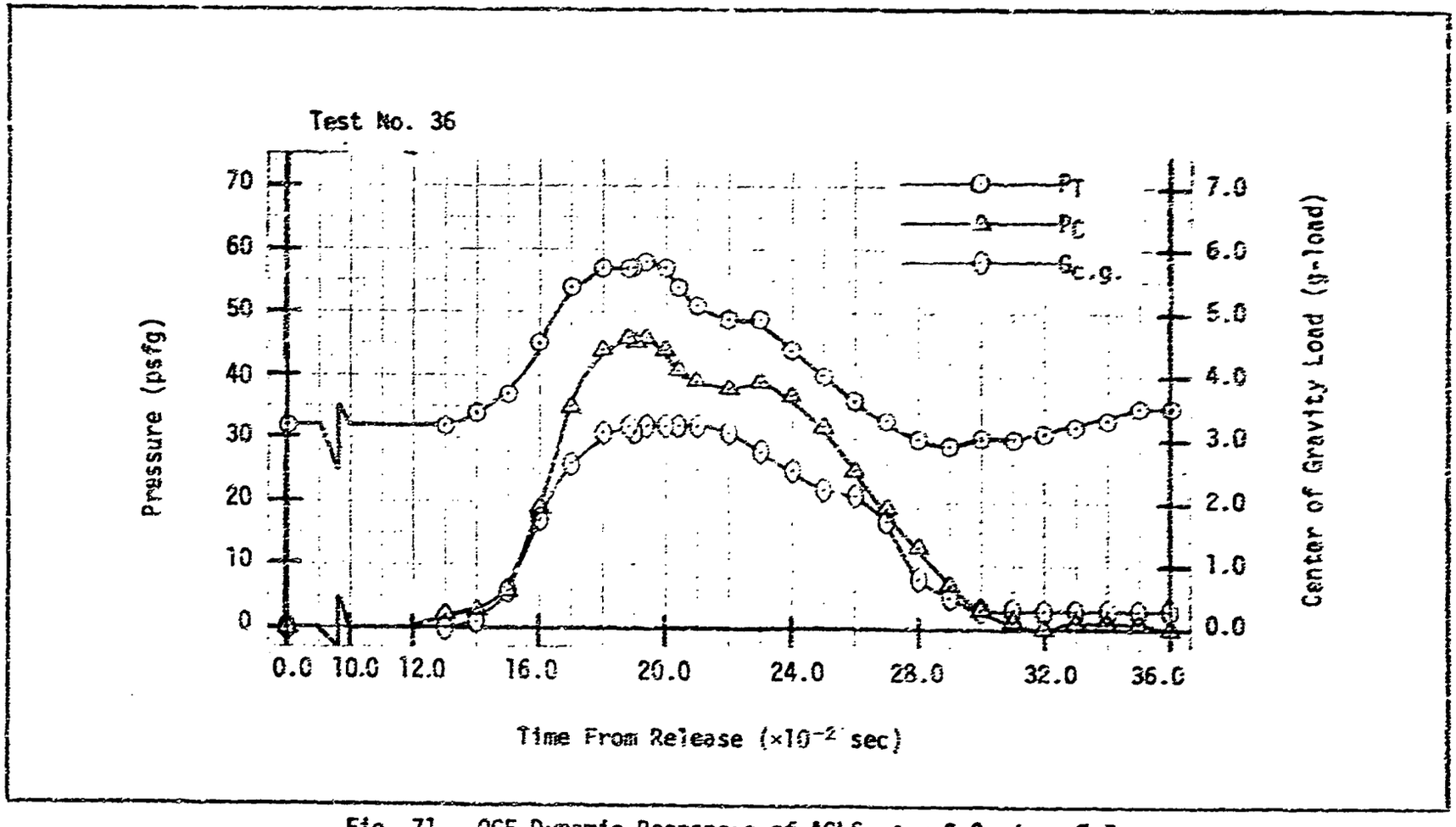

Fig. 71. OGE Dynamic Responses of ACLS, $\theta = 0.0$, $\phi = -7.5$

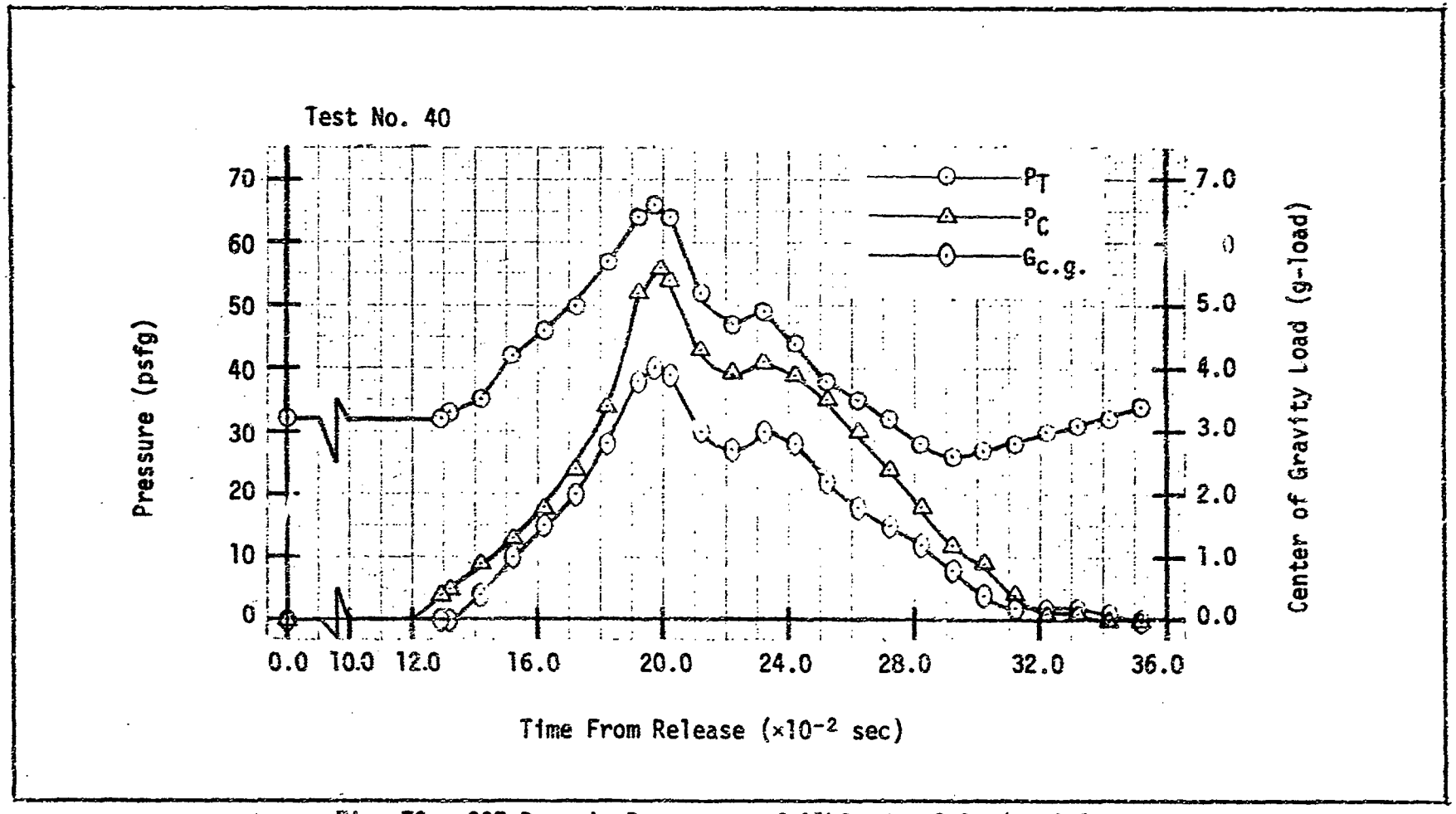

Fig. 72. OGE Dynamic Responses of ACLS, θ = 6.0, ϕ = 0.0

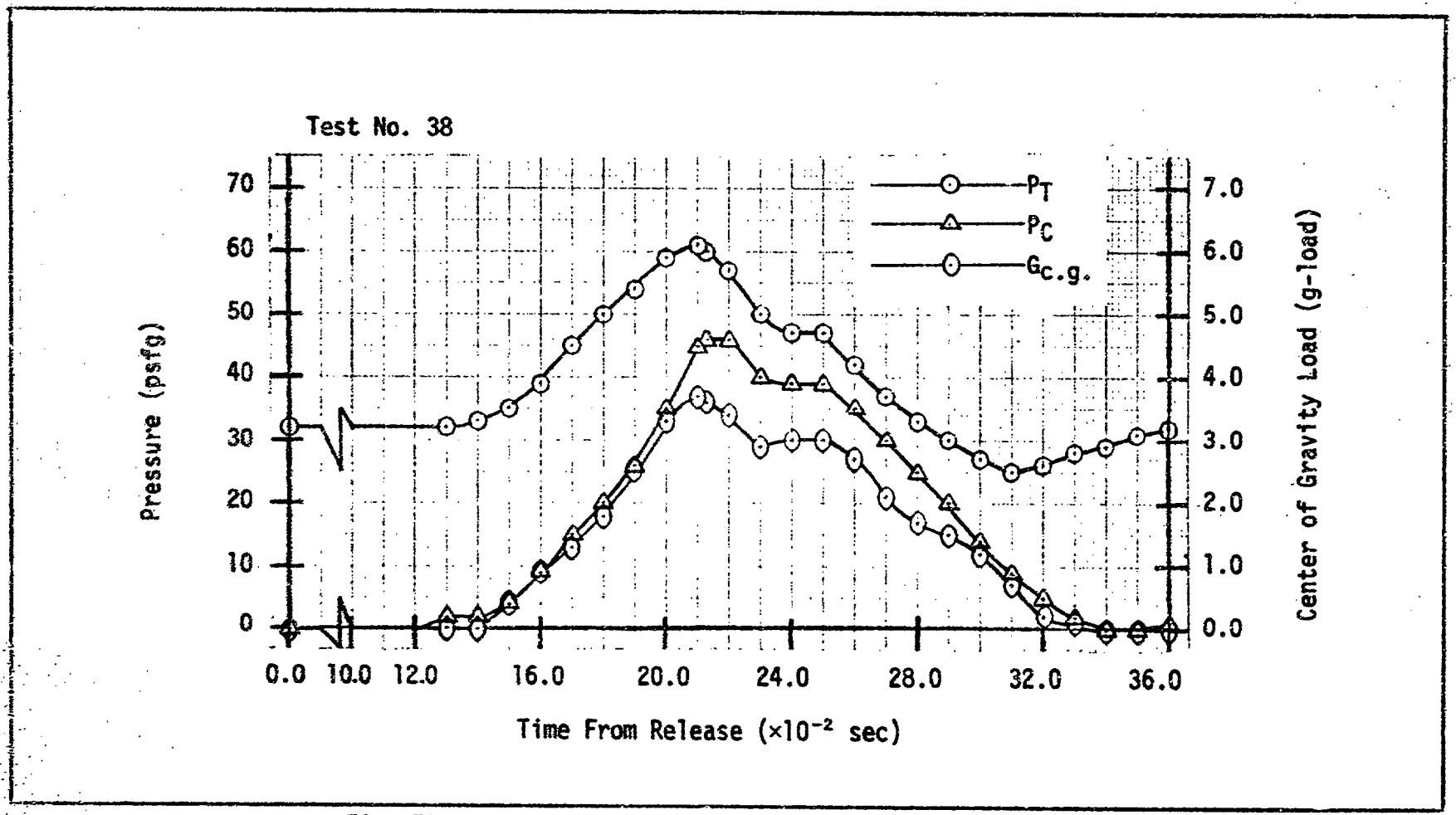

Fig. 73. OGE Dynamic Responses of ACLS, θ = 6.0, ϕ = -7.5

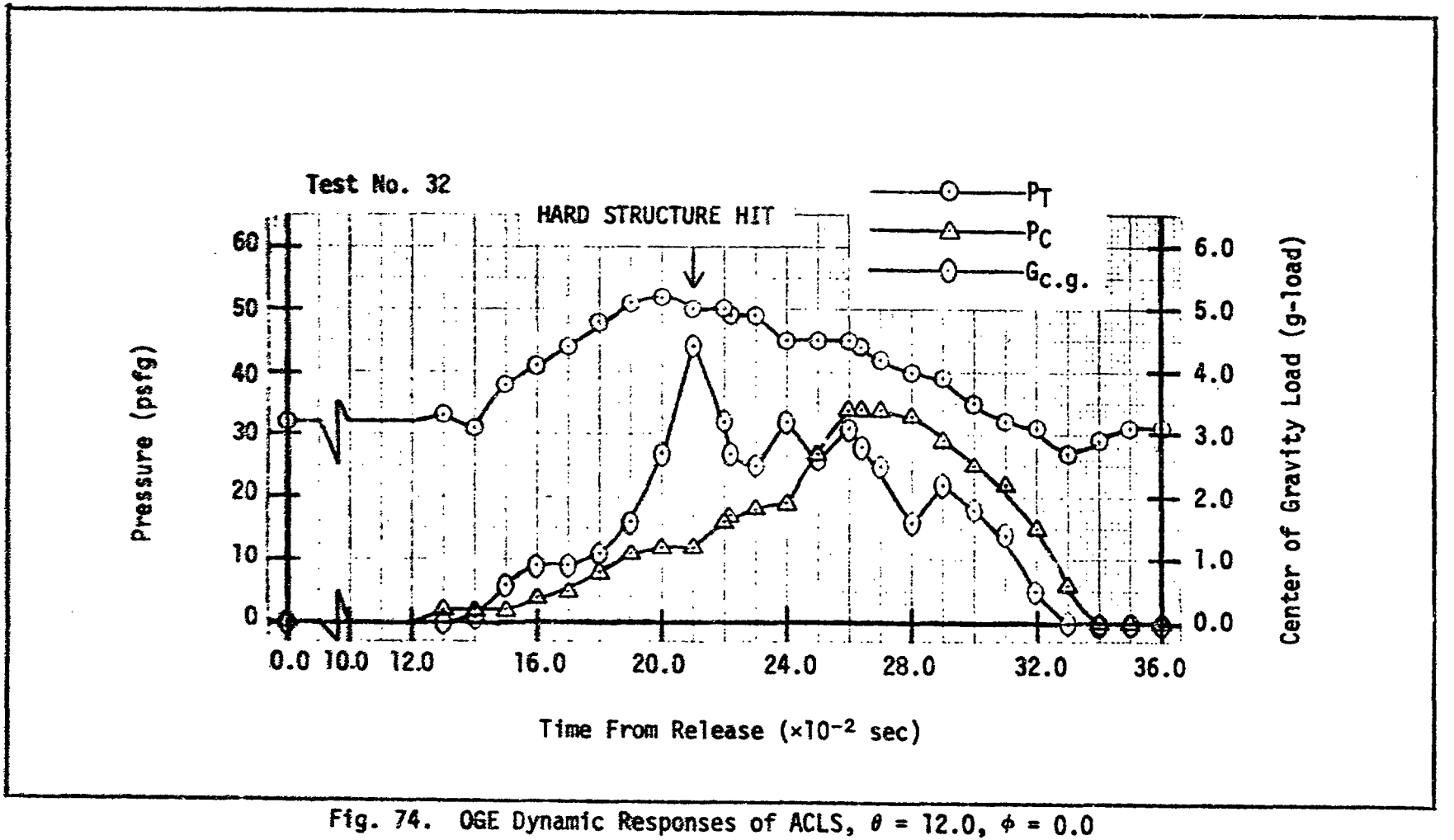

Fig. 74. OGE Dynamic Responses of ACLS, θ = 12.0, ϕ = 0.0

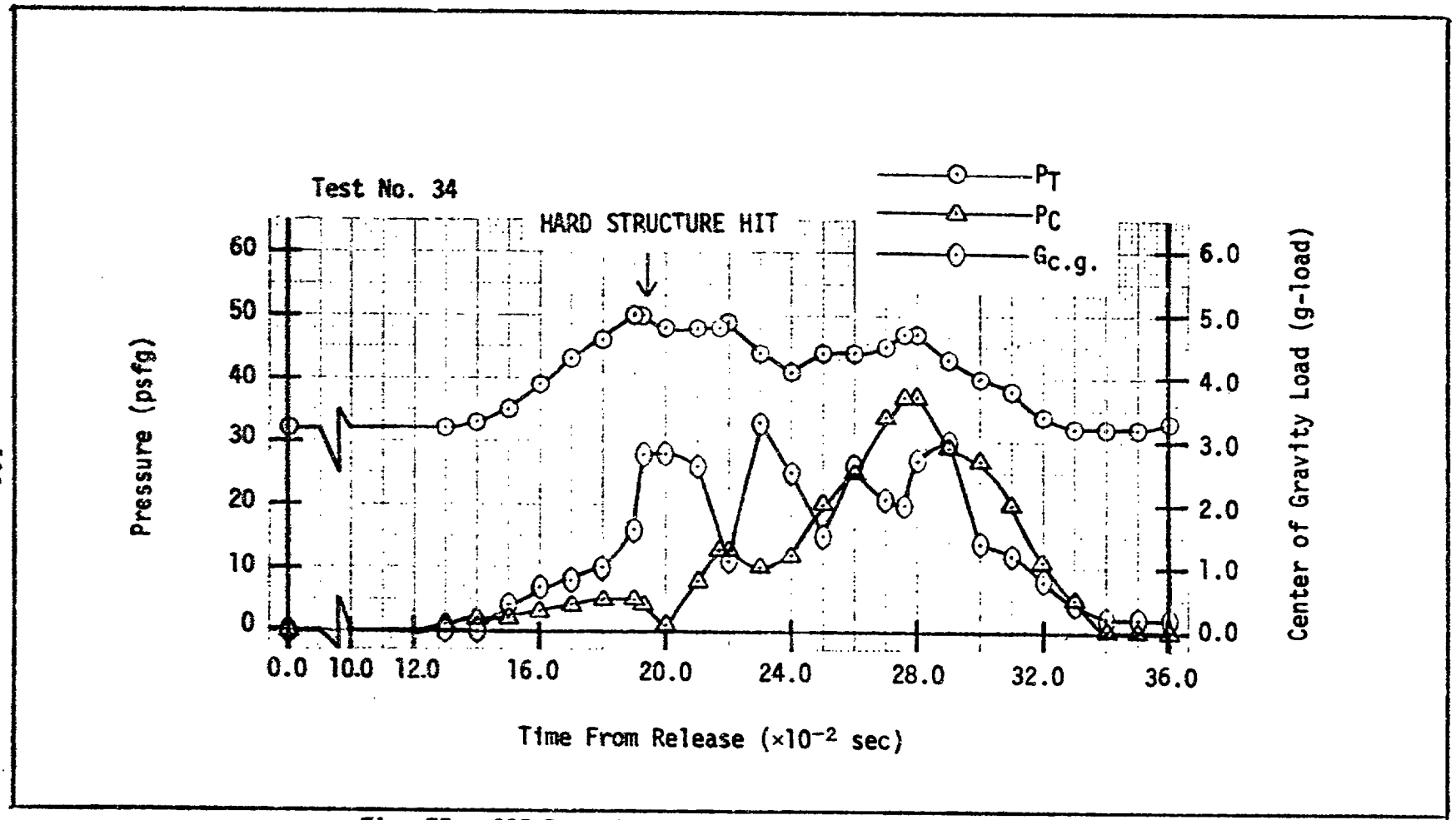

Fig. 75. OGE Dynamic Responses of ACLS, θ = 12.0, ϕ = -7.5

TABLE XX

OGE Drop Test Data, 8.0 fps, $\theta = 0.0$, $\phi = 0.0$
(Test No. 42)

Time (sec)	Event	P_T (psfg)	P_C (psfg)	$G_{c.g.}$ (g-load)
0.000	Release	32	0	0.0
0.108	Touch	32	2	0.0
0.134	Peak trunk pressure	56	44	2.3
0.144	Peak cushion pressure	53	46	2.7
0.169	Peak $G_{c.g.}$-load	50	40	3.0
0.284	Top of first bounce	33	1	0.0

TABLE XXI

OGE Drop Test Data, 8.0 fps, $\theta = 0.0$, $\phi = -7.5$
(Test No. 43)

Time (sec)	Event	P_T (psfg)	P_C (psfg)	$G_{c.g.}$ (g-load)
0.000	Release	32	0	0.0
0.106	Touch	32	2	0.0
0.156	Peak trunk pressure	56	40	2.8
0.166	Peak cushion pressure and $G_{c.g.}$-load	55	42	3.1
0.336	Top of first bounce	36	1	0.2

TABLE XXII

OGE Drop Test Data, 8.0 fps, θ = 6.0, ϕ = 0.0
(Test No. 41)

Time (sec)	Events	P_T (psfg)	P_C (psfg)	$G_{c.g.}$ (g-load)
0.000	Release	32	0	0.0
0.109	Touch	32	4	0.0
0.180	Peak trunk pressure	60	47	3.3
0.184	Peak cushion pressure and $G_{c.g.}$-load	60	48	3.3
0.350	Top of first bounce	35	0	0.0

TABLE XXIII

OGE Drop Test Data, 8.0 fps, θ = 6.0, ϕ = -7.5
(Test No. 39)

Time (sec)	Event	P_T (psfg)	P_C (psfg)	$G_{c.g.}$ (g-load)
0.000	Release	32	0	0.0
0.107	Touch	32	1	0.0
0.189	Peak trunk pressure	58	35	3.1
0.202	Peak cushion pressure and $G_{c.g.}$-load	55	43	3.3
0.360	Top of first bounce	35	1	0.2

TABLE XXIV

OGE Drop Test Data, 8.0 fps, θ = 12.0, ϕ = 0.0
(Test No. 33)

Time (sec)	Event	P_T (psfg)	P_C (psfg)	$G_{c.g.}$ (g-load)
0.000	Release	32	0	0.0
0.108	Touch	32	2	0.0
0.184	Peak trunk pressure	52	9	2.1
0.195	Peak $G_{c.g.}$-load	50	9	3.6
0.261	Peak cushion pressure	45	38	2.1
0.374	Top of first bounce	34	2	0.0

TABLE XXV

OGE Drop Test Data, 8.0 fps, θ = 12.0, ϕ = -7.5
(Test No. 35)

Time (sec)	Event	P_T (psfg)	P_C (psfg)	$G_{c.g.}$ (g-load)
0.000	Release	32	0	0.0
0.109	Touch	32	1	0.0
0.176	Peak trunk pressure	48	4	1.8
0.187	Peak $G_{c.g.}$-load	45	1	4.3
0.263	Peak cushion pressure	45	32	2.8
0.340	Top of first bounce	48	35	2.3

APPENDIX D

Static Test Procedures and Data Reduction

Introduction

Details of load application, data collection, and data reduction for the vertical stiffness, roll stiffness, pitch stiffness, and pressure footprint tests are explained in this appendix.

Loading of Model Over Center of Gravity and Center of Pressure

Loads for all the vertical load tests were applied using the same methods. Under 39.1 pounds, load was removed on the ACLS by lifting the model by its support cables using an overhead hoist. The support cables were attached to a Chatillons spring scale with a range from 0 to 100 pounds in 1-pound increments. As the model was lifted, the scale measured the lifting force. This lifting force was subtracted from the normal weight of the model to obtain the load on the ACLS acting at the center of gravity. Over 39.1 pounds the load was applied using lead shot bags, 18 inches long by 6 inches wide, weighing approximately 10 pounds each. Twelve bags were used and numbered from 1 to 12. The bags were weighed cumulatively, in the same order as they were used in the tests, on a Toledo Scale with a range from 0 to 800 pounds in 1/2-pound increments; and thus the loads are within ±1/2 pound. The lead shot bags were placed over the center of gravity or the center of pressure of the model as shown in Fig. 76 to create the desired additional load over 39.1 pounds.

The load on the ACLS was applied after the design trunk pressure was checked at a fan rotation of 8600 rpm in the hover load on ACLS condition, 39.1 pounds. Load was applied in increments of 10 pounds.

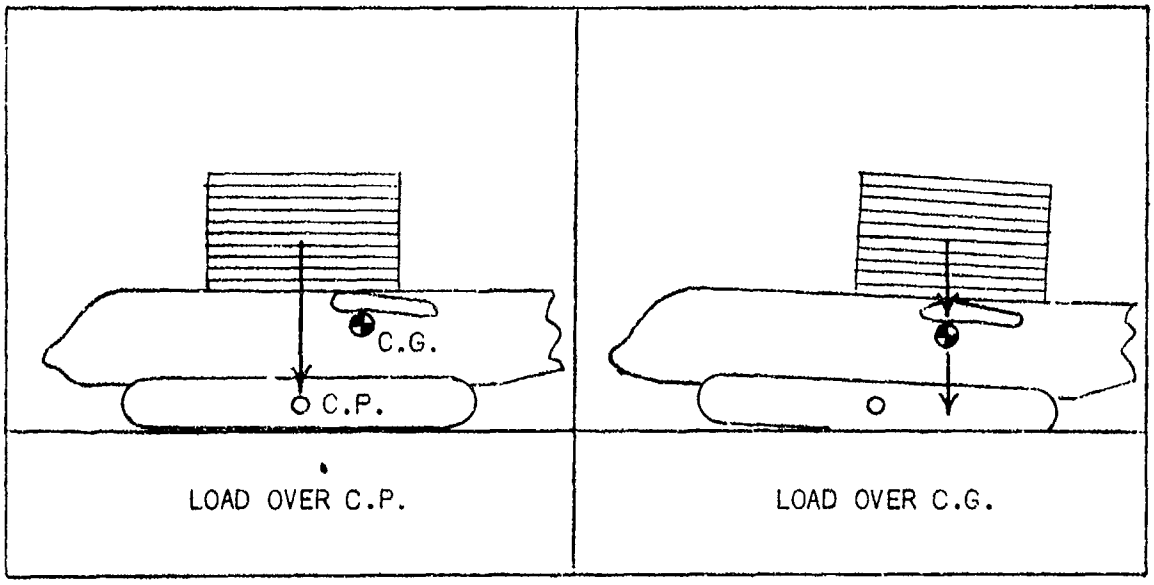

Fig. 76. Load Application

At each load, cushion pressure, trunk pressure, pitch attitude, and height of the center of gravity above the floor were measured. Pressures were measured with the same water manometers used to measure initial cushion and trunk pressures of the drop tests. Pitch attitude was measured using the same procedure used for pitch determination of the drop tests as was explained in Appendix B. The center of gravity height above the floor was measured using a 19-inch vernier-equipped ruler accurate to 0.001 inches. Because of the model's slight movement during measurement it was decided to reduce the accuracy of the center of gravity height measurement to the nearest 0.1 inches or ±0.05 inches. The measurement was made at the center of gravity marker on the port side of the model fuselage. Thus the following data were recorded at each load: cushion pressure, trunk pressure, load, center of gravity height, pitch marker height.

Cushion and trunk pressure data were recorded in inches of water and then converted to psfg, accurate to ±0.5 psfg. It was decided to

keep the accuracy of this data to the same level as that of drop test data.

The deflection of the trunk was calculated from the measurement of the center of gravity height data. With zero load on the ACLS, there was no deflection of the trunk, and the height of the center of gravity above the floor at this point was considered the baseline or zero reference. With H_0 representing zero reference height and H_L the height at each load, deflection D is calculated as

$$D = H_0 - H_L \qquad (D\text{-}1)$$

Roll Stiffness

For roll stiffness, torque was applied about the model's center of gravity as shown in Fig. 77. A plastic cup was attached to parachute cord

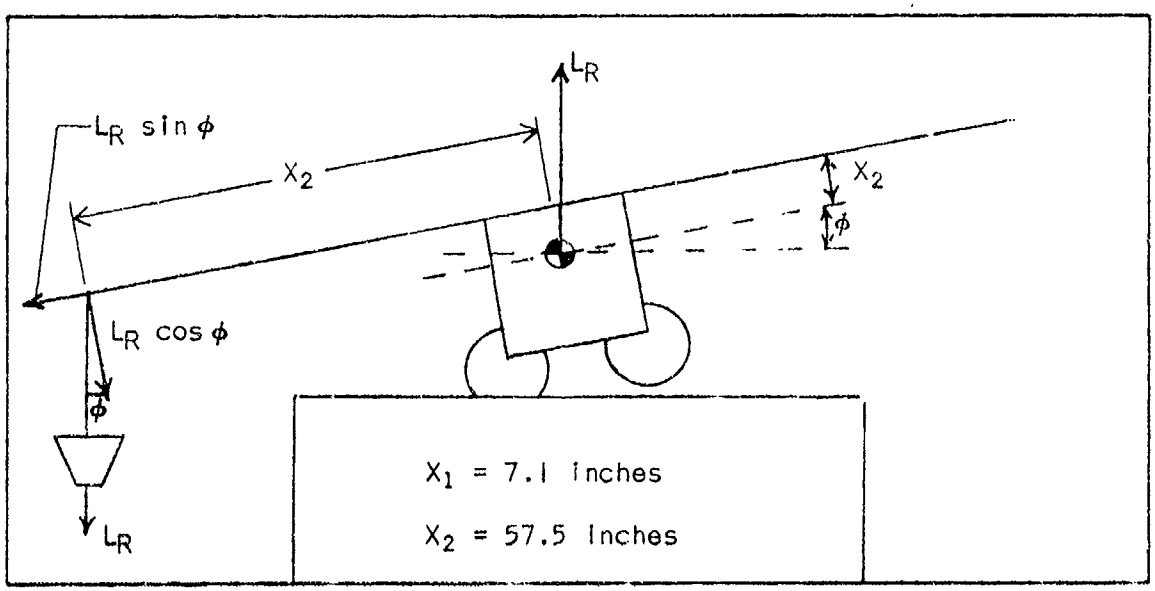

Fig. 77. Roll Torque Application

which in turn was connected to the wing tip of the model on a line directly starboard of the center of gravity and 7.1 inches above it. The cup, string, and the lead weights used to create the torque were weighed on a Toledo

Scale with a 25-pound capacity and accurate to 0.001 pounds. The loads used ranged from 0.000 to 0.800 pounds. To keep the load on the ACLS at 39.1 pounds during roll stiffness tests, an approximate load equal in magnitude but opposite in direction to the torque load was applied at the center of gravity of the model as shown in Fig. 77. Lift load was created by the overhead hoist and measured by a spring scale with a 25-pound range.

The roll angle was measured using the same procedure for roll determination as in the drop tests outlined in Appendix B. It should be noted that the model was pitched at 2 degrees during the roll angle measurements; and thus, the height differences obtained for roll angle calculation were not actually in the roll plane. However, the difference between the correct height and the heights actually measured was negligible as can be seen in Fig. 78. Thus, the offset height was measured and used to determine the roll angle to ±0.05 degrees.

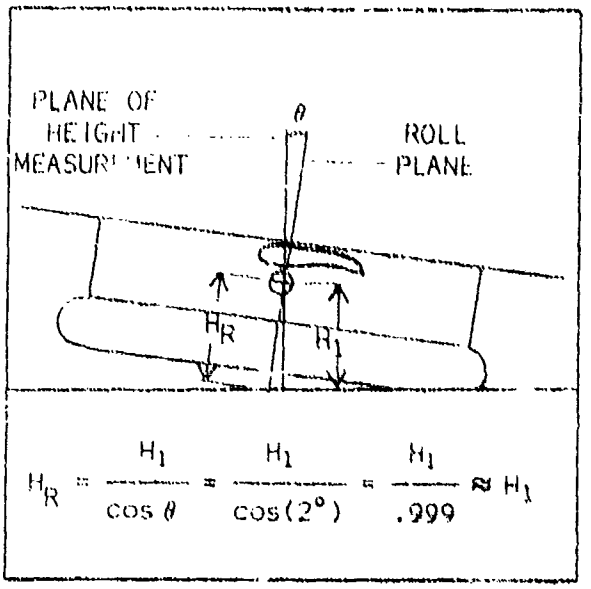

Fig. 78. Roll Angle Measurement

For every load or torque applied, the following raw data were collected: height of the center of gravity from the floor on the port and starboard side of the fuselage, and the load placed on the wing tip. From this collected data the roll angle was calculated, as was explained in Appendix B, and the torque was calculated using the following equation (see Fig. 77):

$$\tau_R \text{ (in-lb)} = L_R \cos\phi(57.5 \text{ in}) + L_R \sin\phi(7.1 \text{ in}) \qquad \text{(D-2)}$$

from this reduced data the roll stiffness curve was developed.

Pitch Stiffness

For pitch stiffness, load was applied at the tail of the model creating positive and negative torque about the center of gravity as shown in Fig. 79. The torque load was applied and measured in exactly 1/2-pound increments using a spring scale with a 25-pound range. The load was applied at a point 61.1 inches directly aft of the center of gravity and 5.6 inches above it. For positive torque, the load was applied in a downward direction forcing the model to pitch positively. For each downward load applied, a lift force equal to the load was placed at the model's center of gravity using the overhead hoist. A similar spring scale to that used to create torque load was used to measure the lift load. Thus the load on the ACLS was kept at a constant 39 pounds. To create negative torque, a stand supported the spring scale above the tail, and force was applied in the upward direction forcing the model to pitch negatively. Again, for each lift torque load an equal downward load was applied over the center of gravity in the form of 0.50-pound lead shot bags. The bags were weighed on a Toledo Company scale with a 25-pound capacity and an accuracy to the nearest 0.001 pound. Positive torque loads ranged from 0.0 to 5.0 pounds while negative torque loads ranged from 0.0 to 7.5 pounds. The pitch angle was calculated from the height difference measurements, as was explained in Appendix B for the drop tests. The model did not roll during these tests.

Thus for each load or torque created, the following data were collected: height of the center of gravity above the floor, pitch angle marker height above the floor, and the load applied. From this collected

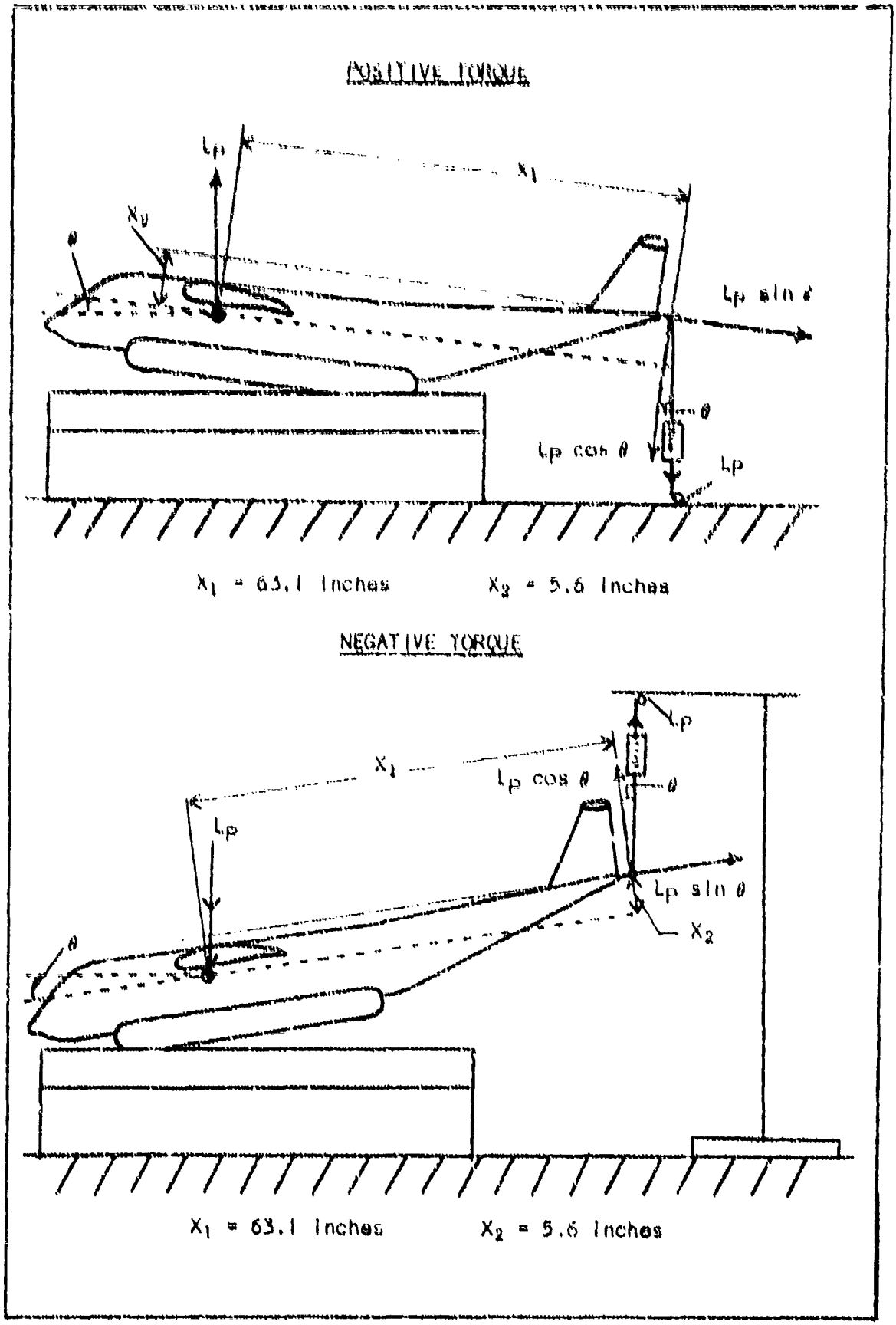

Fig. 79. Pitch Torque Application

data the pitch angle was calculated to the 05 degrees, and positive torque was calculated to the nearest 0.1 foot-pound using the following equation (see Fig. 79):

$$\tau_{p+}\ (\text{ft-lb}) = L_p \cos\theta\left(\frac{63.1}{12}\ \text{ft}\right) + L_p \sin\theta\left(\frac{5.6}{12}\ \text{ft}\right) \qquad (D\text{-}3)$$

Negative torque accurate to the nearest 0.1 ft-lb used the following equation (see Fig. 79):

$$\tau_{p-}\ (\text{ft-lb}) = -L_p \cos\theta\left(\frac{63.1}{12}\ \text{ft}\right) + L_p \sin\theta\left(\frac{5.6}{12}\ \text{ft}\right) \qquad (D\text{-}4)$$

The reduced data were then used to create a pitch stiffness curve.

Pressure Footprint

A pressure footprint was made for each of several loads on the ACLS over the center of gravity. The loads were applied as was explained in the beginning of this appendix. Figure 40 of Chapter IV showed the arrangement of the pressure taps beneath the ACLS. Figure 80 shows the plastic tubing connection to the plate taps. The metal connector forced the plastic tubing against the walls

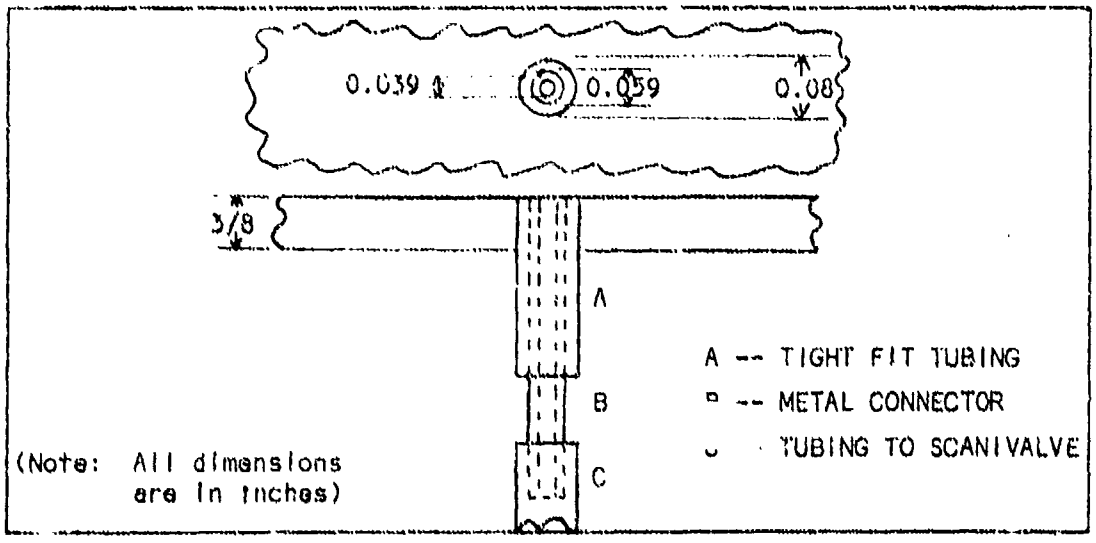

Fig. 80. Pressure Footprint Tubing Installation

of the hole in the plate providing a tight, leak-free fit. Ten feet of plastic tubing was led from the metal connector of each tap to the 48 pressure ports of the Scanivalve measuring instrument.

The Scanivalve measured all 48 pressure taps in 20 seconds. The Scanivalve measured these pressures with the use of one differential pressure transducer, ±2.5 psi range, vented to the atmosphere. Pressure is supplied to the transducer by means of a rotating pressure pickup. The operation of the Scanivalve is shown schematically in Fig. 81. Pressure is being constantly supplied to each port from the plate. The pickup

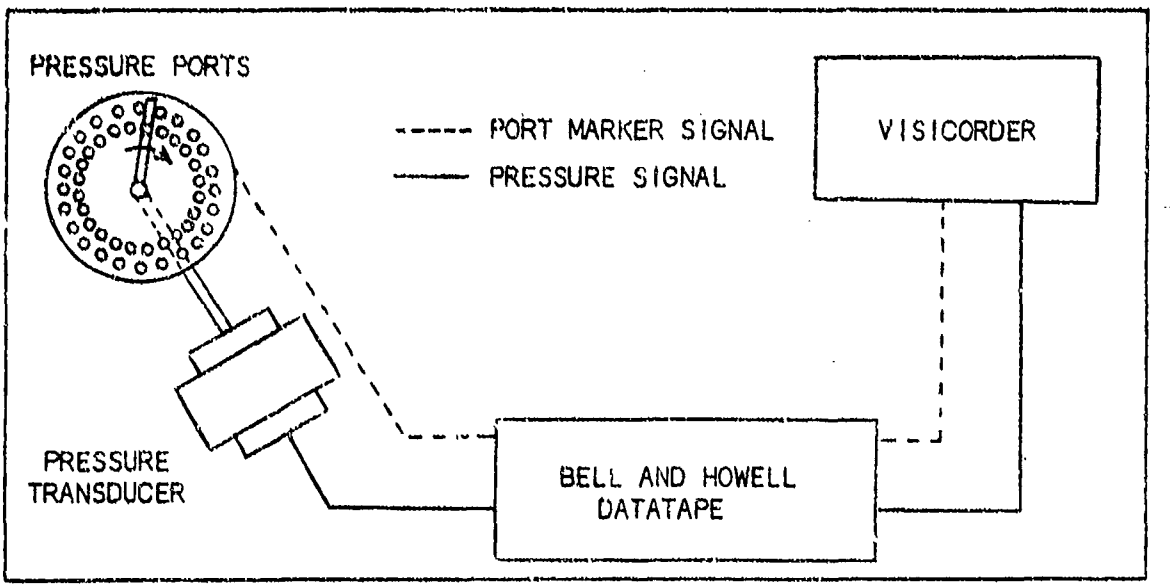

Fig. 81. Scanivalve Operation Schematic

rotates over each port in a sequential numbering order, picking up the pressure and sending it to the transducer which measures that pressure and outputs an electrical signal. Before a new port pressure is picked up, the previous pressure in the rotating pickup tube is vented. The pressure taps on the plate were numbered to correspond to the respective pressure measuring ports on the Scanivalve. Pressure signals from the transducer were sent to the Bell and Howell Datatape and Honeywell

Visicorder in the same manner as were the drop test data. As the pressure pickup rotated, it sent out a marking signal to the Visicorder via the signal conditioning unit on the Bell and Howell Datatape. This marking signal was received on the Visicorder paper above the trace of the 48 pressures, and the marker identified where each pressure was taken. The Honeywell Visicorder was allowed to run at 2 inches per second of paper travel for 30 seconds at each load in order to record all 48 pressure taps.

The pressure transducer on the Scanivalve was calibrated before the series of tests was run by supplying a known air pressure to one port of the Scanivalve and recording the deflection caused by that pressure on the Visicorder paper. Air pressures of 0, 5, 10, and 12 inches of water were supplied to the transducer and recorded. The pressure was measured with a 40-inch Type W Meriam water manometer. The calibration factor used to reduce the data from the Visicorder traces was 21 psfg per inch of trace deflection.

For each load the following raw data were recorded: pressures at the 48 taps, cushion pressure, trunk pressure, and load over the center of gravity on the ACLS. The raw pressure data were reduced to final form in the same manner as drop test data discussed in Appendix B but using the calibration factor obtained above. Data were accurate to ±2 psfg as was the calibration factor. Footprint pressures may be 1 to 2 psfg higher than actual values, since pressures were recorded only on the low side (±0.5 psi) of the ±2.5 psi transducer. The cushion and trunk pressure data were recorded in inches of water and then converted to pounds per square foot with an accuracy of ±0.5 psfg. These reduced data were used to obtain the pressure footprints of Chapter IV.

APPENDIX E

Braking Tests--Simulation, Procedure, and Data Reduction

Introduction

A discussion of brake modeling, the location of brake blocks, details on brake test procedures, and data reduction methods is contained in this appendix.

Brake Modeling

The braking system of the ACLS was designed with the intent that each brake pillow would have 300 square inches, full scale, of surface contact during braking (Ref 3:7). Bell Aerospace has conducted full-scale testing on a two-dimensional section of the CC-115 proposed trunk with a brake pillow, and they have measured the contact area for an initial IGE design trunk pressure of 342 psfg. Although unpublished, the results have revealed that a brake contact area of 254 square inches, full scale, per each brake pillow is the most to be expected. Attachment point and surface contact dimensions are centered above and below each other and should not change for varying brake heights in order to stay within the designs of the braking system. Therefore, to simulate the brakes, wooden blocks were constructed at the fixed attachment point and surface contact dimensions of Fig. 50 of Chapter V but with varying nominal heights of 2-1/2, 2, 1-1/2, 1, and 1/2 inches. Rubber pads, approximately 0.1 inch thick and of the same surface contact dimensions as the blocks, were glued to the contact area of the blocks in order to simulate a coefficient of static friction of 0.8 between the blocks and a brown paper surface on the testing platform. The heights of the five sets of blocks including

rubber pads were measured with a 19-inch vernier-equipped steel ruler and found to be as follows: 2.60, 2.08, 1.56, 1.08, and 0.57 inches. The use of wooden blocks was the only method capable of insuring that surface contact area and brake height would remain at the desired values during a test.

Brake Block Locations

The tenth-scale model trunk contained six locations where no jet holes were situated. These locations were areas where brake pillows would normally be attached. The locations of these six areas with respect to the model's center of pressure on an inflated trunk is found in Fig. 82. The forward to af ngth of each area is 3.9 inches. Each wooden brake block was centered on this 3.9 inches of length along the ground tangent line of the trunk, as shown in Fig. 82. Two-way stick masking tape was placed on the attachmant surface of each block to secure the block to the trunk. In addition, strips of masking tape were used on the edges of the block and attached to the trunk to keep the blocks as stationary as possible with respect to the trunk during a test.

Data Collection and Reduction

One test was run for each brake height. Brakes were attached to the trunk while it was inflated at an OGE trunk pressure of 26 psfg (4.8 inches of water). This is the OGE pressure for the normal IGE design pressure of 34 psfg as was explained in Chapter V. After brakes were attached, the model was lowered onto the platform with ACLS and brakes supporting the full weight of the model. At that point trunk and cushion pressures were measured on water manometers to ±0.05 inches of water. After pressure measurements, the model was pulled forward by hand via a

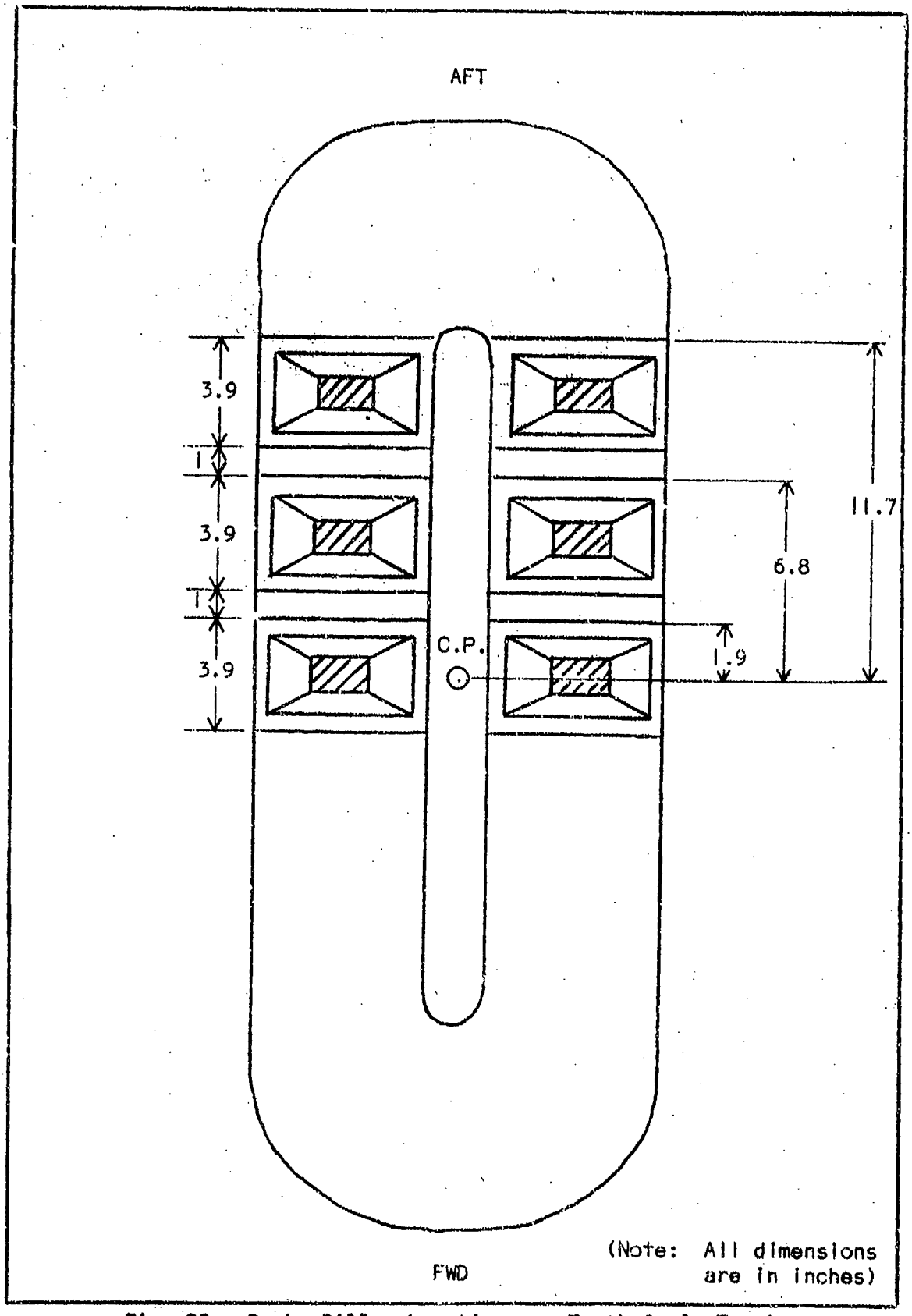

Fig. 82. Brake Pillow Locations on Tenth-Scale Trunk

cable attached directly to the model's center of gravity as shown in Fig. 83. Attached to the cable was a spring scale with a 0 to 25 pound range in 1/2 pound increments. Force was applied to the center of gravity and observed on the spring scale until the first forward motion of the brake blocks was noticed. The force measured was the static drag or frictional force due to the brakes and decreased cushion support. During the pull the cable was kept as parallel as possible to the floor of the testing platform.

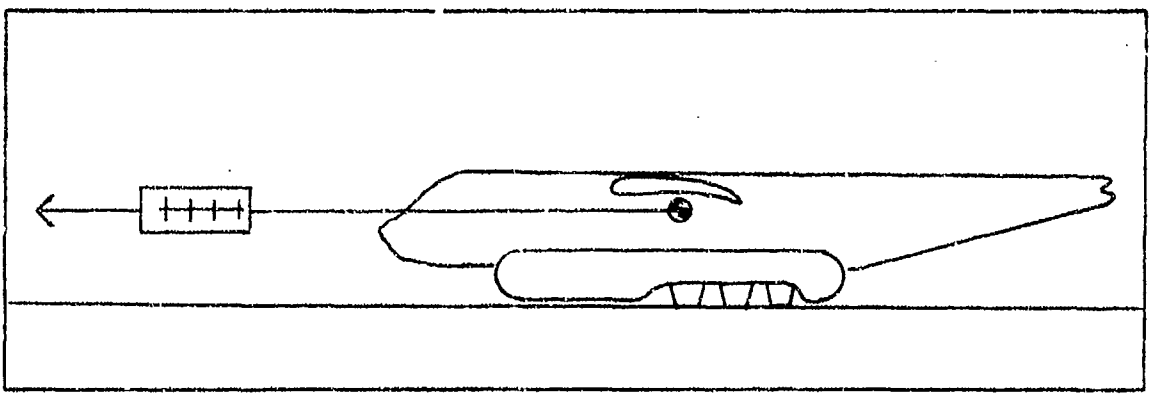

Fig. 83. Pulling Model for Brake Drag

Thus for each test the following raw data were recorded: brake height, cushion pressure, trunk pressure, and frictional force on the spring scale. Cushion and trunk pressure readings in inches of water were converted to pounds per square foot to ±0.5 psfg. Drag forces were read directly from the spring scale to the nearest 0.5 pounds.

Deceleration rates for each brake height were calculated from the measured drag data. Assuming a constant forward velocity (zero acceleration) before applying brakes, the drag force F felt by the brakes caused deceleration A_D; and

$$F = MA_D \qquad \text{(E-1)}$$

where

$$M = \frac{W_A}{g_e} \tag{E-2}$$

or

$$\frac{F}{M} = \frac{F}{W_A} g_e = A_D \tag{E-3}$$

In terms of the number of g_e's,

$$A_D = \frac{F}{W_A} \tag{E-4}$$

In order to obtain accurate deceleration rates, each set of six blocks was weighed and the weight was added to the initial 39.1 pounds weight of the model. This net weight W_A was used to obtain the deceleration rate A_D as shown above. The net weight of the model at each brake height was as follows (±0.05 pounds):

Brake Height (inches)	Model Net Weight (pounds)
2.60	41.6
2.08	41.1
1.56	40.6
1.08	39.9
0.57	39.3
0.00	39.1

These reduced data were used to formulate the graphs of Chapter V.